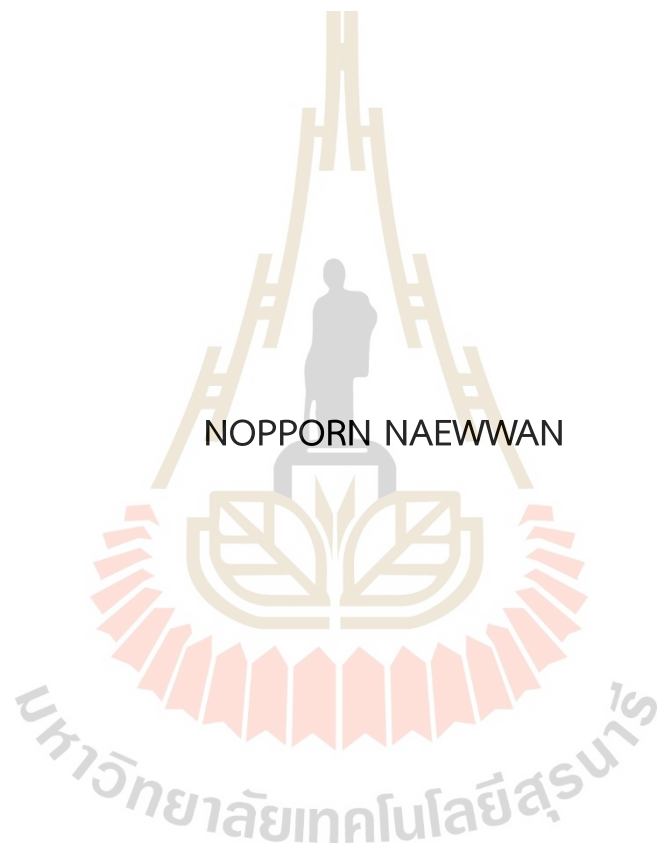


DEVELOPMENT OF SEVERE ACUTE RESPIRATORY SYNDROME
CORONAVIRUS 2 DETECTION BASED ON CRISPR-Cas12a



A Thesis Submitted in Partial Fulfilment of the Requirements for the
Degree of Master of Science in Translational Medicine
Suranaree University of Technology
Academic Year 2023

การพัฒนาชุดตรวจโรคติดเชื้อไวรัสโคโรนา 2019 ด้วยเทคนิค CRISPR-Cas12a



วิทยานิพนธ์นี้เป็นส่วนหนึ่งของการศึกษาตามหลักสูตรปริญญาวิทยาศาสตรมหาบัณฑิต

สาขาวิชาเวชศาสตร์ปริวรรต

มหาวิทยาลัยเทคโนโลยีสุรนารี

ปีการศึกษา 2566

DEVELOPMENT OF SEVERE ACUTE RESPIRATORY SYNDROME
CORONAVIRUS 2 DETECTION BASED ON CRISPR-Cas12a

Suranaree University of Technology has approved this thesis submitted in partial fulfillment of the requirements for a Master's Degree.

Thesis Examining Committee

Jeeraphong T.

(Asst. Prof. Dr. Jeeraphong Thanongsaksrikul)

Chairperson

Kanyarat T.

(Dr. Kanyarat Thueng-in)

Member (Thesis Advisor)

N. Namvichaisirikul

(Dr. Niwatchai Namvichaisirikul, M.D.)

Member (Thesis Co-advisor)

Sanong

(Dr. Sanong Suksaweang)

Member

T. Sim

(Dr. Theeraya Simawaranon)

Member

Chatchai Jothityang

(Assoc. Prof. Dr. Chatchai Jothityangkoon)

Vice Rector for Academic Affairs

and Quality Assurance

S. Pinjaroen

(Assoc. Prof. Sutham Pinjaroen, M.D.)

Dean of Institute of Medicine

นพพร แนววัน : การพัฒนาชุดตรวจโรคติดเชื้อไวรัสโคโรนา 2019 ด้วยเทคนิค CRISPR-Cas12a (DEVELOPMENT OF SEVERE ACUTE RESPIRATORY SYNDROME CORONA-VIRUS 2 DETECTION BASED ON CRISPR-Cas12a) อาจารย์ที่ปรึกษา :
อาจารย์ เทคนิคการแพทย์ ดร.กัญญารัตน์ ถึงอินทร์, 118 หน้า.

คำสำคัญ : โรคโควิด 19; ไวรัสโคโรนาสายพันธุ์กลุ่มอาการทางเดินหายใจเฉียบพลันรุนแรง 2;
คริสเปอร์-แคสทเวลพ์เอ; การตรวจสารพันธุกรรม; การตรวจหาไวรัส

การแพร่ระบาดของโรคติดเชื้อไวรัสโคโรนา 2019 (COVID-19) มีสาเหตุมาจากเชื้อไวรัสโคโรนากลุ่มอาการทางเดินหายใจเฉียบพลันรุนแรง 2 (SARS-CoV-2) ซึ่งทำให้เกิดปัญหาสาธารณสุขอย่างร้ายแรง วิธีทดสอบมาตรฐานในปัจจุบันที่เป็นที่ยอมรับในการตรวจวินิจฉัยโรคโควิด-19 คือวิธี real-time reverse transcription polymerase chain reaction (real-time RT-PCR) ซึ่งเป็นวิธีการที่มีความไวและความจำเพาะในการตรวจหาเชื้อ SARS-CoV-2 อย่างไรก็ตาม เครื่องมือนี้ไม่มีจำหน่ายทั่วไปในท้องตลาด เนื่องจากต้องใช้เครื่องมือและต้องมีการตรวจทางห้องปฏิบัติการ ซึ่งค่าใช้จ่ายสูง พร้อมทั้งบุคลากรที่ต้องได้รับการฝึกอบรมมาเป็นอย่างดี ในการศึกษาครั้งนี้ เราใช้โปรตีน Nonstructural Protein (NSP2) ซึ่งเป็นโปรตีนจำเพาะในเชื้อไวรัสโคโรนา 2 เป็นเป้าหมายในการตรวจวินิจฉัย โดยอาศัยเทคนิค clustered regularly interspaced short palindromic repeats associated proteins (CRISPR-Cas12a) ที่ใช้ชุดแถบทดสอบแบบ lateral flow strips test เพื่อพัฒนาชุดตรวจ ซึ่งช่วยให้สามารถอ่านผลตรวจได้ด้วยตาเปล่า รวมไปถึงเทคนิค recombinases polymerase amplification (RPA) ซึ่งช่วยให้ทราบผลตรวจเร็วขึ้นภายใน 50 นาที การประเมินผลการตรวจหาเชื้อ COVID-19 NSP2 ด้วยวิธีการใหม่นี้ ซึ่งให้ผลการทดสอบความสอดคล้องกับผลการทดสอบด้วยวิธีทดสอบมาตรฐาน real time RT-PCR 100% การศึกษานี้แสดงให้เห็นว่า ชุดแถบทดสอบแบบ lateral flow strips test และเทคนิค CRISPR-Cas12a ร่วมกับเทคโนโลยี RPA ในการตรวจหาเชื้อ SARS-CoV-2 เป็นอีกหนึ่งทางเลือกที่มีความเป็นไปได้ในการตรวจวินิจฉัยเชื้อ SARS-CoV-2 ในตัวอย่างโดยไม่จำเป็นต้องใช้อุปกรณ์พิเศษ

สาขาวิชาเวชศาสตร์ปริวรรต

ปีการศึกษา 2566

ลายมือชื่อนักศึกษา..... นพพร แนววัน

ลายมือชื่ออาจารย์ที่ปรึกษา..... นพพร แนววัน

ลายมือชื่ออาจารย์ที่ปรึกษาร่วม..... นพพร แนววัน

NOPPORN NAEWWAN : DEVELOPMENT OF SEVERE ACUTE RESPIRATORY
SYNDROME CORONAVIRUS 2 DETECTION BASED ON CRISPR-Cas12a. THESIS
ADVISOR : KANYARAT THUENG-IN, Ph.D. 118 PP.

Keyword: COVID-19; SARS-CoV-2; CRISPR-Cas12a; nucleic acid detection; virus
detection

The coronavirus disease 2019 (COVID-19) pandemic is caused by the severe acute respiratory syndrome coronavirus 2 (SARS-CoV-2) virus, which causes serious public health problems. The current gold standard accepted for diagnosing COVID-19 is the real-time reverse transcription polymerase chain reaction (real-time RT-PCR), which is a sensitive and specific method to detect SARS-CoV-2. However, they are not available in resource-constrained regions, equipment is required and requires expensive laboratory settings with well-trained personnel. In this study, we used nonstructural protein 2 (NSP2) as a target for development of a clustered regularly interspaced short palindromic repeats (CRISPR)-CRISPR associated proteins (Cas) 12a based lateral flow strips test, which can be visualized by the naked eye. We also combine with recombinases polymerase amplification (RPA) that allows the sample to result can be achieved in 50 minutes. Evaluation of the new COVID-19-NSP2 assay showed 100% concordance with real-time RT-PCR reference assay. This study shows that CRISPR-Cas12a based lateral flow assay combined with RPA technology are viable alternatives for diagnosing SARS-CoV-2 in samples without the need for special equipment.

School of Translational Medicine
Academic Year 2023

Student's Signature.....*Nopporn N.*.....
Advisor's Signature.....*Kanyarat T.*.....
Co-Advisor's Signature.....*N. Namdeksirikul*.....

ACKNOWLEDGEMENTS

I would like to express my sincere gratitude to my graduate advisor, Dr. Kanyarat Thueng-in, for giving me the opportunity to be a M.Sc. student and do a M.Sc. in her laboratory and for her continued assistance, teaching, kindness, encouragement and mentoring throughout the years.

I would like to sincerely thank and be grateful to Dr. Niwatchai Namvichaisirikul, M.D., my graduate co-advisor for his innumerable help, suggestions, support, and kindness. This thesis has been finished under their suggestion. The most significant factor in my success was their inspiration, patience, and guiding light.

Furthermore, I would also like to thank my thesis committee; Asst. Prof. Dr. Jeeraphong Thanongsaksrikul, Dr. Sanong Suksaweang, and Dr. Theeraya Simawaranon for giving their time to serve on my thesis committee, and for unconditional help, suggestion, support, kindness, and advice on the conduction of this work. This thesis has been finished under their suggestion.

I am most grateful to all members of Dr. Kanyarat's laboratory both past and present who helped and shared the experiences and also for their cheering and friendship. I would like to thank all of lecturers at Translational Medicine Program, Institute of Medicine, and Suranaree University of Technology, who I was introduced to the field of Translational Medicine and for the opportunity to undertake an M.Sc.

Special thanks to Chao Phraya Aphaiphubet Hospital, Translational Medicine's laboratory, Institute of Medicine, Suranaree University of Technology for the laboratory facilities support.

Finally. I would like to thank my amazing family, particularly my parents for their continued love, support, guidance, and encouragement as I pursued my education at the Suranaree University of Technology.

Nopporn Naewwan

TABLE OF CONTENTS

	Page
ABSTRACT (THAI).....	I
ABSTRACT (ENGLISH).....	II
ACKNOWLEDGEMENT.....	III
TABLE OF CONTENTS.....	IV
LIST OF TABLES.....	VIII
LIST OF FIGURES.....	IX
SYMBOLS AND ABBREVIATIONS.....	XII
CHAPTER	
I INTRODUCTION.....	1
1.1 Background and problem.....	1
1.2 Research hypothesis.....	3
1.3 Ultimate objective.....	3
1.4 Specific objective.....	3
1.5 Expected benefit.....	4
II THEORY AND LITTERATURE REVIEW.....	5
2.1 SARS-CoV-2 virus.....	5
2.1.1 SARS-CoV-2 life cycle.....	13
2.1.2 Genome organization of SARS-CoV-2.....	15
2.2 Nonstructural protein 2 (NSP2).....	20
2.3 Nucleic acid amplification tests (NAATs).....	23
2.4 Isothermal amplification technology for SARS-CoV-2 diagnostic.....	27
2.5 CRISPR-Cas12a	33
2.6 Lateral flow assay (LFA).....	38

TABLE OF CONTENTS (Continued)

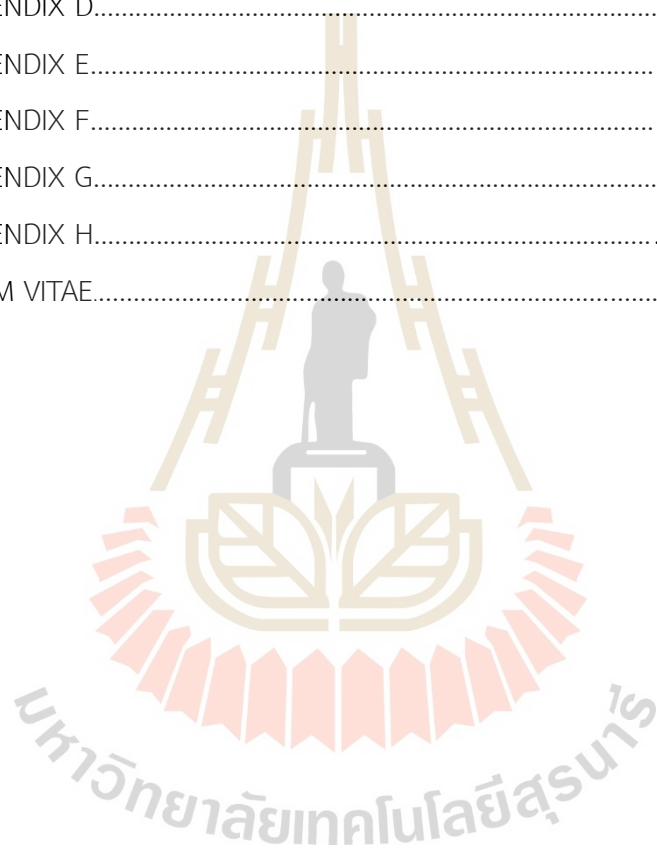
	Page	
2.7	General mechanism of CRISPR-Cas12a mediated detection of nucleic acids via LFA.....	41
III	RESEARCH METHODOLOGY.....	44
3.1	Total RNA extraction.....	44
3.2	conversion of total RNA to cDNA.....	45
3.3	Molecular PCR amplification of NSP2 sequence.....	45
	3.3.1 Primer design.....	45
	3.3.2 PCR amplification of the NSP2 sequence.....	46
	3.3.3 Agarose gel electrophoresis.....	47
3.4	Purification of NSP2 cDNA.....	47
3.5	Ligation of DNA sequence coding for NSP2 into cloning vector.....	48
3.6	Preparation of chemically competent DH5 α <i>E. coli</i>	48
3.7	Transformation and screening for DH5 α <i>E. coli</i> transformations.....	49
3.8	Extraction of the NSP2/pTG19-T plasmids.....	51
3.9	Verification of carrying recombinant plasmids with inserted DNA coding for NSP2.....	52
3.10	Production of the CRISPR-Cas12a digestion reaction.....	52
	3.10.1 LbCas12a.....	52
	3.10.2 crRNA design and synthesis.....	52
3.11	CRISPR-Cas12a digestion.....	53
3.12	Production of the lateral flow strips test based on CRISPR-Cas12a combined with RPA for SARS-CoV-2 NSP2 detection.....	54

TABLE OF CONTENTS (Continued)

	Page
3.12.1 RPA.....	54
3.12.2 RPA-CRISPR-Cas12a-reporter assay.....	56
3.12.3 Target gene detection using RPA-Cas12a and LFA.....	56
IV RESULTS.....	60
4.1 NSP2 gene PCR amplification.....	60
4.2 Cloning of the DNA amplicons coding for NSP2 into cloning vector.....	61
4.3 Extraction of NSP2/pTG19-T plasmid.....	63
4.4 Verification of DNA sequences coding for NSP2.....	64
4.5 The Cas12a can directly detect SARS-CoV-2 NSP2 in NSP2/ pTG19-T plasmid using specific crRNA.....	65
4.6 Establishment of NSP2/pTG19-T plasmid digestion by Cas12a assay for SARS-CoV-2 NSP2 detection and directly visualized the results on LFA.....	67
4.7 SARS-CoV-2detection using RPA-Cas12a and LFA.....	69
4.8 The evaluation of the diagnostic performance of the assay for the detection of SARS-CoV-2.....	72
V DISCUSSION.....	76
VI CONCLUSION AND RECOMMENDATION.....	80
REFERENCES.....	82
APPENDIX	
APPENDIX A.....	99
APPENDIX B.....	101
APPENDIX C.....	104

TABLE OF CONTENTS (Continued)

	Page
APPENDIX D.....	106
APPENDIX E.....	109
APPENDIX F.....	112
APPENDIX G.....	114
APPENDIX H.....	116
CURRICULUM VITAE.....	118



LIST OF TABLES

Table	Page
2.1	Comparison of common isothermal amplification methods.....29
3.1	RPA and PCR primer sequences for the NSP2 gene..... 46
3.2	Guide RNA sequences for the SARS-CoV-2 NSP2 detection based on CRISPR-Cas12a..... 53
4.1	The RPA-Cas12a-LFA results were consistent with the real-time PCR results with 15 of 15 samples showing NSP2 detection..... 75

LIST OF FIGURES

Figure	Page
2.1	Timeline of the key events of the COVID-19 outbreak..... 5
2.2	Classification of coronaviruses in order <i>Nidovirales</i> and taxonomy of SARS-CoV-2..... 8
2.3	World map depicting the geographical distribution of SARS-CoV-2 variants..... 9
2.4	Timeline showing the SARS-CoV-2 epidemic wave in Thailand..... 10
2.5	Anterior-posterior (AP) chest radiograph of a patient with severe COVID-19 pneumonia..... 11
2.6	Pathological presentations of COVID-19 versus multisystem inflammatory syndrome (MIS)..... 12
2.7	SARS-CoV-2 viral entry and replication cycle in virus susceptible host cells..... 14
2.8	Schematic representation of the SARS-CoV-2 viral particle..... 19
2.9	Genomic representation of SARS-CoV-2 consisting of open reading frames that encode structural, non-structural, and accessory proteins..... 19
2.10	Heat maps of conserved genomic regions of SARS-CoV-2. SARS-CoV-2 genomes are divided into ten regions and the frequency of mutations is in different regions worldwide..... 22
2.11	Detection of SARS-CoV-2 by the commonly used manual real-time RT-PCR procedure..... 26
2.12	Isothermal SARS-CoV-2 diagnostics..... 28
2.13	RPA amplification scheme..... 32
2.14	Schematic representation of the fundamental components of Cas12a..... 36

LIST OF FIGURES (Continued)

Figure	Page
2.15 Model for PAM-dependent and PAM-independent activation of cis and trans-cleavage by Cas12a.....	37
2.16 Schematic representation of a typical diagram and several components of LFA and working mechanism.....	40
2.17 Schematics of RPA-Cas12a-LFA detection.....	42
2.18 Difference of test result interpretation for use of the CRISPR-Cas12a via LFA.....	43
3.1 Schematic illustration of a SARS-CoV-2 detection-based LFA.....	59
4.1 Gel electrophoresis image of PCR amplification of SARS-CoV-2 NSP2 cDNA fragments.....	60
4.2 Gel electrophoresis image of PCR amplicons of the NSP2 sequences (~200 bp; arrow) from randomly picked transformed NSP2 plasmid transformed <i>E. coli</i>	62
4.3 Gel electrophoresis image of plasmid extraction of NSP2/pTG19-T plasmid amplicons ~3080 bp from plasmids extraction at the expected size.....	63
4.4 DNA multiple alignment of NSP2.....	64
4.5 1% Agarose gel electrophoresis showing NSP2/pTG19-T plasmid digestion by Cas12a.....	66
4.6 The LFA result interpretation of NSP2/pTG19-T plasmid digestion by Cas12a assay after 2, 5 and 15 min.....	68
4.7 Gel electrophoresis image of RPA amplification of SARS-CoV-2 NSP2 cDNA fragments.....	70
4.8 The LFA result interpretation of SARS-CoV-2 NSP2 cDNA fragment digestion by Cas12a assay after 2, 5 and 15 min.....	71

LIST OF FIGURES (Continued)

Figure	Page
4.9 Gel electrophoresis image of RPA amplicons (200 bp; arrow) of SARS-CoV-2 NSP2 cDNA fragments.....	73
4.10 The qualitative analysis results of LFA.....	74



LIST OF ABBREVIATIONS

%	Percent
°C	Degree Celsius
µg	Microgram
µL	Microliter
µM	Micromolar
AP	Anterior-posterior
bp	Base pairs
C-line	Control line
cDNA	Complementary deoxy-nucleic acid
CRISPR	Clustered regularly interspaced short palindromic repeats
crRNA	CRISPR RNA
COVID-19	Coronavirus Disease 2019
DMVs	Double-membrane vesicles
dNTP	Deoxyribonucleotide triphosphates
dsDNA	Double-stranded DNA
DW	Distilled water
E	Envelope protein
<i>E. coli</i>	<i>Escherichia coli</i>
<i>e.g.</i>	<i>Exempli gratia</i>
ER	Endoplasmic reticulum
ERGIC	Endoplasmic reticulum golgi intermediate compartment
<i>etc.</i>	<i>Et cetera</i>
FDA	Food and Drug Administration
g	Gram

LIST OF ABBREVIATIONS (Continued)

hACE2	Human angiotensin-converting enzyme 2
HCoVs	Human coronavirus
HDA	Helicase dependent amplification
kb	Kilo bases
LB	Luria-Bertani
LbCas12a	<i>Lachnospiraceae bacterium</i>
LFA	Lateral flow assay
LAMP	Loop-mediated isothermal amplification
M	Membrane protein
MDA	Multiple displacement amplification
MERS-CoV	Middle East Respiratory Syndrome Coronavirus
mg	Milligram (s)
min	Minute (s)
MIS	Multisystem inflammatory syndrome
mL	Milliliter (s)
mM	Millimolar
Mpro	Main-protease
N	Nucleocapsid protein
NAATs	Nucleic acid amplification tests
NASBA	Nucleic acid sequence based amplification
NEAR	Nicking enzyme amplification reaction
ng	Nanogram (s)
nm	Nanometer (s)
NSPs	Nonstructural protein
NTC	Negative test control
NTS	Non target DNA strands

LIST OF ABBREVIATIONS (Continued)

nt	Nucleotide
ORFs	Open reading frames
PAM	Protospacer-adjacent motif
PCR	Polymerase chain reaction
PHB1	Prohibiting
PLpro	Papain-like protease
PP	Polyproteins
PRF	Programmed ribosomal frameshifting
qRT-PCR	Quantitative reverse transcription polymerase chain reaction
RCA	Rolling circle amplification
RdRp	RNA dependent RNA polymerase
RNA	Ribonucleic acid
rnx	Reaction
RPA	Recombinases polymerase amplification
RTC	Replication and transcription complex
RT-PCR	Reverse transcription polymerase chain reaction
S	Spike protein
SARS-CoV-2	Severe Acute Respiratory Syndrome Coronavirus 2
sec	Second (s)
SMART	Signal mediated amplification of RNA technology
spp./sp.	Species / specie
STAT	Signal transducer and activator of transcription
T-line	Test line
Tm	Time of mobile phase
TMPRSS2	Transmembrane protease serine protease-2
Ts	Target DNA strands

LIST OF ABBREVIATIONS (Continued)

UDW	Ultrapure distilled water
VOCs	Variants of concern
VOIs	Variants of interest
VUMs	Variants under monitoring
WHO	World Health Organization



CHAPTER I

INTRODUCTION

1.1 Background and problem

Coronavirus Disease 2019 (COVID-19) is an acute respiratory disease caused by Severe Acute Respiratory Syndrome Coronavirus 2 (SARS-CoV-2) infection. The incubation period is 4-5 days but can be up to 14 days (Parasher, 2021). The respiratory system is the main target of SARS-CoV-2 which can progress to severe pneumonia in secondary infection and multiple organ failure (C. Huang et al., 2020). Globally, the emergence of the COVID-19 has had a significant impact on life (Onyeaka, Anumudu, Al-Sharify, Egele-Godswill, & Mbaegbu, 2021). The need for ongoing SARS-CoV-2 screening employing inexpensive and quick diagnostic approaches is becoming increasingly significant in people's daily lives, given the ongoing pandemic and variations in vaccine administration in resource-constrained regions.

Since the early stages of the pandemic, the World Health Organization (WHO) has recommended the use of quantitative real time reverse transcription polymerase chain reaction (real time RT-PCR) for nucleic acid amplification as the gold standard diagnostic for SARS-CoV-2. However, real time RT-PCR still suffers from disadvantages such as the technique is dependent on sophisticated instruments as well as well-trained personnel. It cannot meet the growing demand for rapid testing and available only in limited places (Song et al., 2021; Xiong et al., 2020; Y. Zhang, Y. Chai, et al., 2022; Y. Zhang, Z. Huang, et al., 2022). Therefore, new nucleic acid detection devices are being developed. However, because the SARS-CoV-2 is a rapidly evolving virus, the emergence of strongly infectious mutants of the new coronavirus, the need for

the specific detection of mutant strains is also increasing (Jeong, Lee, Ko, Ko, & Seo, 2022; Y. Zhang, Z. Huang, et al., 2022).

To our knowledge, hardly SARS-CoV-2 assay targeting the nonstructural protein 2 (NSP2) coding region has been used as a target for the molecular diagnosis of SARS-CoV-2 and rarely published previously due to function is not well clear (Raj, 2021; Yip et al., 2020). However, the current NSP2 assay was highly specific without cross-reaction with other common respiratory viruses and conserved regions of NSP2 successfully detected SARS-CoV-2 variant of concern RNA samples in experimental RT-PCR validations (Jeong et al., 2022; Yip et al., 2020). Therefore, NSP2 gene can be used to identify novel primer targets in SARS-CoV-2 and should be a priority strategy in the event of novel SARS-CoV-2 variants pandemic.

In the wake of a pandemic, the development of rapid, simple, and accurate molecular diagnostic tests can significantly aid in reducing the spread of infections. Recombinases polymerase amplification (RPA) has been developed as an attractive alternative to conventional PCR (Feng et al., 2021). RPA can be used to achieve DNA amplification at constant temperature, the usual optimum being 37 °C. The property of RPA reaction greatly simplifies equipment requirements and short reaction times (Lobato & O'Sullivan, 2018; Munawar, 2022; Tan et al., 2022). Unfortunately, RPA can exponentially amplify DNA rapidly to improve analytical sensitivity but is susceptible to nonspecific amplification (Feng et al., 2021). Following isothermal exponential amplification, Clustered Regularly Interspaced Short Palindromic Repeats-CRISPR associated proteins (CRISPR-Cas) based nucleic acid detection have been emerged because of their simplicity, sensitivity, specificity, and wide applicability (Talwar et al., 2021). This method is one of the nucleotide-based methods approved by the US Food and Drug Administration (FDA) for SARS-CoV-2 detection (Guglielmi, 2020). Nucleic acid detection with CRISPR-Cas12a specifically detects the amplicon of target molecules and thus improves analytical specificity (Talwar et al., 2021). Because the Cas12a recognizes the protospacer adjacent motif (PAM) site by guided CRISPR RNA

(crRNA) can be advantageous when differentiating between two sequences that are highly similar and add another layer of specificity observed in the PAM region (Talwar et al., 2021).

Nowadays, researchers across the world are working on the development of an easy-to-use rapid diagnostic method for SARS-CoV-2 detection. In this study, we present an approach for the visual detection of the NSP2 gene of SARS-CoV-2 using CRISPR-Cas12a system. By the combination of a sample processing method and the RPA technology with Cas12a-based detection, the detection time could be obtained in 50 minutes with a lateral flow strip readout. Because our assay needs minimal equipment for a visual detection of SARS-CoV-2, its application may be an alternative way of SARS-CoV-2 diagnosis.

1.2 Research hypothesis

This study presents results as proof of concept by using NSP2 gene as a target to detect for develop The lateral flow strips test based on NSP2-CRISPR-Cas12a combined with RPA could be used to detect SARS-CoV-2 with high sensitivity and specificity.

1.3 Ultimate objective

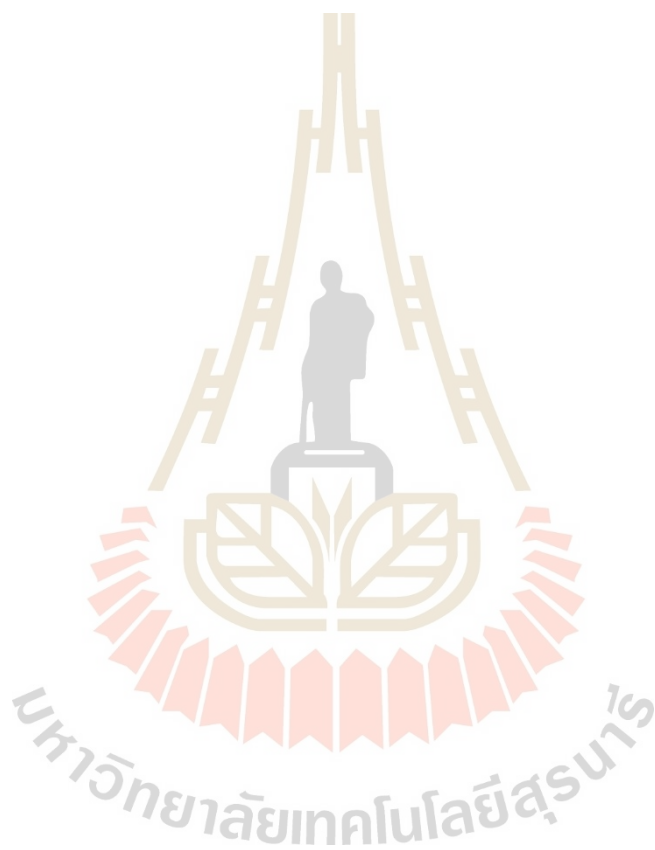
To develop NSP2-CRISPR-Cas12a based lateral flow strip for SARS-CoV-2 detection.

1.4 Specific objectives

- 1.4.1 To extract the RNA of SARS-CoV-2.
- 1.4.2 To produce recombinant NSP2 plasmid of SARS-CoV-2.
- 1.4.3 To design crRNA that is specific to NSP2 gene.
- 1.4.4 To detect SARS-CoV-2 and evaluate COVID-19 detection based on CRISPR-Cas12a.

1.5 Expected Benefits

This approach could be adapted for emerging mutations and implemented in laboratories already conducting SARS-CoV-2 nucleic acid amplification tests using existing resources and extracted nucleic acid.



CHAPTER II

THEORY AND LITERATURE REVIEW

2.1 SARS-CoV-2 virus

Severe acute respiratory syndrome coronavirus 2 (SARS-CoV-2) is a highly transmissible and pathogenic coronavirus. The pandemic of acute respiratory disease, named “Coronavirus disease 2019” (COVID-19) emerged in late 2019, which threatens human health and public safety (B. Hu, Guo, Zhou, & Shi, 2021). The first recorded cases were reported in December 2019 in Wuhan, China (Figure 2.1). Over the course of the following 10 months, more than 30 million cases have been confirmed worldwide (B. Hu et al., 2021). According to the WHO, globally there have been 761,769,759 confirmed cases of COVID-19 including 6,784,181 deaths across 240 nations of the world as of 20 September 2023.

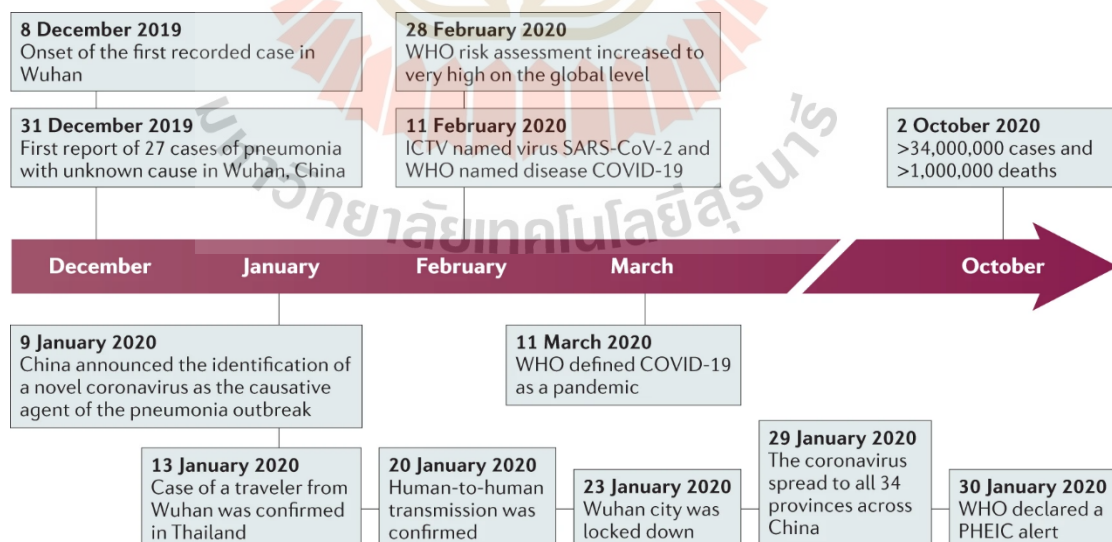


Figure 2.1 Timeline of the key events of the COVID-19 outbreak (B. Hu et al., 2021).

Human *Coronaviruses* (HCoVs) are a diverse group of viruses infecting many different animals, and they can cause diseases in humans and vertebrates (Y. Chen, Liu, & Guo, 2020). Before 2019, there were only six CoVs including HCoV-229E, HCoV-OC43, HCoV-NL63, HKU1, severe acute respiratory syndrome (SARS-CoV), and Middle East respiratory syndrome (MERS-CoV). HCoV-229E, HCoV-OC43, HCoV-NL63, HKU1 were known to infect human but do not cause severe symptoms in humans (Casella, Rajnik, Aleem, Dulebohn, & Di Napoli, 2023; Liu, Liang, & Fung, 2021), while SARS-CoV and MERS-CoV are zoonotic in origin and can infect lower respiratory tract and cause severe respiratory disease in humans (Cui, Li, & Shi, 2019). A CoVs have been reported since 2002, including SARS-CoV, MERS-CoV, and later in 2019 was identified as SARS-CoV-2 (Sharma, Ahmad Farouk, & Lal, 2021). SARS-CoV-2 is the seventh reported Coronavirus that has infected people after HCoV-229E, HCoV-OC43, HCoV-NL63, HKU1, MERS-CoV, SARS-CoV (Cui et al., 2019; N. Zhu et al., 2020). SARS-CoV-2 taxonomically belongs to the *Coronavirinae* subfamily of the family *Coronaviridae* and fall under the order *Nidoviridae*, *Betacoronavirus* genus and its genome sequence is similar to SARS-CoV and MERS-CoV that was shared 50% with MERS-CoV and 79% genome sequence identity with SARS-CoV (Arya et al., 2021; Liu et al., 2021; Lu et al., 2020; Saberiyan et al., 2022) (**Figure 2.2**). SARS-CoV-2 has become a major public health concern after the outbreak of MERS-CoV and SARS-CoV in 2002 and 2012, respectively. SARS-CoV-2 is an enveloped, positive-sense single-stranded genomic RNA virus. SARS-CoV-2 is contagious in humans and it has rapidly spread through close human interactions or the spilled respiratory droplets such as cough and sneeze of the infected people (Ochani et al., 2021). Since the covid-19 pandemic, the number of confirmed infections has risen to more than 700 million worldwide, with nearly 6 million deaths. Moreover, SARS-CoV-2 has continuously evolved with many variants emerging across the world. These variants are classified from variants of SARS-CoV-2 including variant of interest (VOI), variant of concern (VOC), and variant under monitoring (VUM) (Choi & Smith, 2021; Saberiyan et al., 2022). The emerging

Alpha (B.1.1.7), Beta (B.1.351), Gamma (P.1), Delta (B.1.617.2) and Omicron (B.1.1.529) first reported in the United Kingdom, South Africa, Brazil, India and South Africa respectively (Casella, Rajnik, Aleem, Dulebohn, & Di Napoli, 2022; W. Jiang et al., 2022; Y. Jiang, Wu, Song, & You, 2021). These variants were classified as VOCs which were associated with the increase in transmissibility or more severe disease and reduced effectiveness of treatments or vaccines, or diagnostic detection failures (Choi & Smith, 2021). Genotype B.1.1.7 is predominant worldwide. The distribution area of genotype B.1.1.7 is in the United Kingdom, USA, and many European countries in the second quarter of 2021 (Casella et al., 2023; Chadha, Khullar, & Mittal, 2022; Saberiyan et al., 2022). Genotype P.1 is predominantly distributed in the USA, Brazil, and Italy and commonly in 45 other countries. Genotypes B.1.351 was predominantly distributed and first detected in August 2020 in South Africa. The state of Maharashtra, India is the predominant area of the genotype B.1.617. The genotype B.1.1.529 was mostly found in South Africa in November 2021 (Casella et al., 2023; Chadha et al., 2022) (**Figure 2.3**). According to the viral zone, globally there have been VOCs of COVID-19 including Omicron, Alpha, Beta, Delta, Epsilon, Eta, Gamma, Iota, Kappa, Lambda, Theta, and Zeta as of 7 August 2023. As of September 1, 2023, four VOIs (BQ.1 (BA.5 descendent), BA.2.75 (BA.2 descendent), XBB (BA.2.10.1 / BA.2.75 descendent) and XBB.1.5 (BA.2.10.1 / BA.2.75 descendent) new VOI) and also six VUMs (BF.7 (BA.5 descendent), BA.2.3.20 (BA.2 descendent), CH.1.1 (BA.2.75 descendent), BN.1 (BA.2.75 descendent), XBC (Delta (21I) / BA.2 recombinant) and XAY (Delta (AY.45) / BA.2 recombinant)) have been designated by the WHO. For Thailand, genotype A.6, B.1.36.16, B.1.1.7, B.1.617.2, and B.1.1.529 predominated in the first, second, third, fourth, and fifth epidemic wave respectively. These genotypes are widely distributed throughout the country. There have been approximately 3.4 million reported cases of COVID-19 and over 24,000 deaths in Thailand (Puenpa et al., 2023) (**Figure 2.4**). As compared with MERS-CoV and SARS-CoV, SARS-CoV-2 is spreading faster and the number of deaths is multifold higher (N. Zhu et al., 2020). SARS-CoV-2 infected

patients usually present with severe viral pneumonia (Mohamadian et al., 2021) (Figure 2.5). Also with the complications associated with COVID-19 infection on respiratory, cardiovascular, neurological, and metabolic system of recovered COVID-19 patients (Davis, McCorkell, Vogel, & Topol, 2023; Fraser, Orta-Resendiz, Dockrell, Müller-Trutwin, & Mazein, 2023; Su et al., 2023; Z. Yan, Yang, & Lai, 2021) (Figure 2.6).

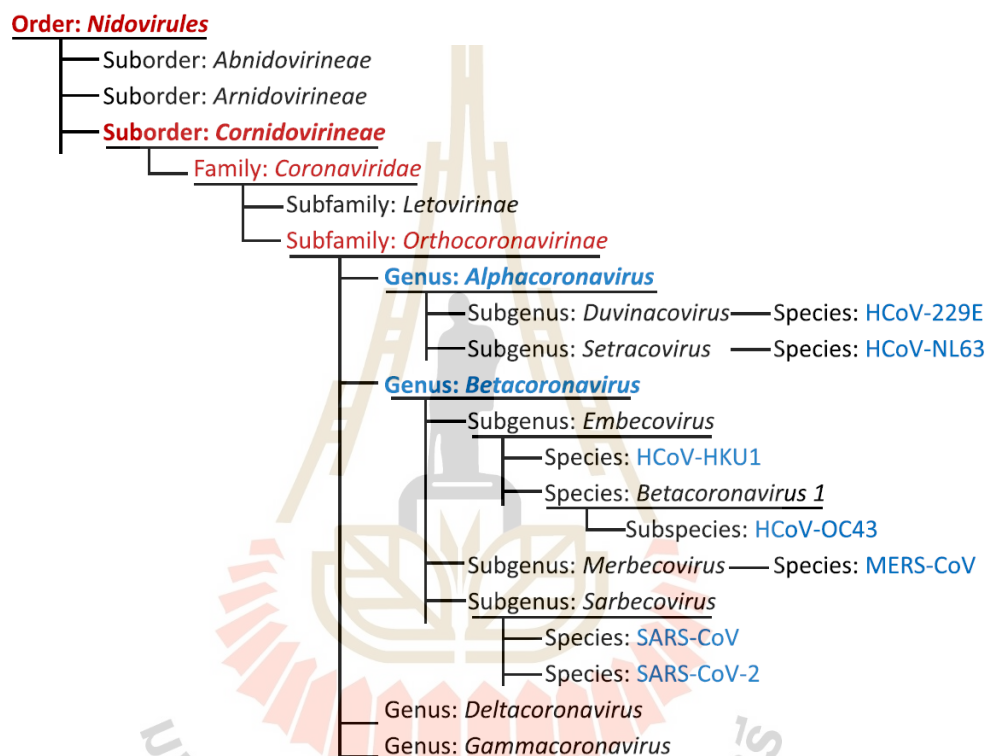


Figure 2.2 Classification of coronaviruses in order *Nidovirales* and taxonomy of SARS-CoV-2 (Liu et al., 2021).

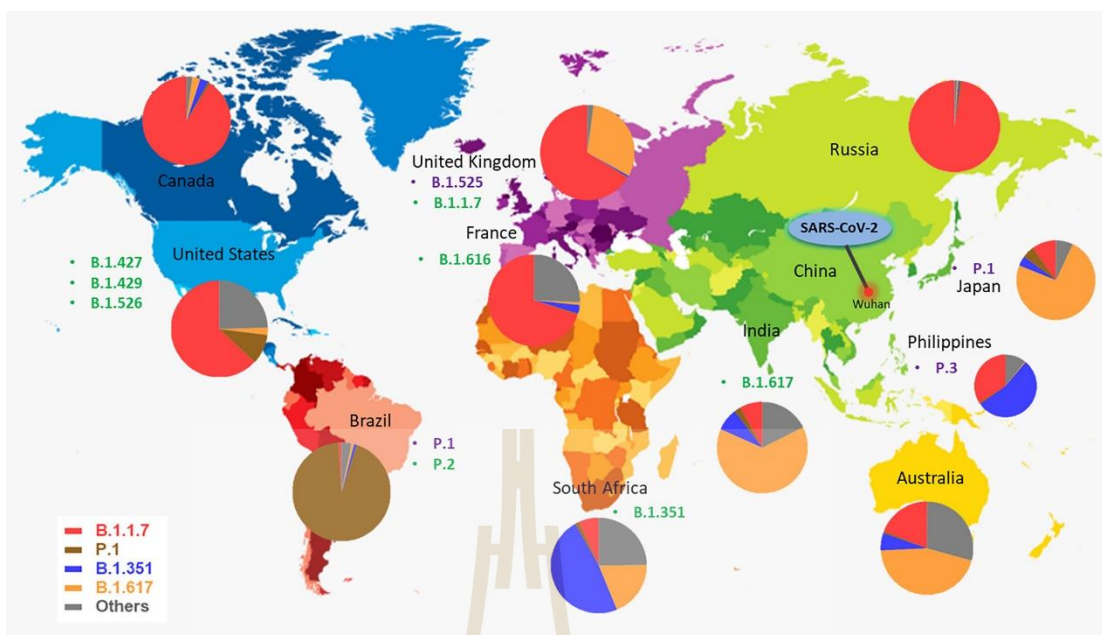


Figure 2.3 World map depicting the geographical distribution of SARS-CoV-2 variants (Chadha et al., 2022).

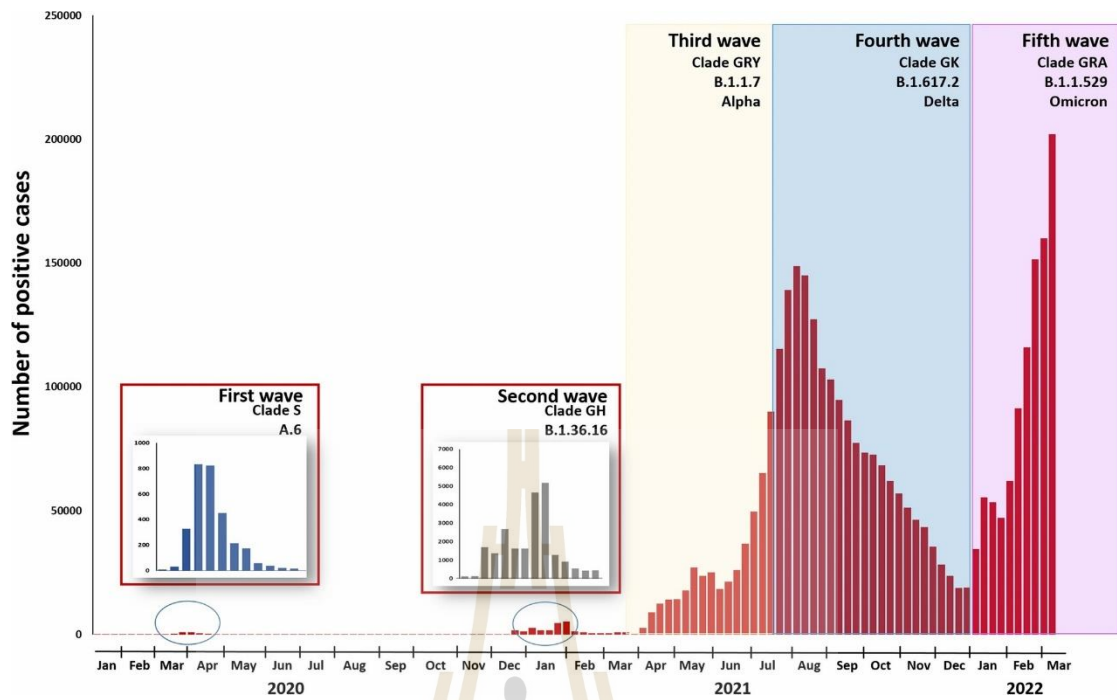


Figure 2.4 Timeline showing the SARS-CoV-2 epidemic wave in Thailand, 2020-2022 (Puenpa et al., 2023).

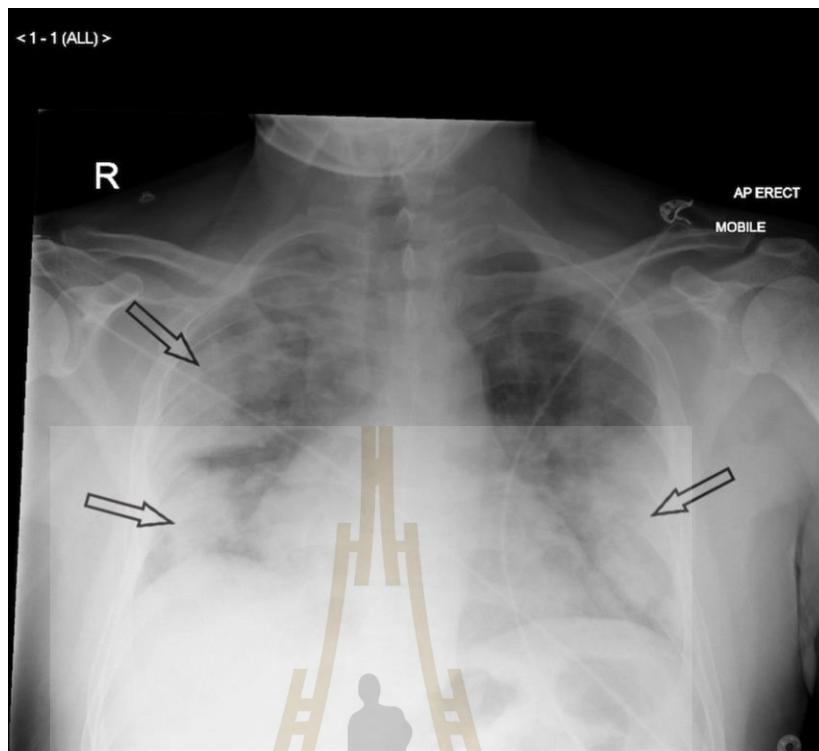


Figure 2.5 Anterior-posterior (AP) chest radiograph of a patient with severe COVID-19 pneumonia, showing bilateral dense peripheral consolidation and loss of lung markings in the mid and lower zones (outlined arrows) (Cleverley, Piper, & Jones, 2020).

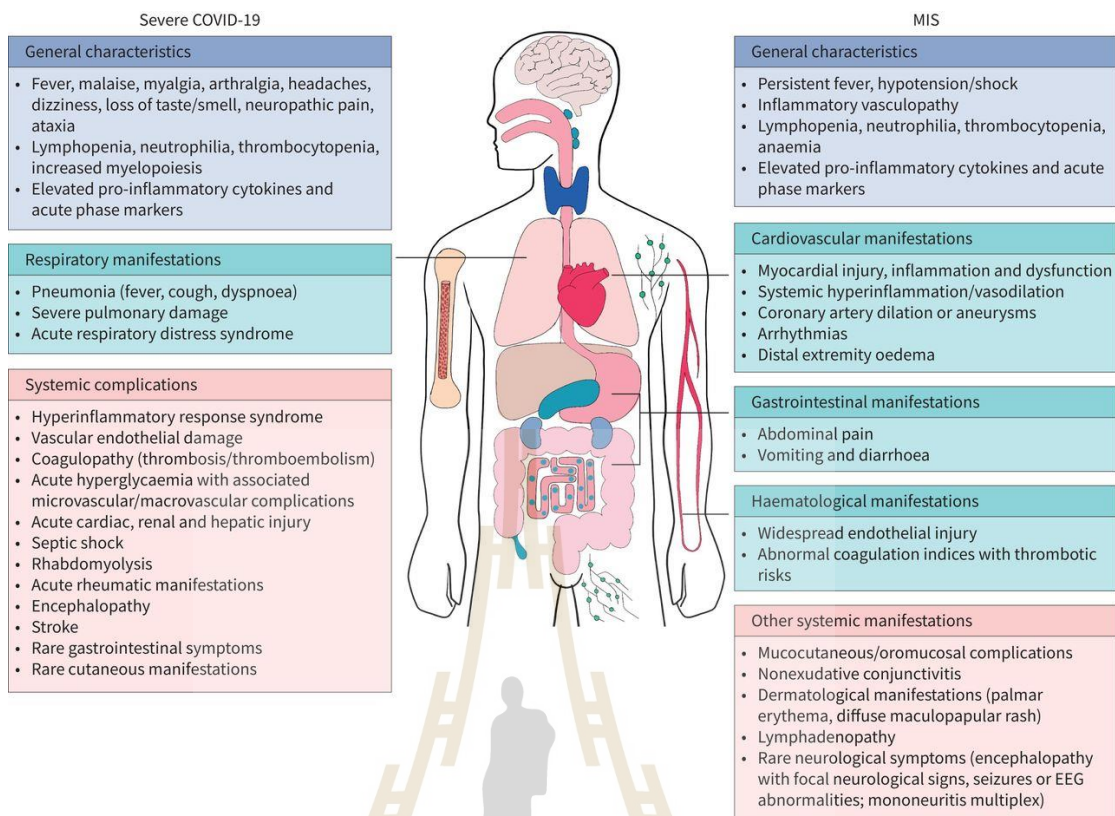


Figure 2.6 Pathological presentations of COVID-19 versus multisystem inflammatory syndrome (MIS) (Fraser et al., 2023).

2.1.1 SARS-CoV-2 life cycle

SARS-CoV-2 is transmitted through direct contact via respiratory materials (cough or sneeze), aerosol droplets, and fomite transmission during the incubation period (J. Y. Li et al., 2020; Ochani et al., 2021; Wölfel et al., 2020; P. Zhou et al., 2020). The SARS-CoV-2 mainly infects lymphatic epithelial cells and type II pneumocytes with the initiation of the human body's innate response by producing interferons (IFNs). However, IFNs activate expression of human angiotensin-converting enzyme 2 (hACE2) which acts as a receptor for virus attachment to host cells (W. Yan, Zheng, Zeng, He, & Cheng, 2022). Upon the SARS-CoV-2 entering the body, the host cell machinery is hijacked to facilitate viral replication and translation of essential proteins. Ultimately, new virion are assembled and released. The life cycle of the SARS-CoV-2 virus infection into the susceptible host cell can be divided into several key steps including (a) attachment and cell entry, (b) transcription of viral replicase, (c) genomic transcription and replication, (d) translation of structural proteins, and (e) virion assembly and release (Machhi et al., 2020). The SARS-CoV-2 infection requires the binding of the S protein to the hACE2 followed by the cleavage of the S2 subunit by transmembrane protease serine protease-2 (TMPRSS-2). Finally, SARS-CoV-2 enters its host cell by endocytosis.

Entry in the cell cytoplasm may occur in two ways: the viral particle is endocytosed before fusing with the endosomal membrane (late pathway), or the viral membrane fuses with the cell membrane at the cell surface (early pathway). Following entry, Two large open reading frames (ORFs), ORF1a and ORF1b, are immediately translated in polyproteins (pp1a and pp1ab). The resulting polyproteins are processed into the individual non-structural proteins (NSPs) that form the viral replication and transcription complex (RTC). The biogenesis of viral genomic RNA replication occurs in protective double-membrane vesicles (DMVs). Transcription and translation of the negative template result in the formation of structural proteins that are inserted into the endoplasmic reticulum (ER) membrane and transit through the ER-to-Golgi intermediate compartment (ERGIC). Here, condensates of newly produced genomic RNA and N proteins interact with E and M proteins resulting in assembly of viral particles. Virions are secreted from the infected cell by exocytosis in two ways:

through the classical exocytosis pathway via the Golgi compartment or through the incorporation in deacidified lysosomes that fuse with the cellular surface membrane (Maison, Deng, & Gerschenson, 2023; Pizzato et al., 2022) (Figure 2.7).

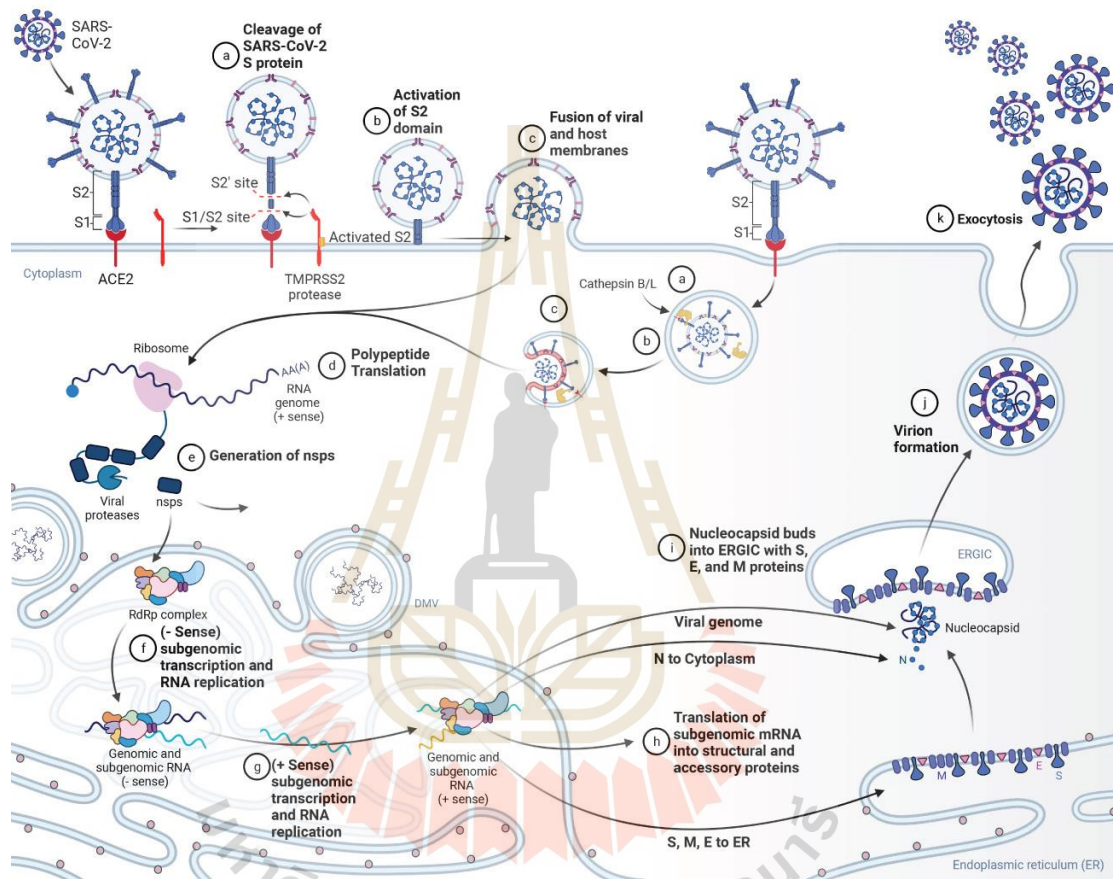


Figure 2.7 SARS-CoV-2 viral entry and replication cycle in virus susceptible host cells (Maison et al., 2023).

2.1.2 Genome organization of SARS-CoV-2

The genome of SARS-CoV-2 is a positive sense single-stranded RNA (ssRNA), which has an approximate length of 29.9 kilobases (kb) packed in the protein envelope (Brant, Tian, Majerciak, Yang, & Zheng, 2021; Kadam, Sukhrmani, Bishnoi, Pable, & Barvkar, 2021; Kandwal & Fayne, 2023; Y. Zhou, Zhang, Xie, & Wu, 2022). The genome contains coding sequence for four structural proteins, 11 accessory proteins, and 16 NSPs. The genomic RNA consists of 5'-end and 3'-poly-A tail structure. From 5'-end to 3'-end, the genome is organized as 5' end structure, 5' -end, ORF1ab, spike protein (S), ORF3a-d, envelope protein (E), membrane protein (M), ORF6, ORF7a-b, ORF8, ORF9b-c, nucleocapsid protein (N), ORF10, 3' -end, and 3'-poly-A tail. In SARS-CoV-2, ORF1a is the longest ORF and occupies almost two-thirds portion of the genome and also ORF1b overlaps with ORF1a. ORF1a and ORF1b, are immediately translated in polyproteins (pp1a and pp1ab) through a -1 programmed ribosomal frameshifting (PRF) that are processed by viral proteases (papain-like protease (PLpro) and main-protease (Mpro) to produce nonstructural proteins (NSPs) (Arya et al., 2021; Maison et al., 2023). The 16 NSPs are identified numerically as NSP1-16. The pp1a protein encoded by ORF1a is proteolytically cleaved into 11 mature non-structural proteins (NSP1-11). The pp1ab protein expressed by ORF1ab is processed into 15 NSPs (NSP1-10 and NSP12-16) (Tam, Lorenzo-Leal, Hernández, & Bach, 2023; A. Wu et al., 2020; F. Wu et al., 2020). A structure near the junction of ORF1a and ORF1b causes PRF which in turn leads to the production of another, longer polyprotein, pp1ab, wherein the short nsp11 is replaced by the RNA-dependent RNA polymerase (RdRp) nsp12 and is followed by nsp13 to -16 (Kung et al., 2022). The four structural proteins are S, E, M, and N (**Figure 2.8**). The structural proteins and the genome form an enveloped virion able to infect cells. The 11 accessory proteins are ORF3a-d, ORF6, ORF7a and b, ORF8, ORF9b and c, and ORF10, and serve various functions from host interaction to immune modulation (Bai, Zhong, & Gao, 2022; Maison et al., 2023) (**Figure 2.9**).

NSP1 is closely associated with the viral infection cycle and host translation regulation (W. Yan et al., 2022). It plays a key role in accelerates mRNA degradation,

inhibiting host translation and blocks innate immune responses (C. Bai et al., 2022; Maison et al., 2023; V'Kovski, Kratzel, Steiner, Stalder, & Thiel, 2021).

NSP2 is an endosome-associated protein and interacts with prohibiting 1 (PHB1) and PHB2 (W. Yan et al., 2022). It plays a key role in modifying the host's environment suitable for viral needs and related to the reduction of IFN β and NF- κ B expression found in human pulmonary cells (Anjum et al., 2022; Lacasse et al., 2023; Maison et al., 2023).

NSP3 is an interferon antagonist and double-membrane vesicle (DMV) formation (V'Kovski et al., 2021). It plays a key role in the viral binds to host proteins and mediates viral replication (C. Bai et al., 2022).

NSP4 is transmembrane domains. It plays a key role in the anchors replication transcription complex to ER and mediates the interaction with cellular membranes (C. Bai et al., 2022; Maison et al., 2023; Raj, 2021).

NSP5 is the main protease with viral polyprotein processing activity. It plays a key role in inhibiting interferon signaling (C. Bai et al., 2022; V'Kovski et al., 2021).

NSP6 is a major contributor to SARS-CoV-2 replication. It plays a key role in the induction of host restricts autophagolysosome expansion and host antiviral defenses (C. Bai et al., 2022; Bills, Xie, & Shi, 2023; Maison et al., 2023).

NSP7 and NSP8 play a key role in cofactors of the RTC, as they interact and regulate the activity of RNA-dependent RNA polymerase and other NSPs (C. Bai et al., 2022; Courouble et al., 2021; V'Kovski et al., 2021).

NSP9 is nucleic acid-binding of single-stranded RNA protein (C. Bai et al., 2022; Maison et al., 2023; V'Kovski et al., 2021). It plays a key role in the modulation of host cells during SARS-CoV-2 infection (Makiyama et al., 2022).

NSP10 interacts with NSP14 and NSP16. It plays a key role in viral mRNA methylation and regulates the function of viral replicase (C. Bai et al., 2022; Maison et al., 2023; V'Kovski et al., 2021).

NSP11 is unknowns function (C. Bai et al., 2022; Maison et al., 2023; V'Kovski et al., 2021; Yadav et al., 2021).

NSP12 is RNA-dependent RNA polymerase. It plays a key role in the viral replication step and catalyzes the synthesis of viral RNA and Inhibit nuclear

translocation of interferon regulatory factor 3 (IRF3) (C. Bai et al., 2022; Maison et al., 2023; Rashid et al., 2022; V'Kovski et al., 2021).

NSP13 interacts with nsp8 and nsp12 and regulates helicase activity (C. Bai et al., 2022). It plays a key role in antagonizing IFN-I signaling by inhibiting signal transducer and activator of transcription (STAT1 and STAT2) phosphorylation (Rashid et al., 2022)

NSP14 plays a key role in decreasing the incidence of mismatched nucleotides (C. Bai et al., 2022).

NSP15 is endoribonuclease. It plays a key role in the evasion of immune response and degrades viral RNA (C. Bai et al., 2022; Maison et al., 2023; V'Kovski et al., 2021).

NSP16 plays a key role in evading innate immunity (C. Bai et al., 2022).

Spike protein is large and multifunctional. It lies in a trimmer on the virion surface and gives the virion a corona or crown-like appearance. It plays a key role in the entry of infectious virion particles into the cell through interaction with various host cellular receptors (Chakravarti et al., 2021).

ORF3a is a viroporin that interferes with ion channel activities in host plasma and endomembrane that exerts its effect on the viral life cycle (J. Zhang et al., 2022). It plays a multifunctional role in importance role in induces apoptosis, pathogenicity and virus release, mediates activation of inflammasome and induces cellular innate and pro-inflammatory immune responses, and suppresses IFN β production (C. Bai et al., 2022; Zandi et al., 2022; J. Zhang et al., 2022).

ORF3b is a potent interferon antagonist. It plays a key role in suppressing the induction of type I interferon (Konno et al., 2020; Zandi et al., 2022).

ORF3c is a protein encoded by an alternative open reading frame within the ORF3a gene. It plays a key role in increased reactive oxygen species (ROS) production and blocks the normal autophagy degradation process and leading to autolysosome accumulation (Mozzi et al., 2023).

ORF3d has been reported to be potent interferon antagonists that may play a role in immune evasion (Hachim et al., 2022).

Envelope protein is the most enigmatic and smallest of the major structural proteins. It plays a multifunctional role in encapsulating the RNA genome, pathogenesis, assembly, and release of the virus (Chakravarti et al., 2021; Dhama et al., 2020).

Membrane protein is the central organizer of coronavirus assembly. It is the most abundant viral protein present in the virion particle and gives a definite shape to the viral envelope (C. Bai et al., 2022).

ORF6 plays a key role in disrupting nucleocytoplasmic trafficking to advance viral replication and activate the NF- κ B pathway (Miyamoto et al., 2022; Nishitsuji, Iwahori, Ohmori, Shimotohno, & Murata, 2022).

ORF7a and ORF7b play a key role related to virus-host interaction and activate the NF- κ B pathway and blocking IFN α signaling and suppressing IFN β by infecting host cells (C. Bai et al., 2022; Nishitsuji et al., 2022; Zandi et al., 2022).

ORF8 is unique among these accessory proteins. It's a rapidly evolving accessory protein that has been proposed to interfere with immune responses (Flower et al., 2021; Vinjamuri, Li, & Bouvier, 2022).

ORF9b and ORF9c play a key role in inhibited types I and III IFN production and NF- κ B activation and facilitate viral replication and suppress antiviral responses in cells (Dominguez Andres et al., 2020; Gao et al., 2022; Han et al., 2021; Zandi, 2022).

Nucleocapsid protein is multipurpose. The multipurpose not only participates in viral replication and assembly but also interferes with the interferon pathway of the host. It plays a role in complex formation with the viral genome, encasing the viral RNA into ribonucleocapsid (RNP), facilitating M protein interaction needed during virion assembly, and enhancing the transcription efficiency of the viral genomic replication (Chakravarti et al., 2021; Dhama et al., 2020; W. Yan et al., 2022).

ORF10 plays a key role in the viral replication and immune evasion processes (Zandi, 2022).

As mentioned above, all of the SARS-CoV-2 proteins have their own functions which are pivotal for the viral life cycle. Many of these structures are also useful as a target for the structure-based drug design against COVID-19 (Arya et al., 2021). Furthermore, several conserved regions in the SARS-CoV-2 genome including S, N, E,

or RdRp protein are usually selected as the standard targets for the design of primers for COVID-19 diagnoses (D. Li, Zhang, & Li, 2020; van Kasteren et al., 2020; Y. Zhou et al., 2022). However, these proteins are high rate recurrent and high-frequency mutations. The rapidly evolving characteristic of SARS-CoV-2 could result in low diagnostic sensitivity (Abbasian et al., 2023; Hassan et al., 2022; Omotoso, Olugbami, & Gbadegesin, 2021; Periwal et al., 2022).

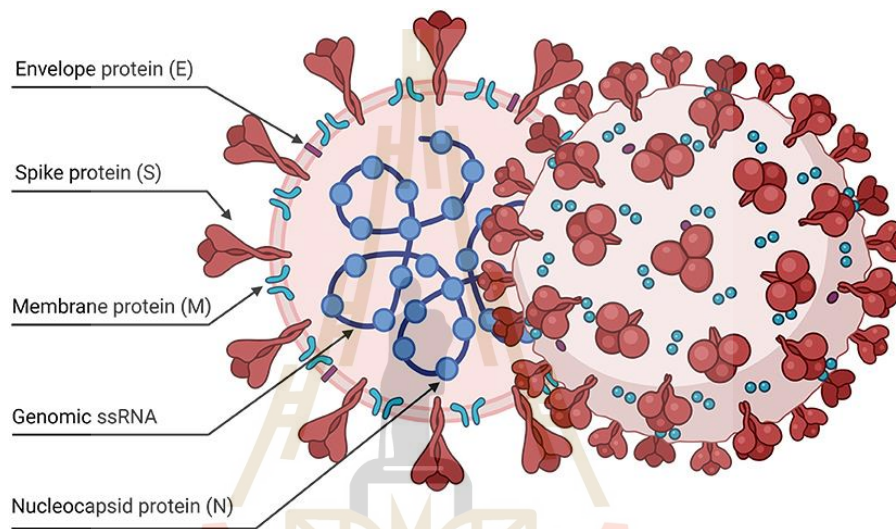


Figure 2.8 Schematic representation of the SARS-CoV-2 viral particle (Pizzato et al., 2022).

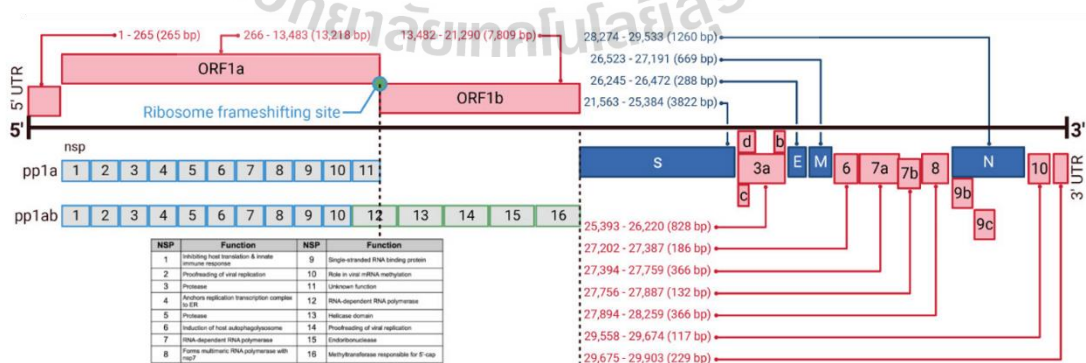


Figure 2.9 Genomic representation of SARS-CoV-2 consisting of open reading frames that encode structural, non-structural, and accessory proteins. (Maison et al., 2023).

2.2 Nonstructural protein 2 (NSP2)

Since SARS-CoV-2 is a rapidly mutated virus, emerging variants harboring nucleotide changes in the primer-binding sites might evade detection, resulting in low diagnostic sensitivity. The rapidly evolving characteristic of SARS-CoV-2 could result in a false negative diagnosis (Jeong et al., 2022). Choosing conserved target genes was a crucial factor for the design of optimal primers. The optimization of laboratory test protocols was important for effective detection (D. Li et al., 2020).

To our knowledge, NSP2 gene is rarely used as a target for the molecular diagnosis of SARS-CoV-2. However, the SARS-CoV-2 NSP2 is a very conserved protein (Zhao, Zhai, & Zhou, 2020). Development of a novel, genome subtraction-derived, SARS-CoV-2 specific covid-19-NSP2 real-time RT-PCR assay and its evaluation using clinical specimens reported that the new COVID-19-NSP2 assay was highly specific without cross-reaction and did not amplify with other human-pathogenic coronaviruses and common respiratory viruses. Further, terms of cycle threshold (Cv) values were satisfactory, with the total imprecision (% CV) values well below 5% and this assay showed 100% concordance using 59 clinical specimens from 14 confirmed cases with COVID-19-RdRp/Hel reference assay. The diagnostic sensitivity and specificity of the NSP2 assay were 100% in comparison with the COVID-19-RNA-dependent RNA polymerase (RdRp)/helicase (Hel) assay (Yip et al., 2020). Yip et al. reported that the specificity of multiplex PCR (mPCR) could be improved by selecting NSP2 which led to the development of the COVID-19-NSP2 assay (Qasem, Shaw, Elkamel, & Naser, 2021; Yip et al., 2020).

The current NSP2 was highly conserved, Jeong et al. reported that the identification of conserved regions from 230,163 SARS-CoV-2 genomes and their use in diagnostic PCR primer design, primer sets targeting the NSP2 was picked that exhibited > 99.9% in silico amplification coverage against the 230,163 genomes when a 5% mismatch between the primers and target was allowed. The primer sets successfully detected nine SARS-CoV-2 VOC RNA samples in experimental RT-qPCR validations (Jeong et al., 2022). Moreover, Abbasian et al. reported that the global landscape of SARS-CoV-2 mutations and conserved regions revealed a NSP2 is a

conserved region in the SARS-CoV-2 genome from 10,287,271 SARS-CoV-2 genome sequence (**Figure 2.10**) (Abbasian et al., 2023). This is a distinct advantage in clinical laboratories, as results can facilitate the sensitivity and specificity of suspected COVID-19 cases and guide infection control.

Since SARS-CoV-2 genome sequences change due to mutation and recombination, novel mutations on the primer binding sites will cause the failure of PCR (Abbasian et al., 2023; D. Li et al., 2020). Therefore, these primers need to be updated and evaluated regularly to ensure that the rapidly evolving genome primers can be amplified. NSP2 may play important roles in SARS-CoV-2 infection and serve as a potential gene target for identifying conserved regions from SARS-CoV-2 genomes and their use in diagnostic primer design development and may offer accurate high-throughput diagnosis during pandemics. Further, detecting hot spot mutations and conserved regions could be applied to improve the SARS-CoV-2 diagnostic efficiency

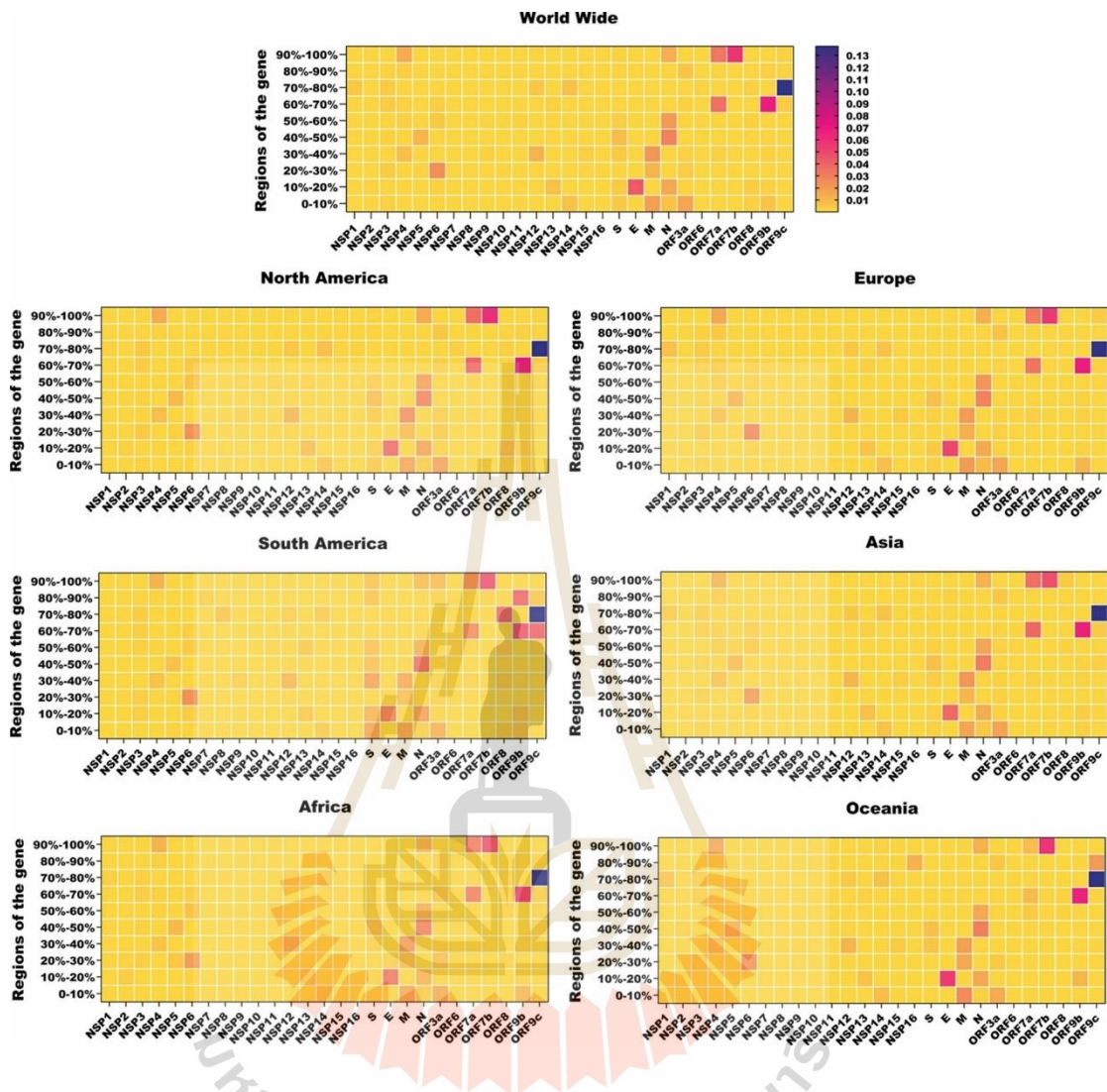


Figure 2.10 Heat maps of conserved genomic regions of SARS-CoV-2. SARS-CoV-2 genomes are divided into ten regions, and the frequency of mutations is in different regions worldwide (Abbasian et al., 2023).

2.3 Nucleic acid amplification tests (NAATs)

A nucleic acid amplification test, or NAATs, is a type of viral diagnostic test for SARS-CoV-2. NAATs for SARS-CoV-2 specifically identify the RNA sequences that comprise the genetic material of the virus. NAATs deliver highly sensitive detection of extremely low-concentrated pathogens in the early stage of diseases, especially newly emerging and re-emerging infectious outbreaks. NAATs are the primary method of diagnosing COVID-19. Since the early stages of the pandemic, the current gold standard for diagnosing COVID-19 is the quantitative real-time reverse transcription-polymerase chain reaction (real-time RT-PCR) among other diagnostic methods for monitoring clinical samples for the presence of the virus (Figuerola et al., 2021; Guo, Ge, & Guo, 2022; Teymouri et al., 2021). Hence, real-time RT-PCR has been deemed to be the gold standard for COVID-19 diagnosis, because it has already been shown to be very sensitive for accurately detecting the viral genome, able to detect a single copy of the viral RNA (Y. Zhou et al., 2022). This method is highly specific with a specificity of almost 100 % (Tahamtan & Ardebili, 2020). This method involves the formation of complementary DNA (cDNA) from SARS-CoV-2 RNA through reverse transcription and subsequent amplification of specific cDNA regions (Udugama et al., 2020). The RT-real time PCR procedure for SARS-CoV-2-infected samples comprises four steps: (a) specimen collection and processing of samples taken from suspected individuals usually through nasopharyngeal swabs from the infected patients; (b) RNA extraction from the isolated sample; (c) cDNA synthesis by reverse transcriptase technique; (d) amplification using target specific primers and detection using real-time RT-PCR method (Chavda et al., 2023; Kabir et al., 2021; Naranbat et al., 2022) (**Figure 2.11**). In the context of the current pandemic caused by the novel coronavirus, molecular detection is not limited to the clinical laboratory but also faces the challenge of the complex and variable real-time detection fields. Unfortunately, routine diagnosis by real-time RT-PCR is still a limitation for many laboratories, especially in developing countries where the cost of a real-time RT-PCR device. This method demands professional skilled personnel and is associated with a high cost of instruments and reagents like primers, probes, and real-time RT-PCR master mix are

even higher than in developing countries due to the importation fees and a laboratory setup with a biosafety level 2 cabinet (Dutta et al., 2022). Despite being regarded as the most reliable technique for virus detection, RT-real time PCR targeting SARS-CoV-2 has several challenges, especially in terms of primer design that necessitate improvements in the way the method is used. Primers are designed to amplify the target regions of the SARS-CoV-2 genome. The novel coronaviruses are RNA viruses and once mutations and recombination occur primers will not be able to effectively amplify the viral sequences. Thus, mutations and recombination can reduce the specificity of the RT-real time PCR (Dramé et al., 2020; D. Li et al., 2020). The current worldwide high demand for reagents supplies and equipment, but the few supplier companies mostly located at high income countries (Dutta et al., 2022; Figueroa et al., 2021; Guo et al., 2022). Moreover, false negative and false positive results have always been a concern for nucleic acid testing. Although the sensitivity and specificity of current detection methods such as real time RT-PCR have almost reached approximately 100% in diagnosing COVID-19, cases of false negatives and positives are continuously reported (Dutta et al., 2022; Y. Zhu, Zhang, Jie, & Tao, 2022). Technically, the RT-real time PCR procedure for SARS-CoV-2-infected samples consists of several steps and needs laboratory equipment making the process time-consuming and difficult to conduct outside the laboratory setting and it cannot meet the growing demand for rapid testing (Talwar et al., 2021; Teymouri et al., 2021). Moreover, this technique requires skilled personnel and specialized equipment (Khan et al., 2020; Y. Zhu et al., 2022).

Currently, rapid RT-PCR is designed to deliver sample-to-result within an hour (Dong et al., 2021). Emergency approval was given both by WHO and the United States Food and Drug Administration (US FDA) for use of Xpert assay platform for COVID-19 testing which is a closed nature platform, requires minimum sample handling, poses minimum biosafety hazard and has less turnaround time (Nitika Dhuria, 2023). Rapid RT-PCR assay delivers results in a relatively short turnaround time of a maximum of 45 min. The test also integrates sample preparation, nucleic acid extraction, RT-PCR amplification, and sequence detection (S. H. Kim & AlMutawa, 2022). However, there are several limitations, such as the results of rapid RT-PCR

assay may lead to a high number of false positives thus affecting its specificity. False-positive results can also the patient must undergo an unnecessary period of self-isolation (Cradic et al., 2020). The cost per test is relatively higher (Nitika Dhuria, 2023). The test has a low throughput rate compared to the lab developed test, which can load hundreds of samples at once. It also costs expensive per kit (S. H. Kim & AlMutawa, 2022). The ideal performance of the SARS-CoV-2 detection test is determined based on its accuracy and examination time. However, accurate results from testing for SARS-CoV-2 are more critical than fast testing times.



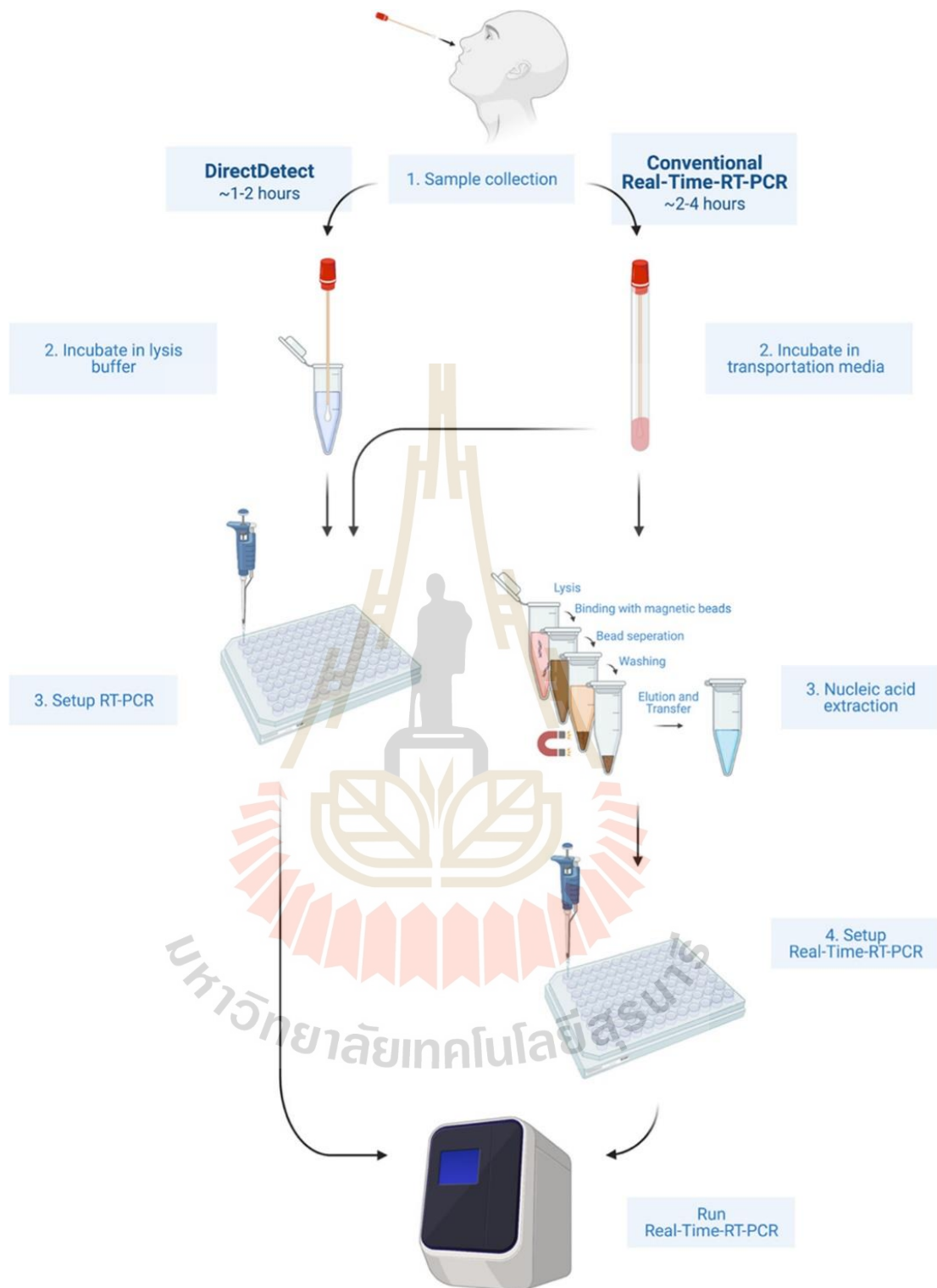


Figure 2.11 Detection of SARS-CoV-2 by the commonly used manual real-time RT-PCR procedure (Naranbat et al., 2022).

2.4 Isothermal amplification technology for SARS-CoV-2 diagnostics

After the outbreak of SARS-CoV-2, nucleic acid testing quickly entered people's lives. In addition to the real-time RT-PCR which was commonly used in nucleic acid testing, isothermal amplification methods were also important nucleic acid testing methods (Tan et al., 2022). Several isothermal amplification techniques for SARS-CoV-2 diagnostics have also been reported (**Figure 2.12**), employ simultaneous, reverse transcriptions, and do not need special instruments.

Isothermal amplification technology is a technique for amplifying nucleotide chains using a simple temperature controller (Boonbanjong, Treeratrakoon, Waiwinya, Pitikultham, & Japrun, 2022). The major difference between isothermal amplification technology and real time RT-PCR consists of two main points: (i) isothermal amplification technology is performed at a constant temperature, whereas real time RT-PCR requires a temperature-changing system; (ii) polymerase enzymes normally extend primers on a single strand of the dsDNA template during real time RT-PCR. In the other hand, some isothermal amplification technology has a special polymerase enzyme that can directly extend primers on a double strand of dsDNA during the amplification process (Boonbanjong et al., 2022). There are three key components of the isothermal amplification technology system: (i) nucleic acid templates; (ii) the initial primer for complementary binding to the target nucleic acids; and (iii) isothermal enzymes for nucleic acid amplification. Both real time RT-PCR and isothermal amplification technology require DNA templates, primers, nucleotide substrates, and amplification enzymes. PCR templates are mostly dsDNA, which require a thermal cycle step to denature, anneal, and elongate the template and amplify the final dsDNA products (Boonbanjong et al., 2022). Isothermal amplification technology can undertake rapid sample and reagent preparation and can also be coupled with a variety of readouts, enhancing their ease-of-use and accessibility (Khan et al., 2020). A comparison of common isothermal amplification methods is shown in **Table 2.1**.

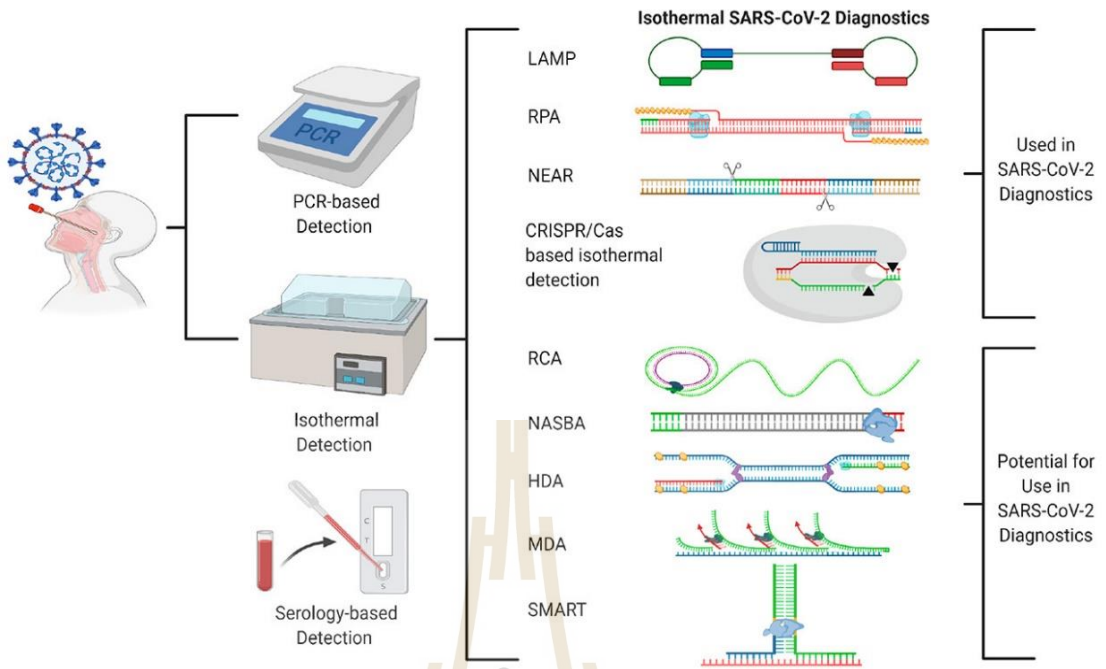


Figure 2.12 Isothermal SARS-CoV-2 diagnostics (Khan et al., 2020).

Table 2.1. Comparison of common isothermal amplification methods (Khan et al., 2020; Tan et al., 2022).

Name	Template	Incubation temperature (°C)	Detection time
Loop mediated isothermal amplification (LAMP)	DNA or RNA	60-65	30-60 min
Recombinases polymerase amplification (RPA)	DNA or RNA	37-42	10-20 min
Nicking enzyme amplification reaction (NEAR)	DNA or RNA	dependent on nicking enzymes and polymerase used	10-20 min
Rolling circle amplification (RCA)	DNA or RNA	37-65	1-3 h
Nucleic acid sequence based amplification (NASBA)	DNA or RNA	37-42	1.5-2 h
Helicase dependent amplification (HDA)	DNA	60-65	30 min
Multiple displacement amplification (MDA)	DNA or RNA	30	4-18 h
Signal-mediated amplification of RNA technology (SMART)	DNA or RNA	41	3 h

Among several common isothermal amplification methods, two isothermal techniques used for rapid and sensitive diagnostics are LAMP (Broughton et al., 2020) and RPA. The method could exponentially amplify DNA rapidly to improve analytical sensitivity and use in SARS-CoV-2 diagnostics (Sharma, Balda, et al., 2021; Tan et al., 2022; Y.-m. Zhang, Zhang, & Xie, 2020). LAMP is the most common method to amplify an interested gene for DNA tests. The designing primers for LAMP is more complicated than RPA and real time RT-PCR (Y.-m. Zhang et al., 2020). Therefore, it is difficult to design new assays and has added complexity due to the increased number of 4-6 primers (Broughton et al., 2020; Talwar et al., 2021; Tan et al., 2022). The primer design is complex and easy to produce nonspecific amplification. RPA was recently paid more attention to (Tan et al., 2022). Primer design for RPA reactions is similar to PCR, and it is thus fairly straightforward to design new assays (Khan et al., 2020). It had the advantages of a simple operation and it could perform isothermal amplification at 37-42 °C. RPA typically operates at a moderate temperature isothermal amplification method to exponentially amplify DNA amount without requiring an additional temperature step and also matching the optimal reaction temperatures of Cas13a and Cas12a (Feng et al., 2021; Talwar et al., 2021; Tan et al., 2022). Hence, a technique for amplifying nucleotide chains using a simple temperature controller, is short reaction time, tolerance of certain mismatches; simple primer design, and support for multiplex amplification reactions (Tan et al., 2022). So, it was very suitable for detection not sophisticated instruments which was very suitable for on-site detection in low resource environments (Cherkaoui, Huang, Miller, Turbé, & McKendry, 2021; Munawar, 2022). Among these isothermal amplification methods, RPA was a relatively simple method. However, non-specific amplification is problematic with these approaches (Yüce, Filiztekin, & Özkaya, 2021). Following isothermal exponential amplification, CRISPR-Cas12a integrated with RPA amplification techniques improves both analytical specificity and sensitivity (Sun et al., 2021). RPA amplification scheme comprises six steps: (I) RPA initiates with binding

of recombinases–nucleotide primer complexes to homologous sequences in the target DNA; (II) The D-loop is stabilized by binding of single-stranded binding proteins to the displaced strands; (III) Synthesis of new DNA strands is initiated by strand displacement polymerases. (IV) The parent DNA strands are separated. (V) DNA synthesis continues until two DNA duplexes are formed; (VI) Exponential amplification was achieved by cyclic repetition of this process (Khan et al., 2020) (**Figure 2.13**).



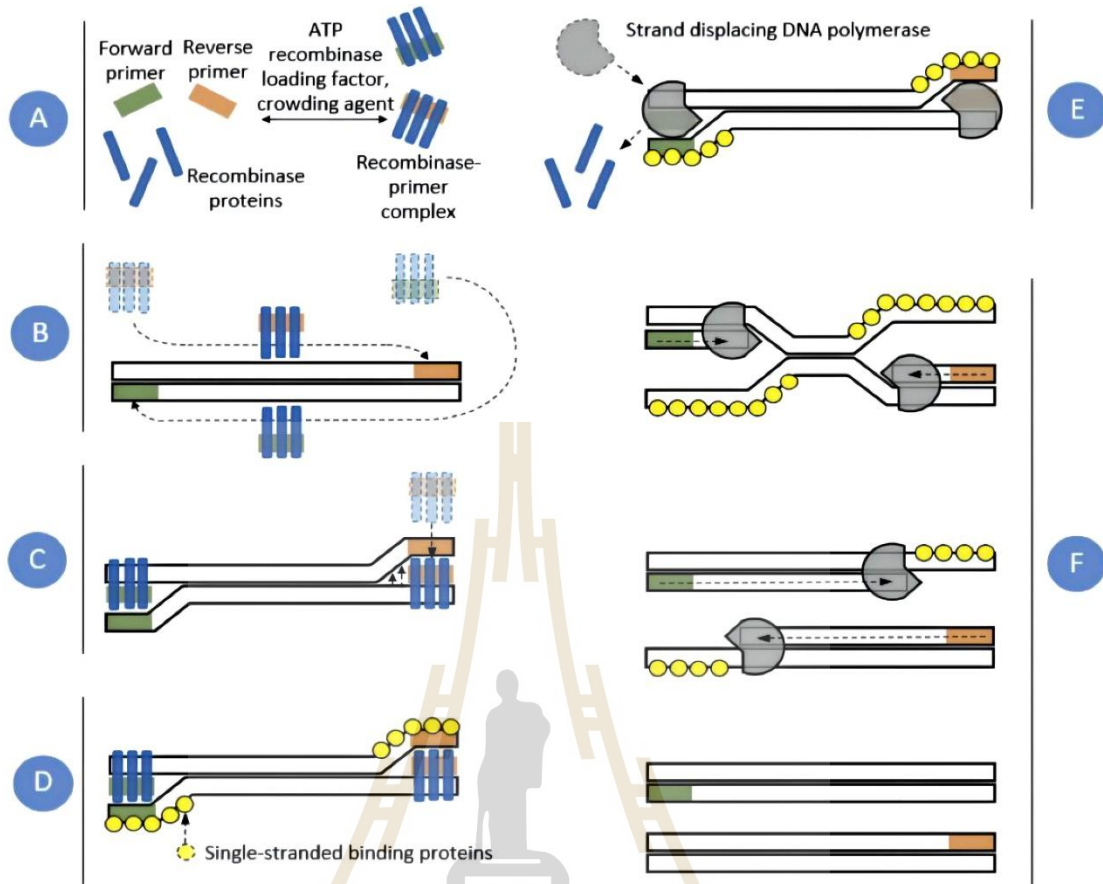


Figure 2.13 RPA amplification scheme (Tan et al., 2022). Recombinases proteins formed complexes with each primer (A), which scanned DNA for homologous sequences (B). The primers were then inserted at the cognate site by the strand-displacement activity of the recombinases (C) and single-stranded binding proteins stabilized the displaced DNA chain (D). The recombinases then disassembled leaving the 3' end of the primers accessible to a strand displacing DNA polymerase (E), which elongated the primer (F). Exponential amplification was achieved by cyclic repetition of this process.

2.5 CRISPR-Cas12a

Clustered regularly interspaced short palindromic repeats (CRISPR)/CRISPR-associated gene (Cas) (CRISPR-Cas) systems was discovered in the genome of adaptive immune prokaryotic organisms that used to cleave invading nucleic acids in nature (Barrangou et al., 2007; Bharathkumar et al., 2022). These systems are gene editing that has emerged as revolutionary genome editing tools in life science (Knott & Doudna, 2018). The CRISPR-Cas systems are also evolving many innovations including several promising nucleic acid detection methods giving hope to the healthcare community (Rahman et al., 2021; Talwar et al., 2021; Tsou, Leng, & Jiang, 2019; Wang et al., 2020). CRISPR-Cas systems are divided generally into two classes (Classes 1 and 2), which are further subdivided into six types (types I through VI) and diverse subtypes possessing signature Cas genes. Class 1 systems (types I, III, and IV) utilize multisubunit Cas proteins, while Class 2 systems (types II, V, and VI) employ a single multiple-domain Cas protein. Because of the concise composition of Class 2 systems, they are more widely researched and applied compared to Class 1 systems. In addition, certain Cas effector proteins, such as Cas9 (type II), Cas12a (subtype V-A), etc., can be reprogrammed with crRNA sequences, allowing researchers to repurpose these crRNA-Cas protein complexes as genetic tools for a wide range of applications, including genome editing, gene silencing, and high-sensitivity nucleic acid detection (Gasiunas, Barrangou, Horvath, & Siksnys, 2012; Nishimasu & Nureki, 2017; Shmakov et al., 2017).

Cas12a (formerly known as Cpf1), the class II type V CRISPR nuclease, has been widely used for genome editing in mammalian cells and plants (Manghwar, Lindsey, Zhang, & Jin, 2019; Safari, Zare, Negahdaripour, Barekati-Mowahed, & Ghasemi, 2019; Shi et al., 2021; L. Zhang et al., 2023). CRISPR-Cas12a is an RNA-guided DNase enzyme that varies in size between 1200 and 1500 amino acids (Shmakov et al., 2015). The key functions as a prokaryotic defense mechanism and comprises diverse family members (F. Zhang, 2019). CRISPR-Cas12a based assay called DNA Endonuclease Targeted CRISPR Trans Reporter (DETECTR) was discovered in 2015 and originally called Cpf1. Cas12a is like the well-known Cas9 protein that UC Berkeley's

Jennifer Doudna and colleague Emmanuelle Charpentier turned into a powerful gene-editing tool in 2012. To date, three members of Cas12a nucleases of diverse species from *Acidaminococcus sp.* (AsCas12a), *Lachnospiraceae bacterium* (LbCas12a), and *Francisella novicida* (FnCas12a) are characterized and used in genome editing (H. Huang et al., 2022; Jiménez, Hoff, & Revuelta, 2020; Mohanraju et al., 2021; Zetsche et al., 2015). Among others, Cas12a protein from Lachnospiraceae bacterium (LbCas12a) is widely used for biomedical research (Misiurina et al., 2022). Cas12a nuclease has bilobed molecular architecture and contains two major parts: a nuclease lobe (NUC) and an alpha-helical recognition lobe (REC). The REC lobe consists of two domains: REC1 and REC2, which have been shown to coordinate the crRNA-target DNA heteroduplex. The NUC lobe is composed of the RuvC domain and additional domains for cleavage of a target (TS) and non-target DNA strands (NTS) (Bandyopadhyay, Kancharla, Javalkote, Dasgupta, & Brutnell, 2020; Misiurina et al., 2022; Shi et al., 2021). NTS is cleaved first and followed by TS and generates double strand staggered break (sticky ends). Unlike other Cas proteins, Cas12a processes its own mature crRNA into 42 to 44 nt without the intervention of tracrRNA. This distinct feature of Cas12a makes it advantageous for multiplex gene editing (Bandyopadhyay et al., 2020; Safari et al., 2019) (**Figure 2.14**).

The mechanisms of Cas12 cleavage activity employ only the RuvC domain that performs the cleavage of the target DNA strands. Cas12a contained two DNA nuclease active sites and cleavage of the target and non-target DNA strands were cleaved by the same catalytic mechanism in a single active site RuvC in Cas12a enzymes. The catalytic activity of Cas12a requires recognition of the protospacer adjacent motif (PAM) sequence located at the 5'-end of the protospacer. PAM is a short DNA sequence that follows the DNA region targeted for cleavage by the CRISPR-Cas12a. Most Cas proteins require a specific PAM which is a short DNA sequence that is located next to the target region (S. Kim, Ji, & Koh, 2021). Cas12a can cleave the target nucleic acid with site-specific cleavage at any locus containing a PAM that can

be achieved with designed crRNA containing appropriate spacer sequences (Ghosh, Saha, & Sharma, 2022). Cas12a has several unique features, as follows. (a) The canonical PAM of CRISPR-Cas12a which is located at the 5' ends of the target site (b) the binding of crRNA to target DNA activated Cas12a for both cleavages of a site-specific double-stranded DNA molecule (dsDNA) and non-specific ssDNA (**Figure 2.15**). A fundamental property of Cas12 nucleases is their ability to cleave the non-specific single-strand DNA (ssDNA) molecules also known as trans-cleavage or collateral activity. For target recognition, the binding of the target dsDNA is initiated by the recognition of the PAM sequence. After cleavage of the target dsDNA, the PAM-distal cleavage product is released, and the PAM-proximal dsDNA remains bind to the Cas12acrRNA complex. Cas12a requires a specific nucleotide sequence of PAM (Misiurina et al., 2022). The key functional activities of the CRISPR-Cas system that are routinely employed in the diagnostic methods: (a) target nucleic acids synthesized with an isothermal amplification process; (b) activation of collateral activity by Cas nucleases cut the target nucleic acid, followed by the sequence-specific binding; (c) the reporters cut by the activated Cas effectors to liberate visual fluorescent signals within detection platforms (S. Kim et al., 2021; Rahman et al., 2021).

In recent years, a new strategy for nucleic acid detection based on CRISPR-Cas seems to offer unprecedented possibilities. The coupling of the CRISPR-Cas technology with isothermal amplification methods is fostering the development of applications in the CRISPR-built next-generation novel coronavirus diagnostics (Bonini et al., 2021; Rahman et al., 2021). The CRISPR-based nucleic acid detection gives rise to several reasonably better diagnostic methods than the others. Firstly, if we compare the time taken for the test. Secondly, the cost associated with each test. Thirdly, their capability of detecting SARS-CoV-2 in the clinical samples. Finally, the CRISPR-based nucleic acid detection can be easily read with paper strips without compromising sensitivity or specificity.

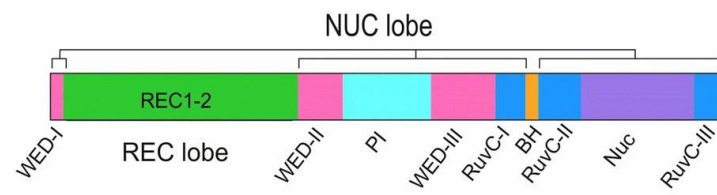


Figure 2.14 Schematic representation of the fundamental components of Cas12a (Safari et al., 2019).

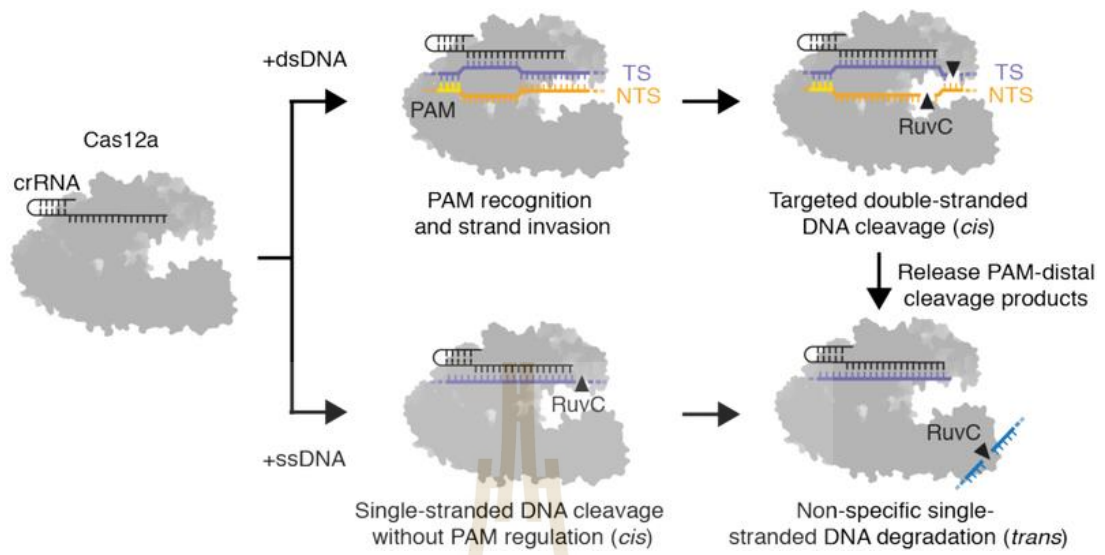


Figure 2.15 Model for PAM-dependent and PAM-independent activation of cis and trans-cleavage by Cas12a (J. S. Chen et al., 2018).

2.6 Lateral flow assay (LFA)

As mentioned above, there are several major testing platforms for diagnosing COVID-19 which detect the SARS-CoV-2 RNA sequences. However, it requires instrumentation and skilled personnel to conduct and interpret the test (Pradhan et al., 2022). Lateral flow assay, a qualitative chromatography, is a very simple, rapid, portable analytical platform that specifically targets the detection of antigens or antibodies and does not require instrumentation for readout because the results are presented as visible colorimetric bands (Alhabbab, 2022). Most LFAs are designed to give a qualitative response ideal for naked-eye detection by non-specialized users (Parolo et al., 2020). Lateral flow assays are technology devices popular in biomedicine, agriculture, food, and environmental science (Koczula & Gallotta, 2016). Broadly, LFA tests can be divided into two categories: (a) lateral flow immunoassay tests, these assays use antibodies to recognize antigens, proteins, or hormones and are classified into two types: (i) sandwich LFA and (ii) competitive LFA; (b) lateral flow nucleic acid tests, these assays can be grouped into two categories (i) nucleic acid LFA (NALF) and (ii) nucleic acid lateral flow immunoassays (NALFIA) (Koczula & Gallotta, 2016). LFA is usually composed of four main parts: a sample pad, a conjugate pad, a membrane with immobilized antibodies, and an adsorbent pad. They are mounted on a nitrocellulose membrane. The membrane binds to the capture bioreceptor that forms the test and control lines (**Figure 2.16**).

Part (1) Sample pad: The sample pad represents the first section of an LFA where the sample is pipetted biological sample gets absorbed at the beginning of the test. This pad may be treated with certain salts or surfactants to maintain the pH or control the flow rate of the sample. The most important role of the sample pad is to control the flow rate of the sample in a smooth, continuous. The characteristics of the sample pad are coated with buffer salts, proteins, surfactants, and other liquids. It should do properties for example pH, ionic strength, viscosity, purity, and concentration of blocking agents suitable for the interaction with the detection

system. Moreover, the pores which are to distribute the sample evenly and can act to direct the sample to reach the conjugate pad (Parolo et al., 2020; Sachdeva, Davis, & Saha, 2021).

Part (2) Conjugate pad: The conjugate pad is the second pad to be encountered by the sample. It consists of immobilized pre-labeled sample recognition elements. Different types of reporter labels – gold nanoparticles, fluorescence quenching labels, and quantum dots can be used (Parolo et al., 2020; Sachdeva et al., 2021).

Part (3) Membrane: The membrane also called detection pad is part of the LFA strip where the signal is generated for capturing the bioreceptor that allows interaction of antigen and antibody or DNA/RNA hybridization. This region contains the test line and the control line. Wherein, the antibody or nucleic acid hybrid specific to the sample is immobilized on the test line and the control line consists of a secondary sample recognition element. We can add several lines in this region of the strip to check for different analyte from the same sample simultaneously. The test line, the main role of the test line is to detect the presence or absence of the analyte by generating a line from the capture bioreceptor that binds the labeled analyte. The control line, which confirms the correct operation of the lateral flow immunoassay strips when the sample reaches the control line then selective capture of the labeled bioreceptor (Parolo et al., 2020; Sachdeva et al., 2021).

Part (4) Adsorbent pad: The adsorbent pad is to control the volume of the sample that a strip can take. This collects excess waste and ensures that there is no backflow of the fluid (Parolo et al., 2020; Sachdeva et al., 2021).

The sample containing the target analyte is absorbed by the sample pad and it moves toward the conjugate pad with the help of capillary forces. Here, the analyte interacts with a specific antibody or DNA/RNA oligonucleotide (labeled with a colored molecule) and forms a mobile conjugate that flows onto the nitrocellulose membrane. The conjugates which are complementary to the immobilized bioreceptor on the test and the control lines, get captured, respectively, whereas, the remaining fluid gets wicked by the adsorbent pad. A signal is generated on the lines as soon as

the conjugate containing the reporter label along with the target analyte binds to its bioreceptor. As a result, a change in the color of the lines can then be seen (Sachdeva et al., 2021).

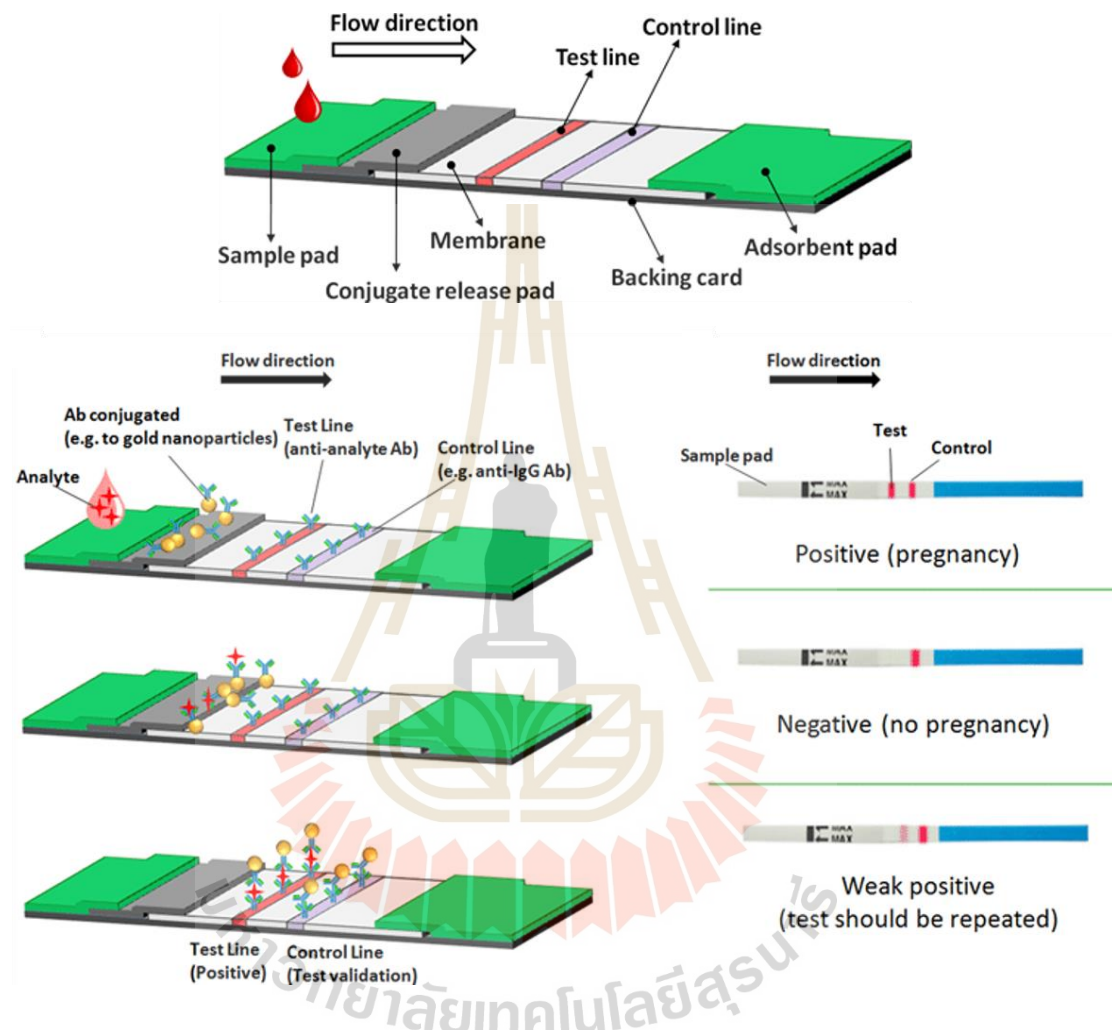


Figure 2.16 Schematic representation of a typical diagram and several components of LFA and working mechanism (Koczula & Gallotta, 2016). A simple LFA test strip consists of a sample pad, a conjugate pad, a test line, a control line, and an absorption pad.

2.7 General mechanism of CRISPR-Cas12a mediated detection of nucleic acids via LFA

CRISPR-Cas12a-based detection of nucleic acids via lateral flow assay methods is generally compatible with a very intuitive and interpreted lateral flow readout. The way LFA is used for CRISPR applications can lead to confusion about the test line (T line) and control line (C line). Cas12a-based detection method interpretation of the test strips can vary using different detection processes. The T line and C line is swapped in Cas12a detection process (Broughton et al., 2020; Sagoe et al., 2023; Tsou et al., 2019; Y.-m. Zhang et al., 2020). Cas12a specifically and sensitively recognizes defined amplicon-related sequences. Successful recognition leads to the activation of the Cas12a associated collateral nuclease activity. The DNA degrading activity is the basis for signal generation in LFA. This is achieved by using the reporter degradation process. The key to the functionality of a Cas12a assay combined with a lateral flow readout is the use of a reporter. The lateral flow test strip is able to give information about the status of a so called reporter. Such a reporter is a short single stranded DNA molecule that carries two specific labels including biotin and FAM or FITC. If the reporter is used in a much defined concentration, the majority of the gold conjugate is trapped at the T-line, which leads to an almost complete extinction of the C-line. It is precisely this effect that enables the T line and C line swap for CRISPR-Cas12a-based detection method. Switching C line and T line, the presence of the gene target leads to a positive test result. In contrast, the absence of the specific genetic target leads to a negative test result. The general mechanism of CRISPR-Cas-mediated detection of nucleic acids via lateral flow readout, the presence of the genetic target leads to a positive test result. The Cas12a recognition of target DNA by the crRNA unleashes collateral activity. Next, activated Cas12a cleaves the dual labeled reporter, which leads to the separation of Biotin and FITC/FAM labels. Reporter cleavage leads to the appearance of the T line during lateral flow analysis. The signal intensity of the C line is weakened. In contrast, the absence of the specific genetic target leads to a negative test result. The Cas12a has no recognition of the target DNA by the crRNA so on no collateral activity. The dual labeled reporter remains intact.

Biotin of the dual labeled reporter is bind by a biotin ligand. The FITC/FAM label is bind by mobile anti FITC-FAM antibodies conjugated to gold particles. This results in a strong C line and a missing T line (**Figure 2.17**).

During LFA, an intact reporter is retained at the C line. The upper T line is not visible (negative test result). Cleaved reporter leads to an increasing amount of C-line overflowing gold conjugate, which is retained at the T line. Therefore, positive results are characterized by an increasing intensity of the T line and a decreasing intensity of the C line (Broughton et al., 2020; Sullivan, Dhar, Cruz-Flores, & Bodnar, 2019) (**Figure 2.18**).

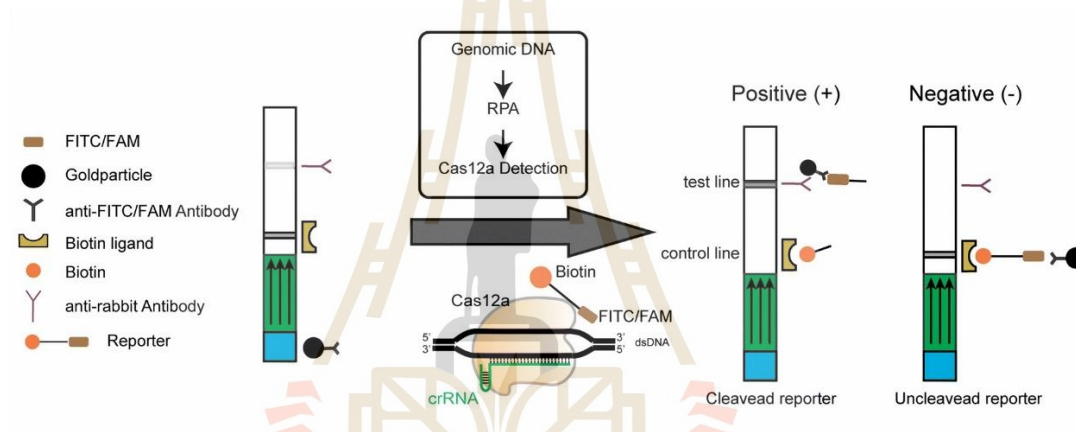


Figure 2.17 Schematics of RPA-Cas12a-LFA detection (Y.-m. Zhang et al., 2020).

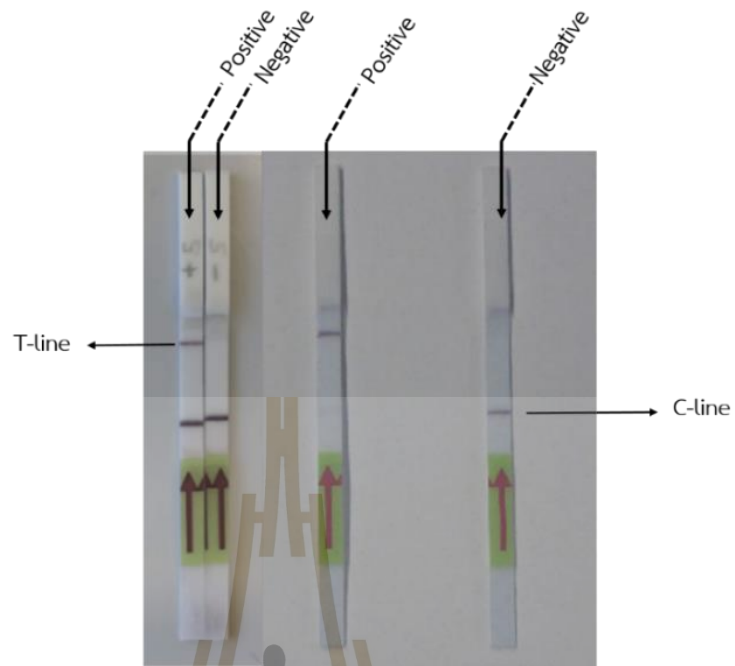


Figure 2.18 Difference of test result interpretation for use of the CRISPR-Cas12a via LFA.

CHAPTER III

RESEARCH METHODOLOGY

3.1 Total RNA extraction

The specimens were collected under protocol approved by the Suranaree University of Technology Institutional Biosafety Committee (SUT IBC). The ribonucleic acids were extracted from the COVID-19-positive specimens by using Trizol™ Universal reagent (Tiangen, Beijing, China). The equal volume of Trizol™ reagent was added into collected specimen tube and mixed well. The homogenization samples were incubated at 25 °C for 5 minutes. After keeping at 25°C for 5 minutes, 500 µL of each suspension were added with 200 µL of chloroform and mixed well by shaking for 15 seconds. After keeping at 25°C for 3 minutes, the suspension was centrifuged at 12,000x g, 4 °C for 15 minutes. The aqueous phase was transferred to a new microcentrifuge tube. 500 µL of isopropanol were added with gentle mix by inverting 5 times. After incubating at 15-30 °C for 10 minutes, the preparations were centrifuged for 10 minutes at 12,000x g at 4 °C. The total RNA was precipitated and formed a white gel- like pellet at the bottom of the tube. After discarding the supernatant, the pellet was washed twice with at least 1 mL of 75 % ethanol per 1 mL of Trizol™ reagent and mixed well by vortexing. The samples were centrifuged at no more than 7500 x g, 4 °C for 15 minutes. At the end of the procedure, the supernatant was again discarded to remove the ethanol and briefly dry the RNA pellet by air-dry or vacuum-dry for 5-10 minutes. To elution the RNA pellet, the pellet was resuspended in 30 µL of ultrapure deionized water (UDW) by pipetting up and down. The concentration and purity of the RNA were measured.

3.2 Conversion of total RNA to cDNA

For conversion of total RNA to cDNA, total RNA extraction from **3.1** was used to convert to cDNA by using RevertAid First Stand cDNA Synthesis Kit (Thermo Scientific, USA), following the manufacturer's recommended procedures. All reagents was mixed as followed:

Ingredient	Volume (μL)
Total RNA	10.0
Random Hexamer primer	1.0
Ultrapure deionized water (UDW)	1.0
Total	12.0
5X Reaction Buffer	4.0
20 U/ μL of RiboLock RNase Inhibitor	1.0
10 mM dNTPs Mix	2.0
200 U/ μL of RevertAid M-MuLV RT	1.0
Total	20.0

3.3 Molecular PCR amplification of NSP2 sequence

3.3.1 Primer design

Oligonucleotide primers specific to NSP2 of SARS-CoV-2 were designed according to gene sequence (accession number NC_045512.2), which access from GENBANK. The detailed RPA and PCR primer sequences for the NSP2 gene is shown in **Table 3.1**. The oligonucleotide primers for PCR amplification of the target sequence were designed from conserved regions from SARS-CoV-2 genomes. The primer sequences were: NSP2 forward: 5'-ATGTTGCTCGAAATCAAAGA-3' and NSP2 reverse: 5'-TTAAGTACTTTATCAATCCT-3'. The primer was dissolved in ultrapure water to a final concentration of 10 μM (**Appendix B**).

Table 3.1 RPA and PCR primer sequences for the NSP2 gene

Gene	Primer	Primer sequences	No	T _m	GC%
NSP2	Forward	5'-ATGTTGCTCGAAATCAAAGA-3'	20 nt	50.1°C	35.0%
NSP2	Reverse	5'-TTAAGTACTTTATCAATCCT-3'	20 nt	43.0°C	25.0%

3.3.2 PCR amplification of the NSP2 sequence

The cDNA from **3.1.2** was used as a DNA template for amplification of target sequence by conventional polymerase chain reaction (PCR). For isothermal amplification, 25 µL complete PCR reaction mix was prepared on ice. The supplementary information for PCR system was followed:

Ingredient	Volume (25 µL rxn)	Final concentration
Ultrapure deionized water (UDW)	15.5	-
10X Taq buffer with KCL ₂	2.5	1X
25 mM MgCl ₂	1.5	1.5 mM
10 µM dNTPs mix	2.0	0.8 µM
10 µM NSP2 forward primer	1.0	0.4 µM
10 µM NSP2 reverse primer	1.0	0.4 µM
Template DNA	1.0	1-500 ng
Taq DNA polymerase (5 U/ µL)	0.5	1.0-2.5 U/ rxn

The PCR thermal cycles were:

1. Initial denaturation	at 94°C for 5 minutes
2. Forty cycles of	
a. Denaturation	at 94°C for 1 minute
b. Annealing	at 94°C for 1 minute
c. Extension	at 94°C for 2 minutes
3. Final extension	at 94°C for 10 minutes

3.3.3 Agarose gel electrophoresis

The PCR amplicon was verified by agarose gel electrophoresis. One point five percent agarose gel was prepared by dissolving the agarose powder (1st BASE, Singapore) in 1x TAE buffer. The suspension was melted by using a hotplate (JOANLAB, Thailand). The gel was set and cooled down. Polymerization of the agarose suspension was allowed to occur in a mini agarose gel electrophoresis apparatus (Mupid-eXu, Thailand). The sample to be resolved was mixed with 1x DNA loading dye and loaded into a slot made in the sample well. The DNA was run in 1x TAE buffer at 100 Volts for 35 minutes. After electrophoresis, the DNA band was revealed by using UV-Vis Spectrophotometer Quantum CX5 (VILBER, Thailand).

3.4 Purification of NSP2 cDNA

The NSP2 DNA amplicons were purified from the respective gel using a gel extraction kit (Universal DNA Purification Kit, Tiangen, China), according to manufacturer's instructions. Column equilibration: Add 500 μ L Buffer BL to the Spin Column CB2 (in a 2 ml Collection Tube). Centrifuge at 12,000 rpm (\sim 13,400 \times g) for 1 min. Discard the flow-through, and set the spin column CB2 back into the collection tube. The target DNA band was cut and transferred into a microcentrifuge tube. After weight the gel block, each microcentrifuge tube was added equal volume of Buffer PC to the volume of gel and incubated at 50°C for about 10 minutes with inverting up and down the microcentrifuge tube. After the agarose gel dissolved completely, transfer the whole solution to the spin column and centrifuge at 12000 \times rpm for 1 minute. After discarding the flow-through completely, each spin column was added 600 μ L of Buffer PW and centrifuged at 12000 \times rpm for 1 minute and washed the column was centrifuged at 12000 \times g for 2 minutes to remove residual and allowed the column to air dry with the cap open for several minutes to dry the membrane. The elution DNA was transferred the column to a microcentrifuge tube, added with 30 μ L of ultrapure deionized water (UDW) was directly onto the column membrane

and stand for 2 minutes. The purified DNA was collected after centrifugation at 12000 x g for 2 minutes.

3.5 Ligation of DNA sequence coding for NSP2 into cloning vector

The purified NSP2 amplicons from **section 3.4** were ligated with TA cloning vector pTG19-T (25ng/ μ L) (Vivantis, Malaysia). The reaction was incubated at 22 °C for 1 hour. The ligation product was transformed into DH5 α *E. coli*. The transformation reaction was spread onto an LB agar plate containing 100 mg ampicillin/mL and screened the colony for colony PCR. The details of the ligation reaction of NSP2/ pTG19-T ligation mixtures were prepared as the following:

Ingredient	Volume (μ L)
pTG19-T vector (25ng/ μ L)	2.0
Fresh PCR product	* (Appendix D)
10X Buffer Ligase	1.0
T4 DNA Ligase (200u/ μ L)	1.0
Ultrapure deionized water (UDW)	to 10.0
Total	10.0

3.6 Preparation of chemically competent DH5 α *E. coli*

The DH5 α *E. coli* was grown in 2 mL of Luria-Bertani (LB) broth in 50 mL tube (**Appendix E**) and incubated at 37 °C with shaking at 200 rpm for 16-18 hours. After overnight culture of DH5 α *E. coli*, 50 mL tube of the overnight culture were incubated at 37°C with shaking at 250 rpm for 3 hours. The cell pellet was collected by centrifugation at 1500 x rpm, 4°C for 5 minutes and removed LB to collect the cell pellet. The pellet was suspended in 1 mL of cold 100 mM MgCl₂ solution, gently mixed and stored on ice for 5 minutes. The cell suspension was centrifuged at 1500 x rpm, for 5 minutes at 4°C, the supernatant discarded, and the cell pellet was resuspended

in 500 μL of cold 100 mM CaCl_2 solution. The cell suspension was mixed very well and aliquot into the micro centrifuge tubes with 100 μL per tube and add 0.5 μL of ligation reaction from **section 3.5** per tube and stored on ice for 20 minutes and heat at 42 $^\circ\text{C}$ for 2 minute in a water-bath for insert gene. Add 1 mL of LB broth non ampicillin and incubated at 37 $^\circ\text{C}$ with shaking at 200 rpm for 1 hour. After incubated, 100 μL of the culture were spread onto LB agar plates containing 100 mg ampicillin/mL (LB-A) (**Appendix E**). LB broth 900 μL were centrifuged at 1500 x rpm for 5 minutes. After discarding the LB broth, take the remaining pellet 50 μL for spread onto LB agar plates containing 100 mg ampicillin/mL (LB-A) and incubated at 37 $^\circ\text{C}$ for 16 hours.

3.7 Transformation and screening for DH5 α *E. coli* transformations

The ligation mixtures from **section 3.5** were introduced into DH5 α *E. coli* competent cells by heat shock method. Briefly, each ligation mixture was mixed with 100 μL of competent cell suspension and kept in an ice-bath for 20 minutes. The mixture was heated at 42 $^\circ\text{C}$ for 2 minutes in a water-bath and immediately moved to an ice-bath for 5 minutes. The preparation was added into 1 mL of LB broth and incubated at 37 $^\circ\text{C}$ with shaking at 250 rpm for 1 hour. The culture was spread onto LB agar plates containing 100 mg ampicillin/mL LB-A. The agar plates were incubated at 37 $^\circ\text{C}$ for 16 hours. The colonies of the transformed *E. coli* transformants were randomly picked to screen for the colonies that carried recombinant plasmid containing NSP2 coding sequence by means of colony PCR. Replica plates for individual colonies were made also on LB-A agar plates (**Appendix E**) for subsequent use. The PCR reaction mixture was prepared as the following:

Ingredient	Volume (12 μ L rxn)	Final concentration
Ultrapure deionized water (UDW)	6.75	-
10X Taq buffer with KCl_2	1.25	1X
25 mM $MgCl_2$	0.75	1.5 mM
10 μ M dNTPs mix	1.0	0.8 μ M
10 μ M NSP2 forward primer	0.5	0.4 μ M
10 μ M NSP2 reverse primer	0.5	0.4 μ M
Template DNA	1.0	1-500 ng
Taq DNA polymerase (5 U/ μ L)	0.25	1.0-2.5 U/ rxn

Thermal cycles of the PCR are shown below. The PCR amplified products were verified by agarose gel electrophoresis as **section 3.3.3**.

1. Initial denaturation at 94°C for 5 minutes
2. Forty cycles of
 - a. Denaturation at 94°C for 1 minute
 - b. Annealing at 94°C for 1 minute
 - c. Extension at 94°C for 2 minutes
3. Final extension at 94°C for 10 minutes

3.8 Extraction of the NSP2/pTG19-T plasmids

The recombinant NSP2/ pTG19-T plasmids were extracted from respective transformed DH5 α *E. coli* clones using GF-1 Plasmid DNA Extraction Kit (Vivantis, Selangor, Malaysia). Individual transformed *E. coli* colonies carrying the respective NSP2/ pTG19-T plasmids were inoculated into 10 mL of LB-A broth and incubated at 37°C with shaking 200 rpm for 12-16 hours. Individual *E. coli* pellets were collected by centrifugation at 6000 x g for 5 minutes to harvest the cells. After discarding the supernatant completely, each bacterial pellet was resuspended in 250 μ L of solution S1 RNase A (DNase-free) and transferred to a new tube. The alkaline lysis was added 250 μ L solution S2 and gently mixed by inverting the tube several times (4-6 times) to obtain a clear lysate and kept at 25°C for 5 minutes. The neutralization was added 400 μ L of Buffer NB, mixed by inverting the tube several times (6-10 times) until a white precipitate formed. The preparation was centrifuged at 14000-16000 x g for 10 minutes. The supernatant containing plasmids was transferred 650 μ L to a column assembled in a clean collection tube. After loading the column, centrifuged at 10000 x g for 1 minute, and wash the column was added 650 μ L of wash buffer and centrifuged at 10000 x g for 1 minute. The upper phase was transferred to a microcentrifuge tube, added with 30 μ L of ultrapure deionized water (UDW) directly onto the column membrane, and stand for 1 minute. The plasmid DNA in the pellet was collected after centrifugation at 10000 x g for 1 minute. Plasmids in the pellet were suspended in 30 μ L of UDW and verified by 1% agarose gel electrophoresis as **section 3.3.3.**

3.9 Verification of carrying recombinant plasmids with inserted DNA coding for NSP2

The presence of the NSP2 inserts in the pTG19-T vector was verified by DNA sequencing. Homologies of the sequences with the database was verified. The recombinant plasmid was further used as positive control in CRISPR-Cas12a cleavage system.

3.10 Production of the CRISPR-Cas12a digestion reaction

3.10.1 LbCas12a

Lba Cas12a and NEBuffer 2.1 were purchased from New England Biolabs Inc. Lba Cas12a (Cpf1) from *Lachnospiraceae* bacterium ND2006 is a site-specific DNA endonuclease guided by a single 41-44 nucleotide guide RNA. Targeting requires a crRNA complementary to the target site as well as a 5' TTTN (N is any DNA oligonucleotide) PAM on the DNA strand opposite the target sequence. Cleavage by EnGen Lba Cas12a occurs ~18 bases 3' of the PAM and leaves 5 nucleotide 5' overhanging ends.

3.10.2 CrRNA design and synthesis

The crRNA was designed to target SARS-CoV-2 NSP2. The crRNA consists of 20 nt of common sequences (repeat) for binding LbCas12a protein and for recognizing target sites. The detailed Guide RNA sequences for the SARS-CoV-2 NSP2 detection based on CRISPR-Cas12a is shown in **Table 3.2**. The crRNA sequence were utilized Benchling Software (<https://benchling.com/editor>) to design specific CRISPR guides. The crRNA was synthesized and delivered from Integrated DNA Technology (America). The crRNA was dissolved in ultrapure water to a final concentration of 300 nM (**Appendix B**) and used in CRISPR-Cas12a digestion reaction.

Table 3.2 Guide RNA sequences for the SARS-CoV-2 NSP2 detection based on CRISPR-Cas12a

Cut Position	Strand	Guide Sequence	PAM	Off-Target Score
131	Positive	GGTGATGACACTGTGATAGA	TTTT	93.9

3.11 CRISPR-Cas12a digestion

The NSP2 plasmid was used as template for target CRISPR-Cas12a digestion reaction. The reactions were mixed as followed according to manufacturer's instructions. The reactions were incubated at 25-37°C for 20-30 minutes. The NSP2/pTG19-T plasmid digestion by Cas12a was verified by agarose gel electrophoresis.

Ingredient	Volume (μ L) (30 μ L rxn)	Final concentration
Ultrapure deionized water (UDW)	20.0	-
10X NE buffer	3.0	1X
300 nM crRNA	3.0	30 nM
1 μ M Cas12a	3.0	0.1 μ M
NSP2/pTG19-T plasmid	1.0	-

3.12 Production of the lateral flow strips test based on CRISPR-Cas12a combined with RPA for SARS-CoV-2 NSP2 detection

3.12.1 RPA

For testing each sample, set up three RPA reactions, for detection of the NSP2 gene target, positive test control, and negative test control respectively. One microliter of the cDNA template was used as direct input into RPA. The RPA reaction was performed and run as instructed using TwistAmp™ Basic Kit (TwistDx, United Kingdom) according to the manufacturer instructions. Briefly, the cDNA was used as a template for RPA reactions. One microliter of the cDNA template was used as direct input into RPA. The 47.5 µL RPA reactions mixture contained the following reagents: 10 µL forward primer, 10 µL reverse primer, primer free rehydration buffer, ultrapure deionized water, and template. 47.5 µL of reaction mixture were mixed with freeze-dried RPA enzyme powder. Resuspended each lyophilized RPA pellet using 47.5 µL of reactions mixture supplied in the RPA kit. Then, 2.5 µL of 280 mM Magnesium Acetate (MgOAc) was added to start RPA reaction. For isothermal amplification, the RPA reaction mixture was prepared on ice and immediately incubated at 39 °C for 20 minutes in the pre-warmed heat box. After incubation, place the reaction back on ice immediately until ready to add to the reaction in the detection of viral RNA sequence using Cas12a. Ten microliters of RPA reaction were used as direct input as **section 3.12.2.**

The RPA reaction mixture is shown below. The RPA reaction mixture was verified by 1% agarose gel electrophoresis.

Ingredient	Volume (μL)
10 μM Forward primer	2.4
10 μM Reverse primer	2.4
Primer free rehydration buffer	29.5
cDNA	1.0
Ultrapure deionized water (UDW)	12.2
280 mM MgOAc	2.5
Total	50.0

The positive test control of RPA reaction mixture is shown below. The RPA reaction mixture was verified by 1% agarose gel electrophoresis in **section 3.3.2**.

Ingredient	Volume (μL)
Primer mix	8.0
Primer free rehydration buffer	29.5
Positive control DNA	1.0
Ultrapure deionized water (UDW)	9.0
280 mM MgOAc	2.5
Total	50.0

The negative test control of RPA reaction mixture is shown below. The RPA reaction mixture was verified by 1% agarose gel electrophoresis in **section 3.3.2**.

Ingredient	Volume (μL)
10 μM Forward primer	2.4
10 μM Reverse primer	2.4
Primer free rehydration buffer	29.5
Negative control DNA	1.0
Ultrapure deionized water (UDW)	12.2
280 mM MgOAc	2.5
Total	50.0

3.12.2 RPA-CRISPR-Cas12a-reporter assay

For target gene detection using Cas12a; the ssDNA reporter (BIOTIN/TTATTATTATTATTATT/FITC) was synthesized (Serve Science Company Limited, Thailand). The detection of viral RNA sequence using Cas12a reaction mixture included the following reagents: 10X NE buffer, 300 nM crRNA, 1 μ M Cas12a enzyme, 25 nM reporter, RPA product, and ultrapure deionized water. For LFA detection, 50 μ L Cas12a digestion reaction mix was incubated with a reporter at 37 °C for 20 minutes. After all reactions are set up, vortex to mix thoroughly and incubate at 37°C for 30 minutes in a pre-warmed heat box. After incubation, place reaction tubes back on ice and analyze by agarose gel electrophoresis. (Figure 3.1). For each NSP2 gene RPA reaction, set up a Cas12a detection reaction as follows:

Ingredient	Volume (μ L) (50 μ L rxn)	Final concentration
10X NE buffer	5.0	1X
300 nM crRNA	6.0	36 nM
1 μ M Cas12a	1.0	0.02 μ M
25 nM Reporter	2.4	1.2 nM
RPA product	10.0	-
Ultrapure deionized water (UDW)	25.6	-

3.12.3 Target gene detection using RPA-Cas12a and LFA

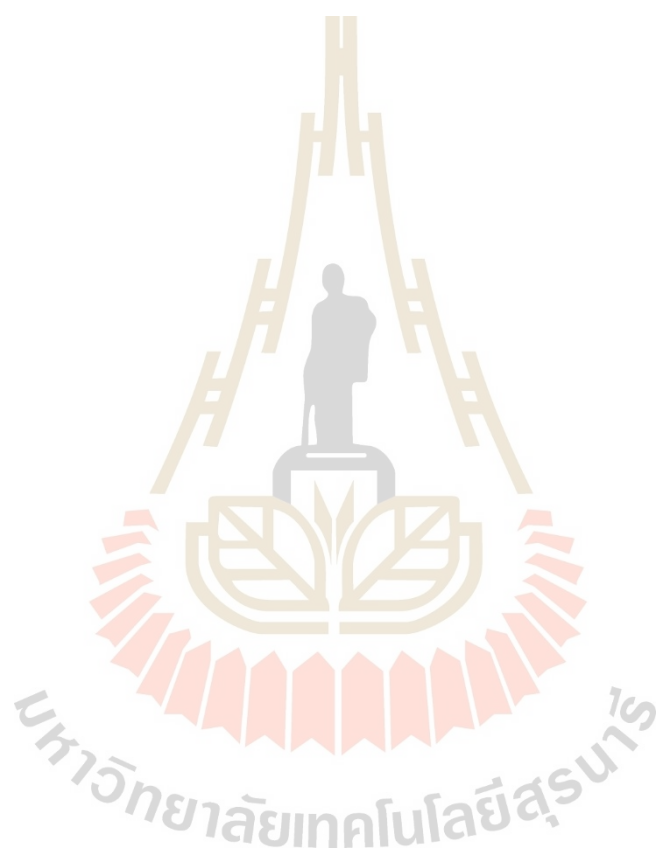
After section 3.12.2, 100 μ L of DNA running buffer was added and mixed thoroughly. Place the diluted reaction in a tube rack and incubate at room temperature for 5 minutes. Place a lateral flow strip into each reaction tube and wait for the reaction to flow through the dipstick. One lateral flow strip was then dipped into the reaction tube and held upright for 5 minutes to develop a visible color in T-line and C-lines. To enable the on-site diagnosis of SARS-CoV-2 NSP2, we designed a lateral flow readout based on the destruction of a biotin and FITC-labelled ssDNA reporter, which allows the presentation of results with a lateral flow strip. In our

lateral flow strip assay, the anti-FITC antibody conjugated gold nanoparticles specifically bind to FITC and show the band signal on the strip. On the control line, the abundant anti-Biotin can bind and capture biotin-labelled ssDNA, and only the CRISPR-Cas12a cleaved ssDNA reporter can flow through the control line. Anti-mouse IgG antibodies on the test line bind the cleaved ssDNA with FITC-gold nanoparticles.

The test starts when a sample is placed on the sample pad (left end). The liquid sample is first loaded onto the sample pad and then allowing for it to migrate to the conjugate pad by capillary force, where previously dried nanoparticle receptors (such as AuNPs) are resuspended in the DNA running buffer. In this process, the target in the sample is captured by an anti-FITC antibody coated nanoparticle embedded in the conjugate pad. As the complexes formed by the analyte and nanoparticles continue to flow forward, they specifically bind to the anti-Biotin capture antibodies, and anti-mouse IgG antibodies are also pre-embedded on the C line and T line in the nitrocellulose membrane. After a few minutes, the target is captured and forms a specific signal at the test line (T line) and control line (C line), representing the presence or absence of the target and the successful completion of the reaction (**Figure 3.1**).

The target gene is cut specifically Cas12a by specifically guide crRNA and induce collateral cleaved so on the reporter were cut by Cas12a. Reporter is labelled by biotin and FITC. After the reporter is cleaved completely, biotin is bind with anti-biotin at C line. Thus, the color do not shown in C line. On the other hand, FITC is bind to both of gold nanoparticle conjugated anti-FITC and anti-mouse IgG antibody and show the band signal on the T line, representing the positive result. However, reporter is not cleaved successful completely by Cas12a that the gold nanoparticle conjugated anti-FITC bind intact biotin-FITC. Thus, the color is shown faint band in C line. However, most of reporter bind to the Gold nanoparticle conjugated Anti-FITC and anti-mouse IgG antibody. Therefore positive results are characterized by an increasing intensity of T line and decreasing intensity of C line. For negative result, crRNA is not bind specificity to target gene. The intact reporter is

bind to anti-biotin with biotin and gold nanoparticle conjugated anti-FITC with FITC. Therefore negative result is characterized by a decreasing intensity of T line and increasing intensity of C line.



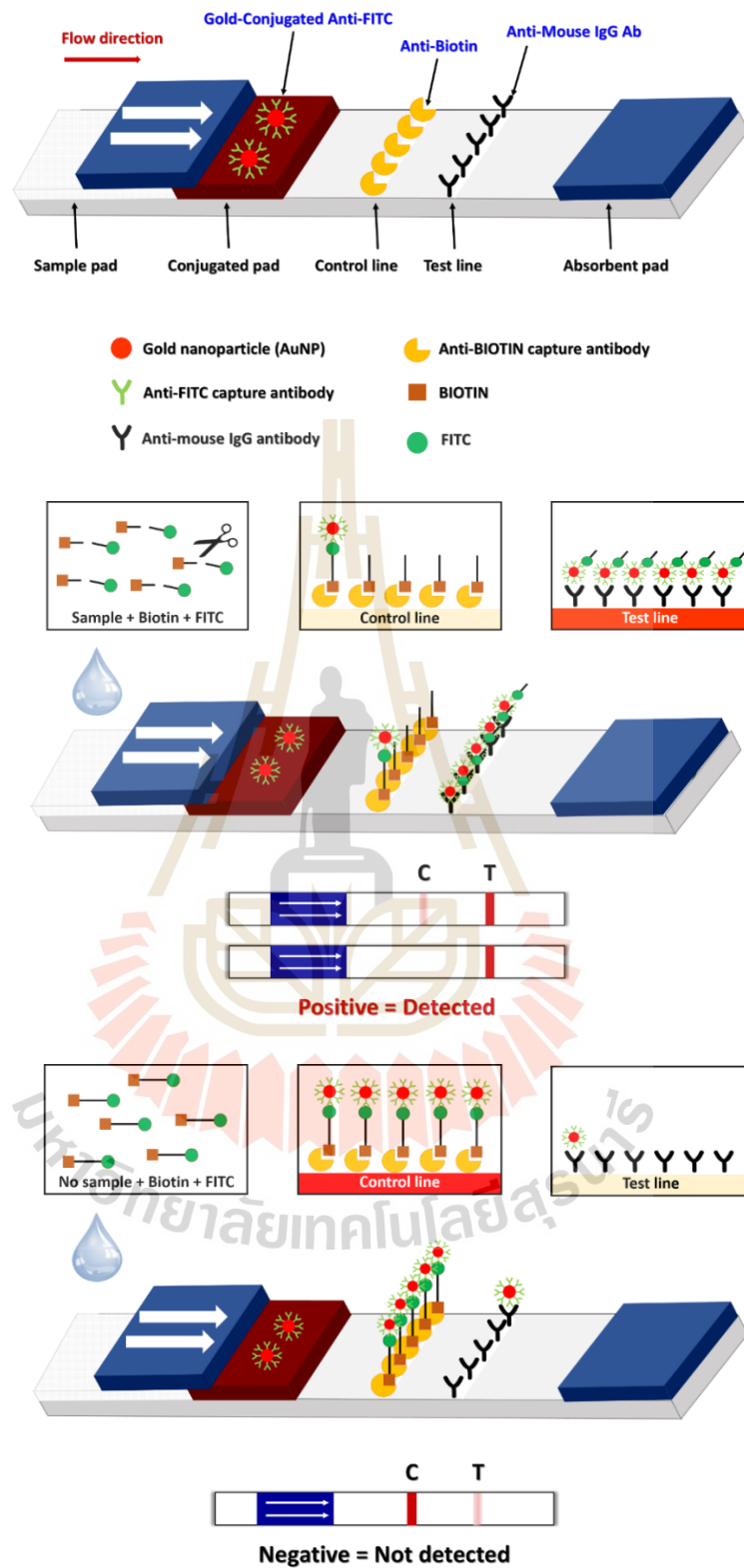


Figure 3.1 Schematic illustration of a SARS-CoV-2 detection-based LFA.

CHAPTER IV

RESULTS

4.1 NSP2 gene PCR amplification

After PCR amplification was performed; the gene fragment was verified by 1.5% agarose gel electrophoresis in TAE buffer. The expected size of NSP2 gene fragment amplicon was 200 bp. In figure 4.1 shown the NSP2 PCR amplification.

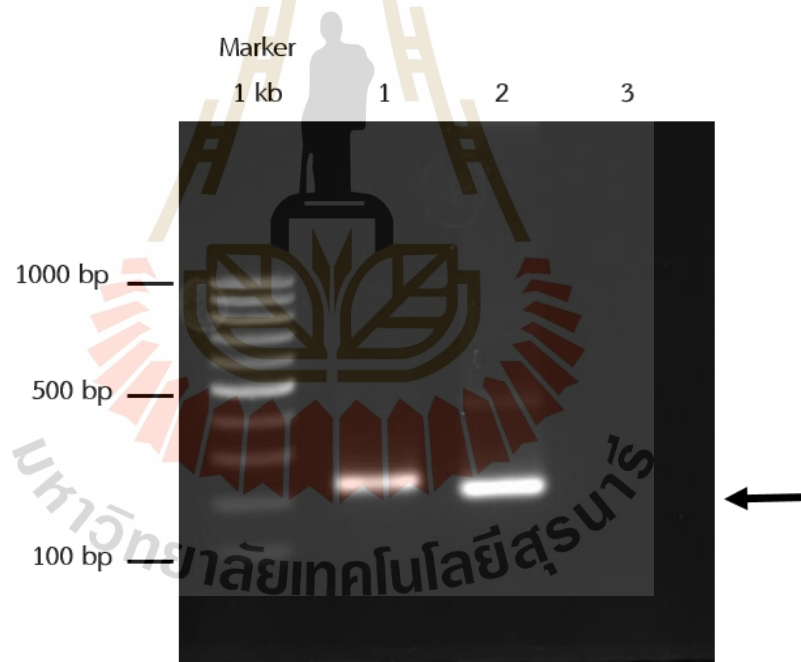


Figure 4.1 Gel electrophoresis image of PCR amplification of SARS-CoV-2 NSP2 cDNA fragments, the expected size was 200 bp and indicated by the respective arrow.

Lane M, Gene Ruler DNA ladder mix 100 bp

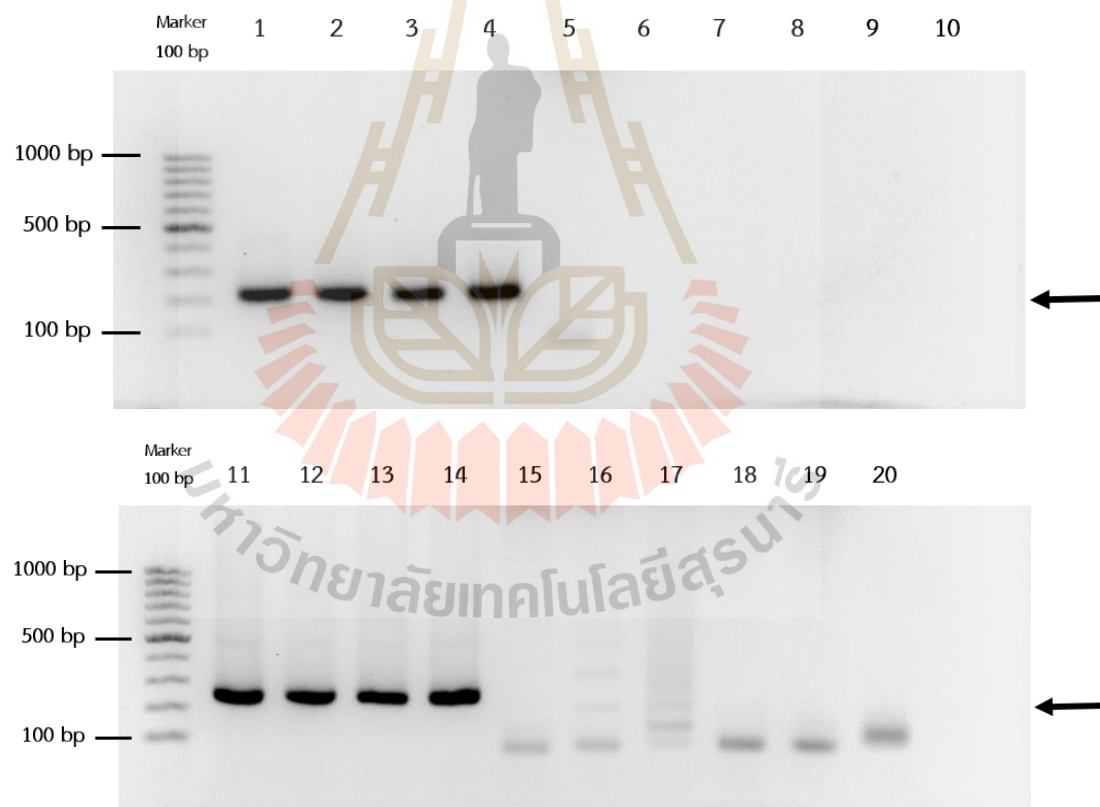
Lane 1-2, NSP2 gene at ~200 bp

Lane 3, Negative control (without DNA template)

Numbers at the left are DNA sizes in bp

4.2 Cloning of the DNA amplicons coding for NSP2 into cloning vector

The PCR amplicons of NSP2 coding sequence were ligated separately into pTG19-T PCR cloning vector. The ligation products were individually transformed into *E. coli* stain DH5 α cloning host. The colonies (transformed *E. coli*) were randomly screened by colony PCR using specific primers. The clones that carried the NSP2 inserts gave positive PCR amplicons at the expected sizes (**Figure 4.2**). The recombinant plasmid confirmed as positive was selected to obtain the NSP2 fragment to be cloned. All positive colonies were collected and kept in 20% glycerol in Luria-Bertani (LB) broth medium at -80 °C as gene stocks.



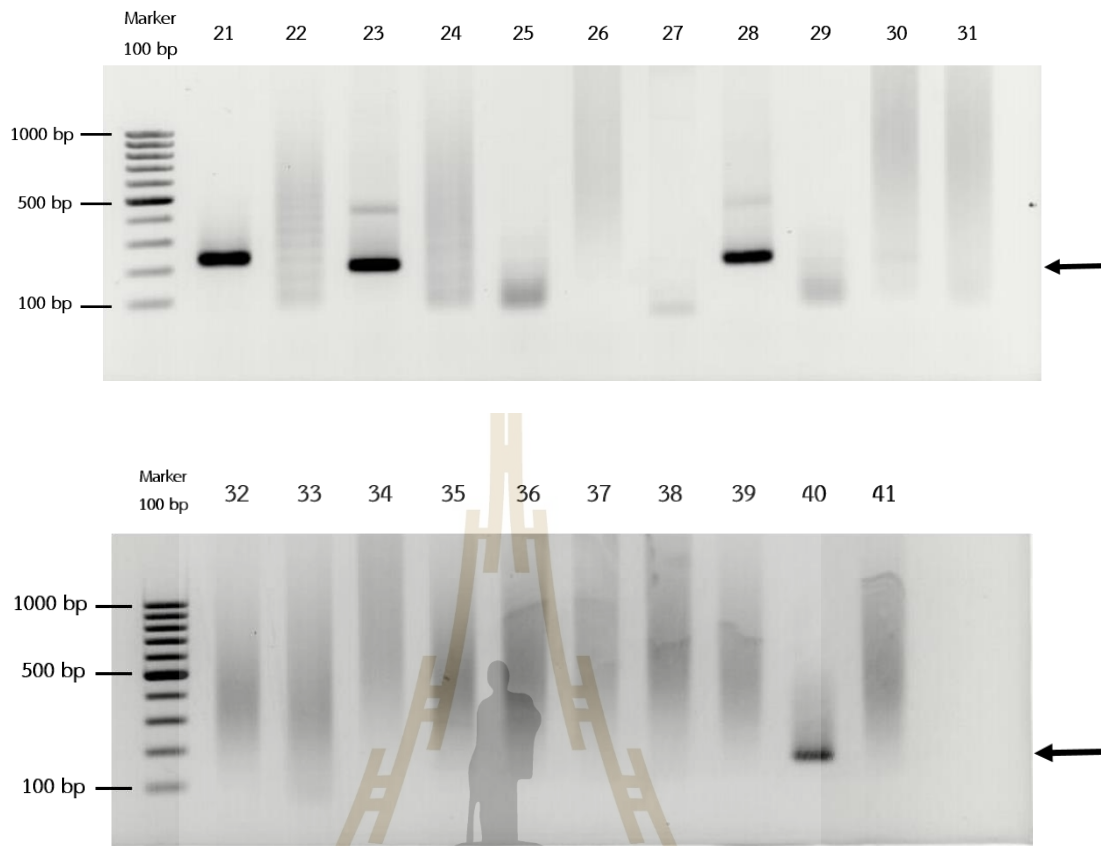


Figure 4.2 Gel electrophoresis image of PCR amplicons of the NSP2 sequences (~200 bp; arrow) from randomly picked transformed NSP2-plasmid-transformed *E. coli*.

Lane M, Gene Ruler DNA ladder mix 100 bp

Lane 1-41, NSP2 amplicons from *E. coli* clones 1-41, respectively

Numbers at the left are DNA sizes in bp

4.3 Extraction of NSP2/pTG19-T plasmid

The recombinant plasmids synthesized by incorporating the cDNA fragment of the SARS-CoV-2 nsp2 gene into a pTG19-T vector were used in this study. The extracted plasmids were initially analyzed with PCR where a clear band was observed for ~3080 bp primers in 1% agarose gel electrophoresis. After a successful confirmation, the plasmid products were subjected to NSP2/pTG19-T plasmid digestion by Cas12a.

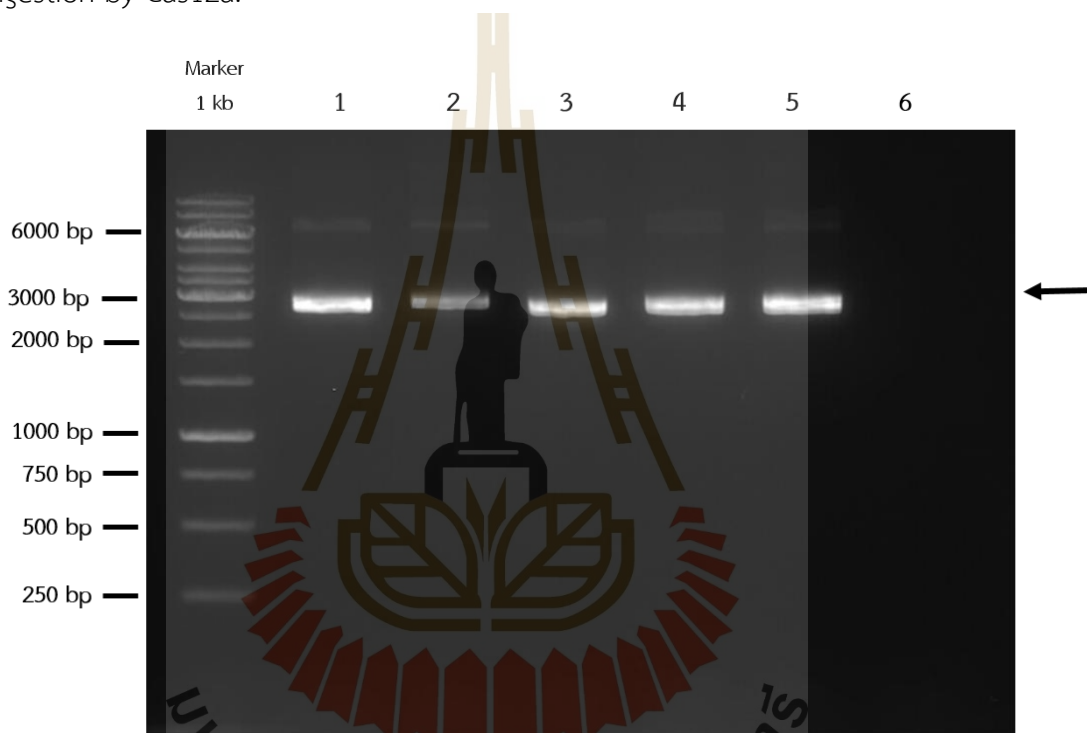


Figure 4.3 Gel electrophoresis image of plasmid extraction of NSP2/pTG19-T plasmid amplicons ~3080 bp from plasmids extraction at the expected size.

Lane M, Gene Ruler DNA ladder mix 1 kb

Lane 1-5, NSP2/pTG19-T plasmid amplicons from *E. coli* clones 1-5 (~3080 bp)
(arrow)

Lane 6, Negative control (without NSP2 plasmids template)

Numbers at the left are DNA sizes in bp

4.4 Verification of DNA sequences coding for NSP2

To verification of DNA sequences coding for NSP2, the DNA sequences were successfully verified as coding sequences of NSP2. The respective sequences were searched for homology by comparing with the sequences in the database. The SARS-CoV-2 NSP2 sequence of specific coronavirus variant as indicated was aligned using NCBI Multiple Sequence Alignment Viewer and Bio Edit Program and found the locations of sequence of NSP2 from 2 NSP2/pTG19-T plasmid were similar to most SARS-CoV-2 NSP2. They were found to have 99.5% similar with the database sequences of the SARS-CoV-2 NSP2 (Figure 4.4). After a successful confirmation, the NSP2/ pTG19-T plasmid were subjected to be known positive for test whether the crRNA could enable CRISPR-Cas12a to specifically detect SARS-CoV-2 NSP2 in NSP2/ pTG19-T plasmid.

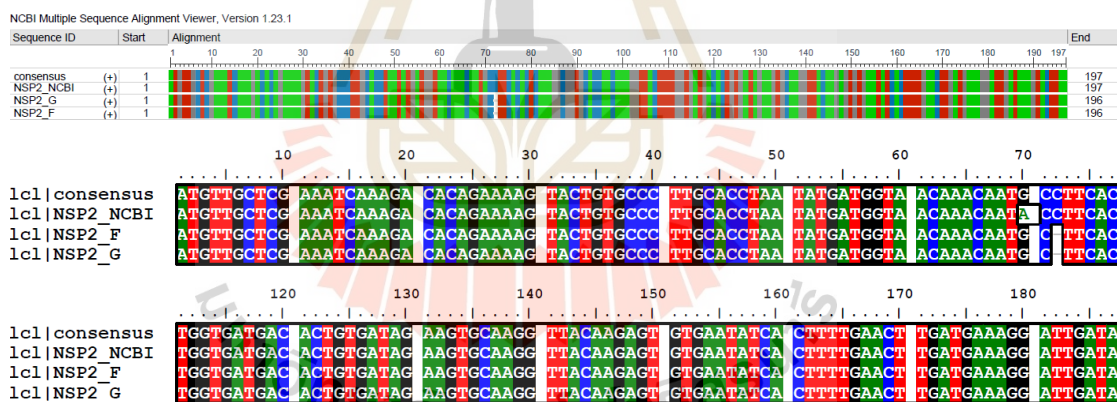


Figure 4.4 DNA multiple alignment of NSP2.

4.5 The Cas12a can directly detect SARS-CoV-2 NSP2 in NSP2/ pTG19-T plasmid using specific crRNA

To obtain efficient and specific crRNA applicable for detecting SARS-CoV-2 NSP2, the recombinant plasmids synthesized by incorporating the cDNA fragment of the SARS-CoV-2 NSP2 gene into a pTG19-T cloning vector were used in this study. To test whether the crRNA could enable CRISPR-Cas12a to specifically detect SARS-CoV-2 NSP2 in NSP2/ pTG19-T plasmid, this method perfectly shows the excellent CRISPR-Cas12a can directly and specifically detect NSP2/ pTG19-T plasmid. Cas12a exhibited variable targeted DNA cleavage efficiencies using crRNA. We used NSP2/ pTG19-T plasmid as an example to apply Cas12a specific digestion test for SARS-CoV-2 diagnosis. These results clearly showed that Cas12a was specific digested when induced with specific crRNA and not digested when left un-induced with no crRNA. The lane 1 indicated Cas12a digested specific crRNA. Lane 2 is a control contamination (Cas12a digestion reaction without plasmid). Lane 3 is a control crRNA specification (Cas12a digestion reaction without gRNA). Lane 4 is an uncut (plasmid without Cas12a digestion reaction). The agarose gel electrophoresis that belongs to **Figure 4.5** showing the NSP2/pTG19-T plasmid digestion by Cas12a.

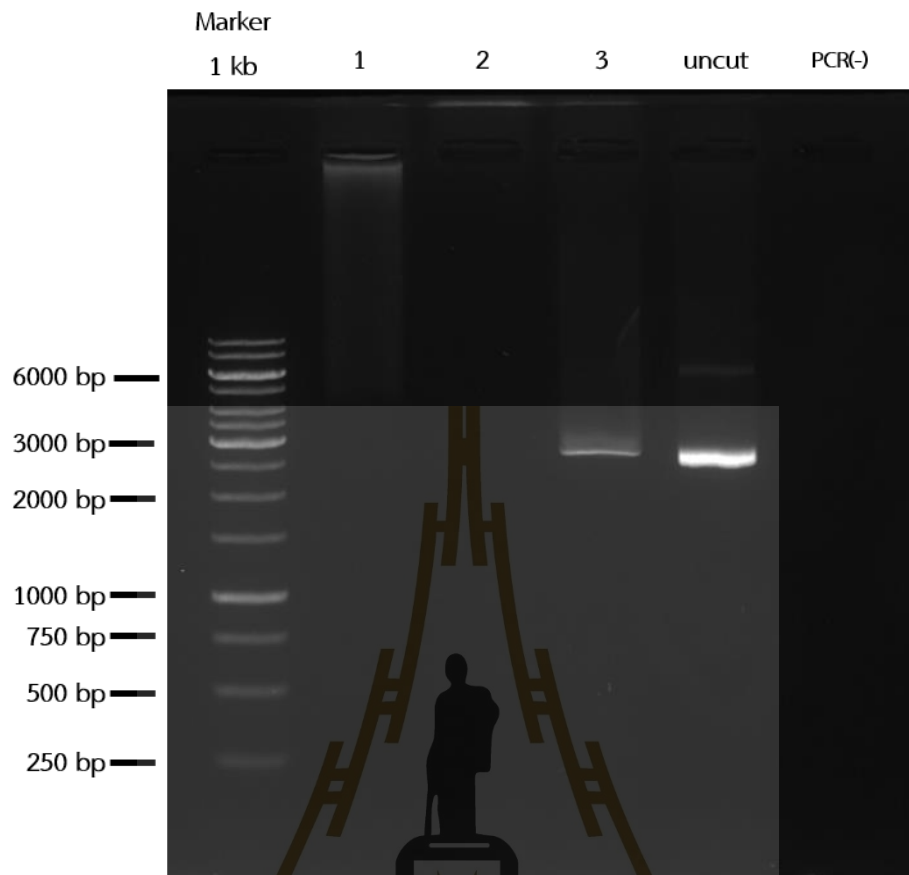


Figure 4.5 1% Agarose gel electrophoresis showing NSP2/pTG19-T plasmid digestion by Cas12a.

Lane M: Gene Ruler DNA ladder mix

Lane 1: NSP2/ pTG19-T plasmid+crRNA+Cas12a

Lane 2: no NSP2/ pTG19-T plasmid+crRNA+Cas12a

Lane 3: NSP2/ pTG19-T plasmid+ no crRNA+ Cas12a

Lane 4: Uncut NSP2/ pTG19-T plasmid

4.6 Establishment of NSP2/pTG19-T plasmid digestion by Cas12a assay for SARS-CoV-2 NSP2 detection and directly visualized the results on LFA

To determine whether the results of NSP2/pTG19-T plasmid digestion by Cas12a assay for SARS-CoV-2 NSP2 detection and could be directly read the results on lateral flow strips, we used DNA dipstick chromatography (Serve Science, Thailand) to readout the results. To obtain efficient and specific crRNA applicable for detecting SARS-CoV-2 NSP2, the recombinant plasmids synthesized by incorporating the cDNA fragment of the SARS-CoV-2 NSP2 gene into a pTG19-T cloning vector were used in this study. The synthesized plasmids were initially analyzed with PCR where a clear band was observed for 3080 bp primers in 1.5% agarose gel electrophoresis. After a successful confirmation, the PCR products were subjected to lateral flow readout of CRISPR-Cas12a activity using biotin-FITC reporter. The lateral flow dipstick was dipped into the reaction mixture and incubated for 15 minutes at room temperature. The results were observed after fifteen minutes. A sample with containing NSP2/pTG19-T plasmid demonstrated a signal significantly increasing strong band intensity on the test line and decreasing on the control line was considered to have a positive result. A sample without NSP2/pTG19-T plasmid was used as a control and had an intense line at the control line. Positive results were recognized by the T-line on the strip's upper side while negative results were recognized by the C-line on the strip's bottom side (**Figure 4.6**).

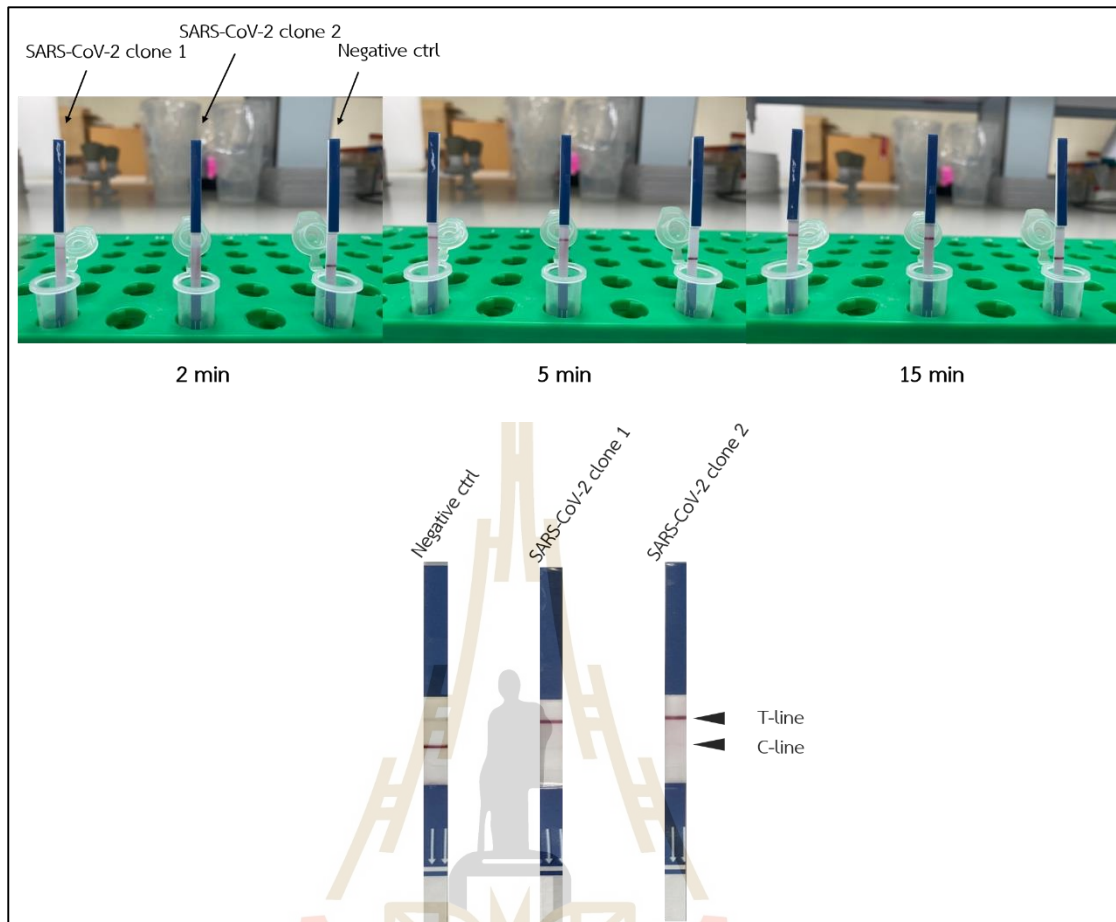


Figure 4.6 The LFA result interpretation of NSP2/pTG19-T plasmid digestion by Cas12a assay after 2, 5, and 15 min.

4.7 SARS-CoV-2 detection using RPA-Cas12a and LFA

To further simplify the detection procedure, we adapted the instrument-free lateral flow assay in RPA-Cas12a detection. The lateral flow strips were used in the reaction. If the target gene was presented in RPA product, the reporter is cleaved by Cas12a and thus develops a dark color at the T line in the LFA strip. By contrast, if the target was not presented, the intact reporter only develops a dark color at the C line. The cDNAs were initially analyzed with RPA where a clear band was observed for 200 bp primers in 1% agarose gel electrophoresis (**Figure 4.7**). After a successful confirmation, the RPA products were subjected to lateral flow readout of CRISPR-Cas12a activity using biotin-FITC reporter. We first examined whether RPA-Cas12a-LFA could detect SARS-CoV-2 NSP2 gene using the RPA products. The crRNA was used RPA-Cas12a-LFA detection. The results showed that sample numbers 19, 35, and 37 developed clear positive T lines, implying successful detection of the NSP2 gene of SARS-CoV-2. In contrast with a negative sample, the crRNA failed to detect the SARS-CoV-2 NSP2, probably due to the target was not presented, the intact reporter only developed a dark color at the C line (**Figure 4.8**). These results indicate that RPA-Cas12a-LFA is able to detect the NSP2 gene of SARS-CoV-2.

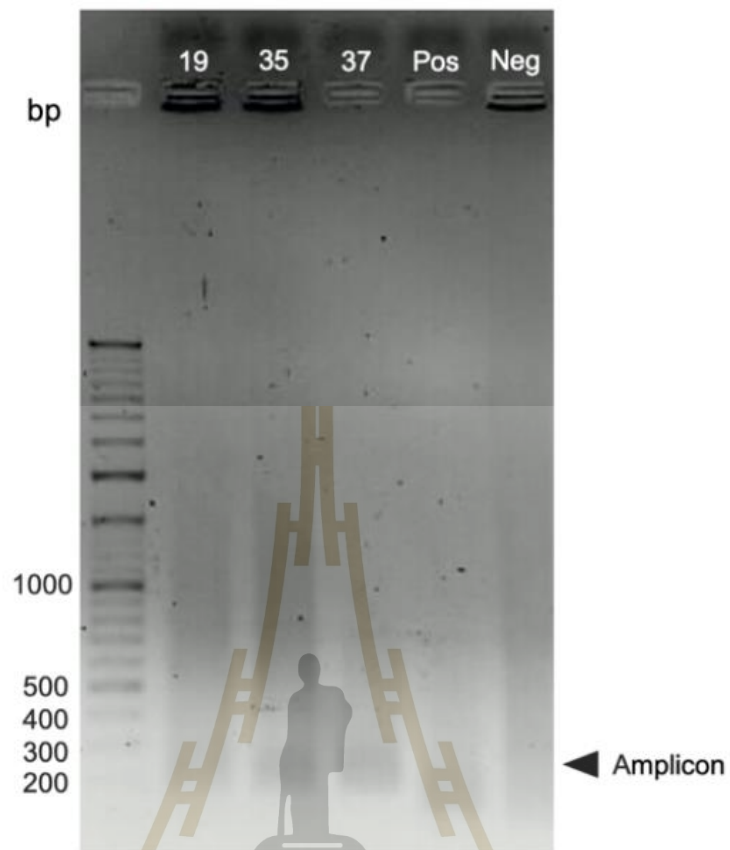


Figure 4.7 Gel electrophoresis image of RPA amplification of SARS-CoV-2 NSP2 cDNA fragments.

Lane numbers 19, 35 and 37, RPA product (~200 bp) (arrow)

Lane Pos, Positive control

Lane Neg, Negative control

Numbers at the left are DNA sizes in bp

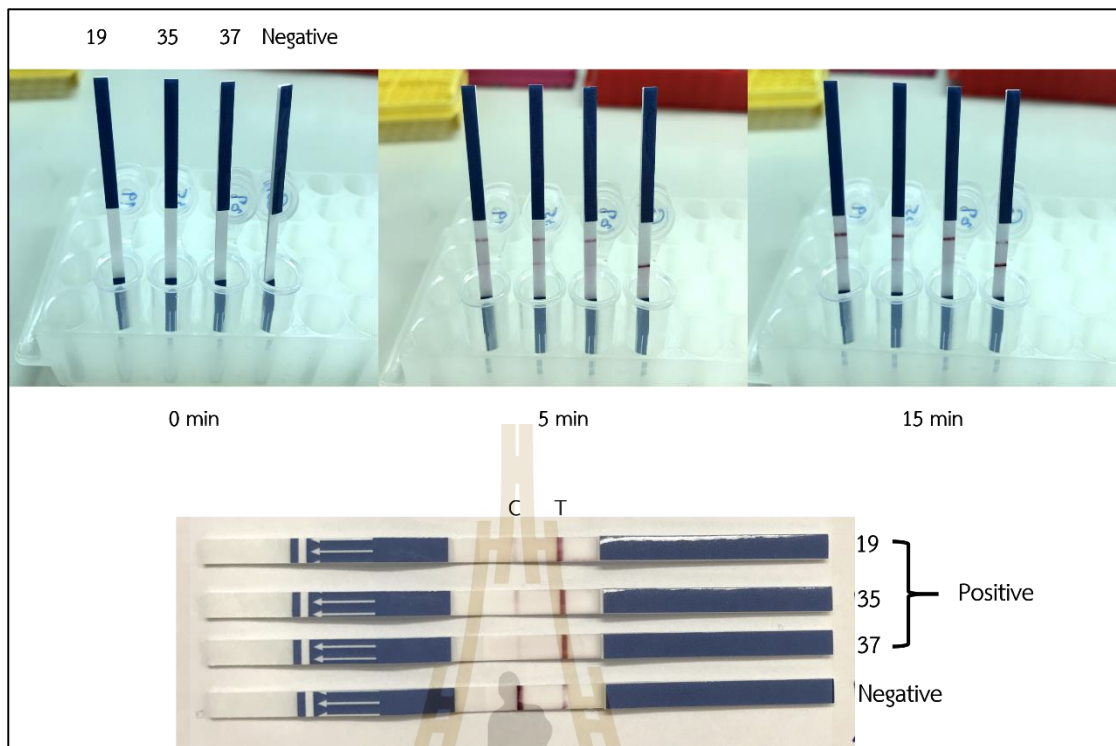


Figure 4.8 The LFA result interpretation of SARS-CoV-2 NSP2 cDNA fragment digestion by Cas12a assay after 2, 5, and 15 min.

4.8 The evaluation of the diagnostic performance of the assay for the detection of SARS-CoV-2

To evaluate the diagnostic performance of the assay for the detection of SARS-CoV-2 in comparison with real time RT-PCR using 15 positive clinical samples. Of these 15 samples, the real time RT-PCR detected 15 samples as positive. In the RPA-Cas12a-LFA assay, the samples were first amplified by RPA and then the amplified products were transferred into the Cas12a solution for cleavage and read out by LFA. The cDNAs were initially analyzed with RPA where a clear band was observed for 200 bp primers in 1% agarose gel electrophoresis (**Figure 4.9**). After a successful confirmation, the RPA products were subjected to lateral flow readout of CRISPR-Cas12a activity using biotin-FITC reporter. The RPA-Cas12a-LFA assay detected 15/15 positive samples as positive. The results from the assay were 100% concordant. The results of the RPA-Cas12a-LFA assay and real time RT-PCR are presented in **Table 4.1**. Two sample, number 1 and 3, which exhibited highest reporter activity in RPA-Cas12a-LFA-assay. The results showed that Cas12a/ crRNA/ NSP2 developed clear positive T-line which is implying successful detection of the targeted gene of SARS-CoV-2 NSP2. However, the other thirteen samples still to detect the target gene but successful detection requires highly active crRNA due to their weak reporter cleavage activities. These results indicate that RPA-Cas12a-LFA is able to detect the SARS-CoV-2 NSP2, but successful detection requires highly active crRNA. The advantage of the RPA-Cas12a-LFA assay for SARS-CoV-2 detection is that it is very convenient without the need for special equipment and the results can be visualized in 50 min.

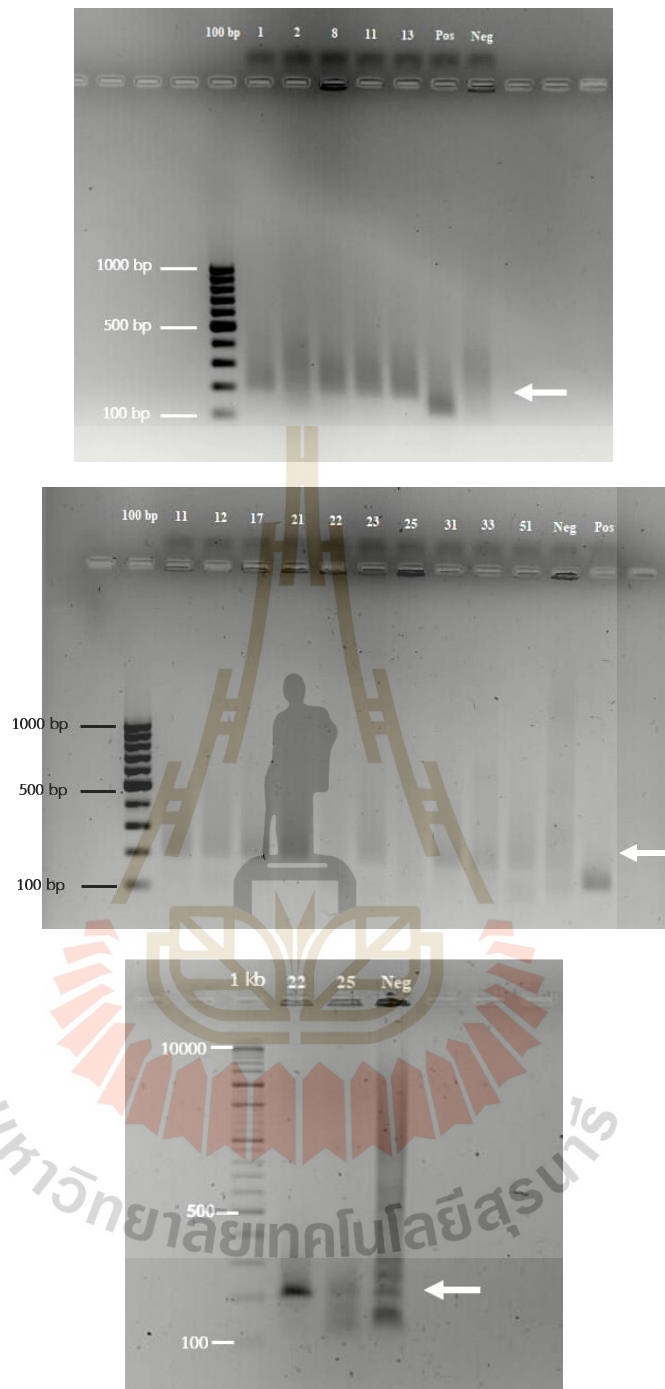


Figure 4.9 Gel electrophoresis image of RPA amplicons (200 bp; arrow) of SARS-CoV-2 NSP2 cDNA fragments. The positive samples of COVID-19 were converted to cDNA, and then were detected by agarose gel electrophoresis. Numbers at the left are DNA sizes in bp. Numbers at the upper are positive samples of COVID-19. “Neg” represents negative control (without DNA template); “Pos” represents positive control.



Figure 4.10 The qualitative analysis results of LFA. The positive samples of COVID-19 were extracted and converted to cDNA, and then were detected by LFA. Numbers at the light are positive samples of COVID-19. “Neg” represents negative control (without DNA template).

Table 4.1 The RPA-Cas12a-LFA results were consistent with the real-time PCR results, with 15 of 15 samples showing NSP2 detection. “/” band in RPA; “Pos” represents the strip test showed positive.

Sample No.	Std. RT-PCR		DNA amount	RPA: NSP2	Strip: NSP2
	ORF1ab/CT	E/CT			
1	18.21	18.59	4.7	/	Pos; T-line only
2	18.35	18.59	5.0	/	Pos; T-line only
8	16.00	16.09	9.1	/	Pos; T-line + C-line
11	16.32	16.46	5.3	/	Pos; T-line + C-line
13	15.93	16.03	4.8	/	Pos; T-line + C-line
31	21.47	21.78	6.3	/	Pos; T-line + C-line
33	22.49	22.61	6.6	/	Pos; T-line + C-line
51	20.77	20.76	7.2	/	Pos; Thin T-line + Thick C-line
11	22.81	23.28	10.5	/	Pos; T-line + C-line
12	22.08	22.21	5.1	/	Pos; T-line + C-line
17	33.16	34.99	5.1	/	Pos; T-line + C-line
21	32.78	34.38	4.8	/	Pos; T-line + C-line
22	28.38	28.71	3.8	/	Pos; T-line + C-line
23	32.79	34.97	5.7	/	Pos; T-line + C-line
25	33.48	35.22	2.9	/	Pos; T-line + C-line

CHAPTER V

DISCUSSION

As the rapidly evolving characteristic of SARS-CoV-2 might evade detection could result in low diagnostic sensitivity (Jeong et al., 2022). Reported prompt availability of the SARS-CoV-2 genome sequences was important for the development of COVID-19 diagnostic procedures notably the real-time RT-PCR (Sagoe et al., 2023). Real time RT-PCR is the current gold standard in COVID 19 diagnostics. The multiple temperatures employed in the real time RT-PCR reaction allow for tuning a range of properties, including primer annealing temperature, denaturation temperature, and extension temperature (Khan et al., 2020). However, this necessitates expensive instrumentation. Similarly, readout requires a skilled technician, or real-time fluorescence readout, requiring a real-time PCR instrument and typically limited to laboratories and requires skilled personnel and specialized equipment (Khan et al., 2020; Y. Zhu et al., 2022). A lack of accessible testing for identifying cases and close contacts has allowed SARS-CoV-2 to spread uncontrollably (Shihong Gao, Zhu, & Lu, 2021). As a result, this study aimed to use SARS-CoV-2 as a model for the development of CRISPR-Cas12a based molecular diagnostic tool that would be more appropriate in environments with resource-constrained regions. In our study, we combined RPA amplification and the advantages of Cas12a for SARS-CoV-2 detection based lateral flow strips test that allows the results could be visualized by the naked eye. The SARS-CoV-2 NSP2 was used for diagnostic primer design. The use of as much sequence data as possible is key to the identification of conserved viral sequences (Jeong et al., 2022). The COVID-19-NSP2 assay was highly specific without cross-reaction and did not amplify with other human-pathogenic coronaviruses and common respiratory viruses. Further, terms of cycle threshold values were satisfactory, with the total imprecision values well below

5% and also this assay showed 100% concordance using 59 clinical specimens from 14 confirmed cases with COVID-19 (Yip et al., 2020). Moreover, the global landscape of SARS-CoV-2 mutations and conserved regions revealed a NSP2 is a conserved region in the SARS-CoV-2 genome from 10,287,271 SARS-CoV-2 genome sequence (Abbasian et al., 2023). Thus, detecting hot spot mutations and conserved regions could be applied to improve the SARS-CoV-2 diagnostic efficiency.

To date, most laboratory diagnostics for COVID-19 require highly trained professional operators and require sophisticated instruments which are difficult to deploy in low resource regions. Hence, a technique for amplifying nucleotide chains using a simple temperature controller, and it is potentially used for point-of-care testing in fields or general laboratories at constant temperature that is of great value for resource-constrained regions. Currently, the outbreak of SARS CoV-2 in 2019 further promoted the application of RPA in nucleic acid detection (Y. Bai et al., 2022). RPA is a technique for amplifying nucleotide chains using a simple temperature controller. The major difference between RPA and real time RT-PCR is that RPA is performed at a constant temperature, whereas real time RT-PCR requires a temperature-changing system. The RPA is a highly sensitive and selective isothermal amplification technique. Due to its advantages like a simple operation, and low requirements for equipment, reaction at 37-42°C, with minimal sample preparation and so on it was expected to replace PCR (Lobato & O'Sullivan, 2018; Talwar et al., 2021; Tan et al., 2022). However, non-specific amplification is problematic with these approaches which weakens analytical specificity if target-specific detection probes are not used (Feng et al., 2021; Yüce et al., 2021). Following isothermal exponential amplification, CRISPR-Cas12a integrated with RPA amplification techniques improves both analytical specificity and sensitivity (Sun et al., 2021). The reaction temperature of the CRISPR-Cas12a is usually compatible with RPA and the optimum reaction temperature of Cas12a is 37 °C (M. Hu et al., 2022). CRISPR diagnostic approaches are high sensitivity and specificity because the sequence specificity needed for both the nucleic acid amplification phase and the CRISPR-Cas detection step (Y. Li, Li, Wang, & Liu, 2019). Cas12a is guided by a crRNA to cleave next to a specific RNA target

sequence and unique collateral cleavage activity (Talwar et al., 2021). Thus, methods of combining RPA with CRISPR-Cas12a have been successfully applied to the detection of SARS-CoV-2, the causative agent of the coronavirus disease of 2019 (COVID-19). CRISPR-Cas12a recognition is possible at room temperature, our approach has significant potential as it can be optimized as a single-step, room-temperature-operable detection tool.

The LFA detection can be used in the readout of Cas-mediated nucleic acid probe cleavage and making it suitable for point-of-care diagnostics (Kaminski, Abudayyeh, Gootenberg, Zhang, & Collins, 2021). In this study, we present an approach for the visual detection of the NSP2 gene of SARS-CoV-2 using CRISPR-Cas12a system. By a combination of a sample processing method and the RPA amplification with Cas12a-based detection, the sample to result can be obtained in 50 minutes via the naked eye. Because our assay does not need special equipment for a visual detection of SARS-CoV-2, its application may help the control of this pandemic.

In this study, the LFA used for the RPA-Cas12a detection has anti biotin and anti-mouse IgG antibodies inserted into the control line (C-line) and test line (T-line). The 5' and 3' ends of the lateral flow reporter were labeled with biotin and FITC, respectively. The dual-labeled reporter, in which the biotin/FITC label is bind by mobile gold conjugated anti-FITC antibodies and the biotin is bind by anti-biotin, will remain intact if the crRNA is unable to recognize the target DNA. In such an incidence, a C-line with strong intensity and faint or no T-line is seen. However, collateral cleavage occurs when the activated Cas12a cuts the dual-labeled reporter if the crRNA recognizes the target DNA. A strong T-line intensity and/or a weak C-line intensity results from the separation of biotin and FITC labels caused by the cleavage. The appearance of the test line indicates that the results are positive, which was the case in our results. When the target was not present, it was found during the experiment that the no template control had a weak T-line present. The presence of a faint T-line could be explained by the dose hook effect, where the amount of reporter added impacts the C- and T-line, which might cause misinterpretation of results, leading to false positive results (Breitbach, 2020).

Finally, we evaluated our system using 15 clinical samples initially diagnosed by real time RT-PCR. The results showed 100% consistency between our assay and the real time RT-PCR readouts for the positive samples. A major limitation of this study is that the size of the cohort (15 cases of positive samples) is small. With the small sample size, the diagnostic performance of the nucleic acid detection using CRISPR-Cas technologies in the clinical specimens could not be reliably evaluated.

The performance of the lateral flow strips based on CRISPR-Cas12a combined with RPA for SARS-CoV detection method does not require sophisticated equipment such as thermocyclers, and, with minimal training, can be carried out by personnel. Thus, our study is the first to develop a novel LFA strip that can be adopted as a simple, rapid, sensitive, on-site, and specific diagnostic tool to benefit future investigations for the detection of SARS-CoV-2 NSP2 and the design of proper prevention and control strategies for this devastating disease, especially in resource-limited areas. These results should be carefully interpreted due to the insufficient number of samples. A larger cohort would be helpful to better understand the sensitivity and specificity and also provide confidence that this assay is adequate to address the pandemic's needs for scalable and accurate testing.

CHAPTER VI

CONCLUSION AND RECOMMENDATION

In this work, we demonstrated the LFA based on CRISPR-Cas12a combined with RPA for the fast detection of SARS-CoV-2 NSP2 with specificity and sensitivity as a proof of concept for COVID-19 diagnosis. The plasmid was prepared by incorporating the NSP2 gene segment of the SARS-CoV-2 genome into a pTG19-T vector and transformed into *E. coli* cells. The presence of the desired gene in the plasmid was confirmed by DNA sequencing and PCR reactions. Additionally, we proved the possibility of a NSP2 gene as a target for detection for developing the lateral flow strips based on CRISPR-Cas12a combined with RPA for detecting SARS-CoV-2 infection. By using lateral flow strips based on CRISPR-Cas12a combined with RPA, the approach shows that CRISPR-Cas12a combined with RPA is a viable alternative for diagnosing SARS-CoV-2 NSP2 in samples. Our assay facilitated in does not require equipment such as thermo cyclers. Altogether, these results demonstrated that the whole test procedure is instrument-free and enables the detection NSP2 gene at body temperature with short incubation time and a robust method for revolutionizing the nucleic acid amplification-based detection of SARS-CoV-2 cDNA fragments. However, a good alternative would be to use more specimens for other respiratory syndrome virus specificity. The study recommends increasing the number of experimental samples as well as conducting tests with other respiratory syndrome viruses with the gold standard for detecting clinical samples and examining their sensitivity and specificity for accuracy and reliability. In the future, we envision bringing the entire process to develop a fully integrated LFA platform for rapid, sensitive, and real-time POC diagnostics of infectious pathogens, which may be a more suitable diagnostic technology for detecting infectious pathogens, including COVID-19 in under- resourced

populations in low- and middle-income nations, as there is still a need for screening and testing. The technology can also be researched for use against similar viral infections and may aid the development of reliable infectious pathogens diagnostic tools or possible other pandemic outbreaks.



REFERENCES

- Abbasian, M. H., Mahmanzar, M., Rahimian, K., Mahdavi, B., Tokhanbigli, S., Moradi, B., . . . Deng, Y. (2023). Global landscape of SARS-CoV-2 mutations and conserved regions. *Journal of Translational Medicine*, *21*(1), 152. doi:10.1186/s12967-023-03996-w
- Alhabbab, R. Y. (2022). Lateral Flow Immunoassays for Detecting Viral Infectious Antigens and Antibodies. *Micromachines (Basel)*, *13*(11). doi:10.3390/mi13111901
- Anjum, F., Mohammad, T., Asrani, P., Shafie, A., Singh, S., Yadav, D. K., . . . Hassan, M. I. (2022). Identification of intrinsically disorder regions in non-structural proteins of SARS-CoV-2: New insights into drug and vaccine resistance. *Molecular and Cellular Biochemistry*, *477*(5), 1607-1619. doi:10.1007/s11010-022-04393-5
- Arya, R., Kumari, S., Pandey, B., Mistry, H., Bihani, S. C., Das, A., . . . Kumar, M. (2021). Structural insights into SARS-CoV-2 proteins. *J Mol Biol*, *433*(2), 166725. doi:10.1016/j.jmb.2020.11.024
- Bai, C., Zhong, Q., & Gao, G. F. (2022). Overview of SARS-CoV-2 genome-encoded proteins. *Sci China Life Sci*, *65*(2), 280-294. doi:10.1007/s11427-021-1964-4
- Bai, Y., Ji, J., Ji, F., Wu, S., Tian, Y., Jin, B., & Li, Z. (2022). Recombinase polymerase amplification integrated with microfluidics for nucleic acid testing at point of care. *Talanta*, *240*, 123209. doi:10.1016/j.talanta.2022.123209
- Bandyopadhyay, A., Kancharla, N., Javalkote, V. S., Dasgupta, S., & Brutnell, T. P. (2020). CRISPR-Cas12a (Cpf1): A Versatile Tool in the Plant Genome Editing Tool Box for Agricultural Advancement. *Front Plant Sci*, *11*, 584151. doi:10.3389/fpls.2020.584151
- Barrangou, R., Fremaux, C., Deveau, H., Richards, M., Boyaval, P., Moineau, S., . . . Horvath, P. (2007). CRISPR provides acquired resistance against viruses in prokaryotes. *Science*, *315*(5819), 1709-1712. doi:10.1126/science.1138140

- Bharathkumar, N., Sunil, A., Meera, P., Aksah, S., Kannan, M., Saravanan, K. M., & Anand, T. (2022). CRISPR/Cas-Based Modifications for Therapeutic Applications: A Review. *Mol Biotechnol*, *64*(4), 355-372. doi:10.1007/s12033-021-00422-8
- Bills, C., Xie, X., & Shi, P. Y. (2023). The multiple roles of nsp6 in the molecular pathogenesis of SARS-CoV-2. *Antiviral Res*, *213*, 105590. doi:10.1016/j.antiviral.2023.105590
- Bonini, A., Poma, N., Vivaldi, F., Kirchhain, A., Salvo, P., Bottai, D., . . . Di Francesco, F. (2021). Advances in biosensing: The CRISPR/Cas system as a new powerful tool for the detection of nucleic acids. *J Pharm Biomed Anal*, *192*, 113645. doi:10.1016/j.jpba.2020.113645
- Boonbanjong, P., Treerattrakoon, K., Waiwinya, W., Pitikultham, P., & Japrun, D. (2022). Isothermal Amplification Technology for Disease Diagnosis. *Biosensors (Basel)*, *12*(9). doi:10.3390/bios12090677
- Brant, A. C., Tian, W., Majerciak, V., Yang, W., & Zheng, Z.-M. (2021). SARS-CoV-2: from its discovery to genome structure, transcription, and replication. *Cell & Bioscience*, *11*(1), 136. doi:10.1186/s13578-021-00643-z
- Breitbach, A. (2020). Lateral Flow Readout for CRISPR/Cas-Based Detection Strategies. Retrieved from <https://www.milenia-biotec.com/en/tips-lateral-flow-readouts-crispr-cas-strategies/>
- Broughton, J. P., Deng, X., Yu, G., Fasching, C. L., Servellita, V., Singh, J., . . . Chiu, C. Y. (2020). CRISPR-Cas12-based detection of SARS-CoV-2. *Nat Biotechnol*, *38*(7), 870-874. doi:10.1038/s41587-020-0513-4
- Cascella, M., Rajnik, M., Aleem, A., Dulebohn, S. C., & Di Napoli, R. (2022). Features, Evaluation, and Treatment of Coronavirus (COVID-19). In *StatPearls*. Treasure Island (FL): StatPearls Publishing
- Copyright © 2022, StatPearls Publishing LLC.
- Cascella, M., Rajnik, M., Aleem, A., Dulebohn, S. C., & Di Napoli, R. (2023). Features, Evaluation, and Treatment of Coronavirus (COVID-19). In *StatPearls*. Treasure Island (FL) ineligible companies. Disclosure: Michael Rajnik declares no relevant financial relationships with ineligible companies. Disclosure: Abdul

Aleem declares no relevant financial relationships with ineligible companies.
 Disclosure: Scott Dulebohn declares no relevant financial relationships with ineligible companies. Disclosure: Raffaella Di Napoli declares no relevant financial relationships with ineligible companies.: StatPearls Publishing

Copyright © 2023, StatPearls Publishing LLC.

- Chadha, J., Khullar, L., & Mittal, N. (2022). Facing the wrath of enigmatic mutations: a review on the emergence of severe acute respiratory syndrome coronavirus 2 variants amid coronavirus disease-19 pandemic. *Environ Microbiol*, *24*(6), 2615-2629. doi:10.1111/1462-2920.15687
- Chakravarti, R., Singh, R., Ghosh, A., Dey, D., Sharma, P., Velayutham, R., . . . Ghosh, D. (2021). A review on potential of natural products in the management of COVID-19. *RSC Adv*, *11*(27), 16711-16735. doi:10.1039/d1ra00644d
- Chavda, V. P., Valu, D. D., Parikh, P. K., Tiwari, N., Chhipa, A. S., Shukla, S., . . . Patravale, V. (2023). Conventional and Novel Diagnostic Tools for the Diagnosis of Emerging SARS-CoV-2 Variants. *Vaccines*, *11*(2), 374. Retrieved from <https://www.mdpi.com/2076-393X/11/2/374>
- Chen, J. S., Ma, E., Harrington, L. B., Da Costa, M., Tian, X., Palefsky, J. M., & Doudna, J. A. (2018). CRISPR-Cas12a target binding unleashes indiscriminate single-stranded DNase activity. *Science*, *360*(6387), 436-439. doi:10.1126/science.aar6245
- Chen, Y., Liu, Q., & Guo, D. (2020). Emerging coronaviruses: Genome structure, replication, and pathogenesis. *J Med Virol*, *92*(4), 418-423. doi:10.1002/jmv.25681
- Cherkaoui, D., Huang, D., Miller, B. S., Turbé, V., & McKendry, R. A. (2021). Harnessing recombinase polymerase amplification for rapid multi-gene detection of SARS-CoV-2 in resource-limited settings. *Biosens Bioelectron*, *189*, 113328. doi:10.1016/j.bios.2021.113328
- Choi, J. Y., & Smith, D. M. (2021). SARS-CoV-2 Variants of Concern. *Yonsei Med J*, *62*(11), 961-968. doi:10.3349/ymj.2021.62.11.961

- Cleverley, J., Piper, J., & Jones, M. M. (2020). The role of chest radiography in confirming covid-19 pneumonia. *BMJ*, *370*, m2426. doi:10.1136/bmj.m2426
- Courouble, V. V., Dey, S. K., Yadav, R., Timm, J., Harrison, J., Ruiz, F. X., . . . Griffin, P. R. (2021). Revealing the Structural Plasticity of SARS-CoV-2 nsp7 and nsp8 Using Structural Proteomics. *J Am Soc Mass Spectrom*, *32*(7), 1618-1630. doi:10.1021/jasms.1c00086
- Cradic, K., Lockhart, M., Ozbolt, P., Fatica, L., Landon, L., Lieber, M., . . . Antonara, S. (2020). Clinical Evaluation and Utilization of Multiple Molecular In Vitro Diagnostic Assays for the Detection of SARS-CoV-2. *Am J Clin Pathol*, *154*(2), 201-207. doi:10.1093/ajcp/aqaa097
- Cui, J., Li, F., & Shi, Z. L. (2019). Origin and evolution of pathogenic coronaviruses. *Nat Rev Microbiol*, *17*(3), 181-192. doi:10.1038/s41579-018-0118-9
- Davis, H. E., McCorkell, L., Vogel, J. M., & Topol, E. J. (2023). Long COVID: major findings, mechanisms and recommendations. *Nat Rev Microbiol*, *21*(3), 133-146. doi:10.1038/s41579-022-00846-2
- Dhama, K., Khan, S., Tiwari, R., Sircar, S., Bhat, S., Malik, Y. S., . . . Rodriguez-Morales, A. J. (2020). Coronavirus Disease 2019-COVID-19. *Clin Microbiol Rev*, *33*(4). doi:10.1128/cmr.00028-20
- Dominguez Andres, A., Feng, Y., Campos, A. R., Yin, J., Yang, C. C., James, B., . . . Ronai, Z. A. (2020). SARS-CoV-2 ORF9c Is a Membrane-Associated Protein that Suppresses Antiviral Responses in Cells. *bioRxiv*. doi:10.1101/2020.08.18.256776
- Dong, X., Liu, L., Tu, Y., Zhang, J., Miao, G., Zhang, L., . . . Qiu, X. (2021). Rapid PCR powered by microfluidics: A quick review under the background of COVID-19 pandemic. *TrAC Trends in Analytical Chemistry*, *143*, 116377. doi:<https://doi.org/10.1016/j.trac.2021.116377>
- Dramé, M., Tabue Teguo, M., Proye, E., Hequet, F., Hentzien, M., Kanagaratnam, L., & Godaert, L. (2020). Should RT-PCR be considered a gold standard in the diagnosis of COVID-19? *J Med Virol*, *92*(11), 2312-2313. doi:10.1002/jmv.25996
- Dutta, D., Naiyer, S., Mansuri, S., Soni, N., Singh, V., Bhat, K. H., . . . Mansuri, M. S. (2022). COVID-19 Diagnosis: A Comprehensive Review of the RT-qPCR Method

- for Detection of SARS-CoV-2. *Diagnostics (Basel)*, *12*(6). doi:10.3390/diagnostics12061503
- Feng, W., Peng, H., Xu, J., Liu, Y., Pabbaraju, K., Tipples, G., . . . Le, X. C. (2021). Integrating Reverse Transcription Recombinase Polymerase Amplification with CRISPR Technology for the One-Tube Assay of RNA. *Anal Chem*, *93*(37), 12808-12816. doi:10.1021/acs.analchem.1c03456
- Figueroa, S., Freire-Paspuel, B., Vega-Mariño, P., Velez, A., Cruz, M., Cardenas, W. B., & Garcia-Bereguian, M. A. (2021). High sensitivity-low cost detection of SARS-CoV-2 by two steps end point RT-PCR with agarose gel electrophoresis visualization. *Sci Rep*, *11*(1), 21658. doi:10.1038/s41598-021-00900-8
- Flower, T. G., Buffalo, C. Z., Hooy, R. M., Allaire, M., Ren, X., & Hurley, J. H. (2021). Structure of SARS-CoV-2 ORF8, a rapidly evolving immune evasion protein. *Proc Natl Acad Sci U S A*, *118*(2). doi:10.1073/pnas.2021785118
- Fraser, R., Orta-Resendiz, A., Dockrell, D., Müller-Trutwin, M., & Mazein, A. (2023). Severe COVID-19 versus multisystem inflammatory syndrome: comparing two critical outcomes of SARS-CoV-2 infection. *European Respiratory Review*, *32*(167), 220197. doi:10.1183/16000617.0197-2022
- Gao, W., Wang, L., Ju, X., Zhao, S., Li, Z., Su, M., . . . Zhang, W. (2022). The Deubiquitinase USP29 Promotes SARS-CoV-2 Virulence by Preventing Proteasome Degradation of ORF9b. *mBio*, *13*(3), e0130022. doi:10.1128/mbio.01300-22
- Gasiunas, G., Barrangou, R., Horvath, P., & Siksnys, V. (2012). Cas9-crRNA ribonucleoprotein complex mediates specific DNA cleavage for adaptive immunity in bacteria. *Proc Natl Acad Sci U S A*, *109*(39), E2579-2586. doi:10.1073/pnas.1208507109
- Ghosh, N., Saha, I., & Sharma, N. (2022). Palindromic target site identification in SARS-CoV-2, MERS-CoV and SARS-CoV-1 by adopting CRISPR-Cas technique. *Gene*, *818*, 146136. doi:10.1016/j.gene.2021.146136
- Guglielmi, G. (2020). First CRISPR test for the coronavirus approved in the United States. *Nature*. doi:10.1038/d41586-020-01402-9

- Guo, J., Ge, J., & Guo, Y. (2022). Recent advances in methods for the diagnosis of Corona Virus Disease 2019. *J Clin Lab Anal*, 36(1), e24178. doi:10.1002/jcla.24178
- Hachim, A., Gu, H., Kavian, O., Mori, M., Kwan, M. Y. W., Chan, W. H., . . . Kavian, N. (2022). SARS-CoV-2 accessory proteins reveal distinct serological signatures in children. *Nat Commun*, 13(1), 2951. doi:10.1038/s41467-022-30699-5
- Han, L., Zhuang, M. W., Deng, J., Zheng, Y., Zhang, J., Nan, M. L., . . . Wang, P. H. (2021). SARS-CoV-2 ORF9b antagonizes type I and III interferons by targeting multiple components of the RIG-I/MDA-5-MAVS, TLR3-TRIF, and cGAS-STING signaling pathways. *J Med Virol*, 93(9), 5376-5389. doi:10.1002/jmv.27050
- Hassan, S. S., Basu, P., Redwan, E. M., Lundstrom, K., Choudhury, P. P., Serrano-Aroca, Á., . . . Uversky, V. N. (2022). Periodically aperiodic pattern of SARS-CoV-2 mutations underpins the uncertainty of its origin and evolution. *Environ Res*, 204(Pt B), 112092. doi:10.1016/j.envres.2021.112092
- Hu, B., Guo, H., Zhou, P., & Shi, Z. L. (2021). Characteristics of SARS-CoV-2 and COVID-19. *Nat Rev Microbiol*, 19(3), 141-154. doi:10.1038/s41579-020-00459-7
- Hu, M., Qiu, Z., Bi, Z., Tian, T., Jiang, Y., & Zhou, X. (2022). Photocontrolled crRNA activation enables robust CRISPR-Cas12a diagnostics. *Proceedings of the National Academy of Sciences*, 119(26), e2202034119. doi:doi:10.1073/pnas.2202034119
- Huang, C., Wang, Y., Li, X., Ren, L., Zhao, J., Hu, Y., . . . Cao, B. (2020). Clinical features of patients infected with 2019 novel coronavirus in Wuhan, China. *Lancet*, 395(10223), 497-506. doi:10.1016/s0140-6736(20)30183-5
- Huang, H., Huang, G., Tan, Z., Hu, Y., Shan, L., Zhou, J., . . . Rong, Z. (2022). Engineered Cas12a-Plus nuclease enables gene editing with enhanced activity and specificity. *BMC Biol*, 20(1), 91. doi:10.1186/s12915-022-01296-1
- Jeong, H., Lee, S., Ko, J., Ko, M., & Seo, H. W. (2022). Identification of conserved regions from 230,163 SARS-CoV-2 genomes and their use in diagnostic PCR primer design. *Genes Genomics*, 44(8), 899-912. doi:10.1007/s13258-022-01264-7

- Jiang, W., Ji, W., Zhang, Y., Xie, Y., Chen, S., Jin, Y., & Duan, G. (2022). An Update on Detection Technologies for SARS-CoV-2 Variants of Concern. *Viruses*, *14*(11). doi:10.3390/v14112324
- Jiang, Y., Wu, Q., Song, P., & You, C. (2021). The Variation of SARS-CoV-2 and Advanced Research on Current Vaccines. *Front Med (Lausanne)*, *8*, 806641. doi:10.3389/fmed.2021.806641
- Jiménez, A., Hoff, B., & Revuelta, J. L. (2020). Multiplex genome editing in *Ashbya gossypii* using CRISPR-Cpf1. *N Biotechnol*, *57*, 29-33. doi:10.1016/j.nbt.2020.02.002
- Kabir, M. A., Ahmed, R., Iqbal, S. M. A., Chowdhury, R., Paulmurugan, R., Demirci, U., & Asghar, W. (2021). Diagnosis for COVID-19: current status and future prospects. *Expert Rev Mol Diagn*, *21*(3), 269-288. doi:10.1080/14737159.2021.1894930
- Kadam, S. B., Sukhramani, G. S., Bishnoi, P., Pable, A. A., & Barvkar, V. T. (2021). SARS-CoV-2, the pandemic coronavirus: Molecular and structural insights. *J Basic Microbiol*, *61*(3), 180-202. doi:10.1002/jobm.202000537
- Kaminski, M. M., Abudayyeh, O. O., Gootenberg, J. S., Zhang, F., & Collins, J. J. (2021). CRISPR-based diagnostics. *Nature Biomedical Engineering*, *5*(7), 643-656. doi:10.1038/s41551-021-00760-7
- Kandwal, S., & Fayne, D. (2023). Genetic conservation across SARS-CoV-2 non-structural proteins - Insights into possible targets for treatment of future viral outbreaks. *Virology*, *581*, 97-115. doi:10.1016/j.virol.2023.02.011
- Khan, P., Aufdembrink, L. M., & Engelhart, A. E. (2020). Isothermal SARS-CoV-2 Diagnostics: Tools for Enabling Distributed Pandemic Testing as a Means of Supporting Safe Reopenings. *ACS Synth Biol*, *9*(11), 2861-2880. doi:10.1021/acssynbio.0c00359
- Kim, S., Ji, S., & Koh, H. R. (2021). CRISPR as a Diagnostic Tool. *Biomolecules*, *11*(8). doi:10.3390/biom11081162
- Kim, S. H., & AlMutawa, F. (2022). Tracheal Aspirate and Bronchoalveolar Lavage as Potential Specimen Types for COVID-19 Testing Using the Cepheid Xpert Xpress SARS-CoV-2/Flu/RSV. *Microbiol Spectr*, *10*(3), e0039922. doi:10.1128/spectrum.00399-22

- Knott, G. J., & Doudna, J. A. (2018). CRISPR-Cas guides the future of genetic engineering. *Science*, *361*(6405), 866-869. doi:10.1126/science.aat5011
- Koczula, K. M., & Gallotta, A. (2016). Lateral flow assays. *Essays Biochem*, *60*(1), 111-120. doi:10.1042/ebc20150012
- Konno, Y., Kimura, I., Uriu, K., Fukushi, M., Irie, T., Koyanagi, Y., . . . Sato, K. (2020). SARS-CoV-2 ORF3b Is a Potent Interferon Antagonist Whose Activity Is Increased by a Naturally Occurring Elongation Variant. *Cell Rep*, *32*(12), 108185. doi:10.1016/j.celrep.2020.108185
- Kung, Y. A., Lee, K. M., Chiang, H. J., Huang, S. Y., Wu, C. J., & Shih, S. R. (2022). Molecular Virology of SARS-CoV-2 and Related Coronaviruses. *Microbiol Mol Biol Rev*, *86*(2), e0002621. doi:10.1128/mmmbr.00026-21
- Lacasse, É., Gudimard, L., Dubuc, I., Gravel, A., Allaëys, I., Boilard, É., & Flamand, L. (2023). SARS-CoV-2 Nsp2 Contributes to Inflammation by Activating NF- κ B. *Viruses*, *15*(2). doi:10.3390/v15020334
- Li, D., Zhang, J., & Li, J. (2020). Primer design for quantitative real-time PCR for the emerging Coronavirus SARS-CoV-2. *Theranostics*, *10*(16), 7150-7162. doi:10.7150/thno.47649
- Li, J. Y., You, Z., Wang, Q., Zhou, Z. J., Qiu, Y., Luo, R., & Ge, X. Y. (2020). The epidemic of 2019-novel-coronavirus (2019-nCoV) pneumonia and insights for emerging infectious diseases in the future. *Microbes Infect*, *22*(2), 80-85. doi:10.1016/j.micinf.2020.02.002
- Li, Y., Li, S., Wang, J., & Liu, G. (2019). CRISPR/Cas Systems towards Next-Generation Biosensing. *Trends Biotechnol*, *37*(7), 730-743. doi:10.1016/j.tibtech.2018.12.005
- Liu, D. X., Liang, J. Q., & Fung, T. S. (2021). Human Coronavirus-229E, -OC43, -NL63, and -HKU1 (Coronaviridae). *Encyclopedia of Virology*, 428-440.
- Lobato, I. M., & O'Sullivan, C. K. (2018). Recombinase polymerase amplification: Basics, applications and recent advances. *Trends Analyt Chem*, *98*, 19-35. doi:10.1016/j.trac.2017.10.015
- Lu, R., Zhao, X., Li, J., Niu, P., Yang, B., Wu, H., . . . Tan, W. (2020). Genomic characterisation and epidemiology of 2019 novel coronavirus: implications for

- virus origins and receptor binding. *Lancet*, 395(10224), 565-574. doi:10.1016/s0140-6736(20)30251-8
- Machhi, J., Herskovitz, J., Senan, A. M., Dutta, D., Nath, B., Oleynikov, M. D., . . . Kevadiya, B. D. (2020). The Natural History, Pathobiology, and Clinical Manifestations of SARS-CoV-2 Infections. *J Neuroimmune Pharmacol*, 15(3), 359-386. doi:10.1007/s11481-020-09944-5
- Maison, D. P., Deng, Y., & Gerschenson, M. (2023). SARS-CoV-2 and the host-immune response. *Frontiers in Immunology*, 14. doi:10.3389/fimmu.2023.1195871
- Makiyama, K., Hazawa, M., Kobayashi, A., Lim, K., Voon, D. C., & Wong, R. W. (2022). NSP9 of SARS-CoV-2 attenuates nuclear transport by hampering nucleoporin 62 dynamics and functions in host cells. *Biochem Biophys Res Commun*, 586, 137-142. doi:10.1016/j.bbrc.2021.11.046
- Manghwar, H., Lindsey, K., Zhang, X., & Jin, S. (2019). CRISPR/Cas System: Recent Advances and Future Prospects for Genome Editing. *Trends Plant Sci*, 24(12), 1102-1125. doi:10.1016/j.tplants.2019.09.006
- Misiurina, M. A., Chirinskaite, A. V., Fotina, A. S., Zelinsky, A. A., Sopova, J. V., & Leonova, E. I. (2022). New PAM Improves the Single-Base Specificity of crRNA-Guided LbCas12a Nuclease. *Life*, 12(11), 1927. Retrieved from <https://www.mdpi.com/2075-1729/12/11/1927>
- Miyamoto, Y., Itoh, Y., Suzuki, T., Tanaka, T., Sakai, Y., Koido, M., . . . Oka, M. (2022). SARS-CoV-2 ORF6 disrupts nucleocytoplasmic trafficking to advance viral replication. *Commun Biol*, 5(1), 483. doi:10.1038/s42003-022-03427-4
- Mohamadian, M., Chiti, H., Shoghli, A., Biglari, S., Parsamanesh, N., & Esmailzadeh, A. (2021). COVID-19: Virology, biology and novel laboratory diagnosis. *J Gene Med*, 23(2), e3303. doi:10.1002/jgm.3303
- Mohanraju, P., Mougiakos, I., Albers, J., Mabuchi, M., Fuchs, R. T., Curcuru, J. L., . . . van der Oost, J. (2021). Development of a Cas12a-Based Genome Editing Tool for Moderate Thermophiles. *Crispr j*, 4(1), 82-91. doi:10.1089/crispr.2020.0086
- Mozzi, A., Oldani, M., Forcella, M. E., Vantaggiato, C., Cappelletti, G., Pontremoli, C., . . . Cagliani, R. (2023). SARS-CoV-2 ORF3c impairs mitochondrial respiratory

- metabolism, oxidative stress, and autophagic flux. *iScience*, 26(7), 107118. doi:10.1016/j.isci.2023.107118
- Munawar, M. A. (2022). Critical insight into recombinase polymerase amplification technology. *Expert Rev Mol Diagn*, 22(7), 725-737. doi:10.1080/14737159.2022.2109964
- Naranbat, D., Schneider, L., Kantor, R., Beckwith, C. G., Bazerman, L., Gillani, F., . . . Tripathi, A. (2022). DirectDetect SARS-CoV-2 Direct Real-Time RT-PCR Study Using Patient Samples. *ACS Omega*, 7(6), 4945-4955. doi:10.1021/acsomega.1c05595
- Nishimasu, H., & Nureki, O. (2017). Structures and mechanisms of CRISPR RNA-guided effector nucleases. *Curr Opin Struct Biol*, 43, 68-78. doi:10.1016/j.sbi.2016.11.013
- Nishitsuji, H., Iwahori, S., Ohmori, M., Shimotohno, K., & Murata, T. (2022). Ubiquitination of SARS-CoV-2 NSP6 and ORF7a Facilitates NF- κ B Activation. *mBio*, 13(4), e0097122. doi:10.1128/mbio.00971-22
- Nitika Dhuria, N. N., Vishal Sharma, Arun Kumar. (2023). Comparison of Cepheid Xpert Xpress SARS-CoV-2 Assay with Standard RT-PCR Test for Detection of COVID-19 Infection: A Retrospective Cohort Study. *Journal of Clinical and Diagnostic Research*, 17(2), DC20-DC23. doi:10.7860/jcdr/2023/59191.17541
- Ochani, R., Asad, A., Yasmin, F., Shaikh, S., Khalid, H., Batra, S., . . . Surani, S. (2021). COVID-19 pandemic: from origins to outcomes. A comprehensive review of viral pathogenesis, clinical manifestations, diagnostic evaluation, and management. *Infez Med*, 29(1), 20-36.
- Omotoso, O. E., Olugbami, J. O., & Gbadegesin, M. A. (2021). Assessment of intercontinents mutation hotspots and conserved domains within SARS-CoV-2 genome. *Infect Genet Evol*, 96, 105097. doi:10.1016/j.meegid.2021.105097
- Onyeaka, H., Anumudu, C. K., Al-Sharif, Z. T., Egele-Godswill, E., & Mbaegbu, P. (2021). COVID-19 pandemic: A review of the global lockdown and its far-reaching effects. *Sci Prog*, 104(2), 368504211019854. doi:10.1177/00368504211019854

- Parasher, A. (2021). COVID-19: Current understanding of its Pathophysiology, Clinical presentation and Treatment. *Postgrad Med J*, 97(1147), 312-320. doi:10.1136/postgradmedj-2020-138577
- Parolo, C., Sena-Torralba, A., Bergua, J. F., Calucho, E., Fuentes-Chust, C., Hu, L., . . . Merkoçi, A. (2020). Tutorial: design and fabrication of nanoparticle-based lateral-flow immunoassays. *Nat Protoc*, 15(12), 3788-3816. doi:10.1038/s41596-020-0357-x
- Periwal, N., Rathod, S. B., Sarma, S., Johar, G. S., Jain, A., Barnwal, R. P., . . . Sood, V. (2022). Time Series Analysis of SARS-CoV-2 Genomes and Correlations among Highly Prevalent Mutations. *Microbiol Spectr*, 10(5), e0121922. doi:10.1128/spectrum.01219-22
- Pizzato, M., Baraldi, C., Boscato Sopetto, G., Finozzi, D., Gentile, C., Gentile, M. D., . . . Volpini, L. (2022). SARS-CoV-2 and the Host Cell: A Tale of Interactions. *Frontiers in Virology*, 1. doi:10.3389/fviro.2021.815388
- Pradhan, M., Shah, K., Alexander, A., Ajazuddin, Minz, S., Singh, M. R., . . . Chauhan, N. S. (2022). COVID-19: clinical presentation and detection methods. *J Immunology Immunochem*, 43(1), 1951291. doi:10.1080/15321819.2021.1951291
- Puenpa, J., Rattanakomol, P., Saengdao, N., Chansaenroj, J., Yorsaeng, R., Suwannakarn, K., . . . Poovorawan, Y. (2023). Molecular characterisation and tracking of severe acute respiratory syndrome coronavirus 2 in Thailand, 2020–2022. *Archives of Virology*, 168(1), 26. doi:10.1007/s00705-022-05666-6
- Qasem, A., Shaw, A. M., Elkamel, E., & Naser, S. A. (2021). Coronavirus Disease 2019 (COVID-19) Diagnostic Tools: A Focus on Detection Technologies and Limitations. *Curr Issues Mol Biol*, 43(2), 728-748. doi:10.3390/cimb43020053
- Rahman, M. R., Hossain, M. A., Mozibullah, M., Mujib, F. A., Afrose, A., Shahed-Al-Mahmud, M., & Apu, M. A. I. (2021). CRISPR is a useful biological tool for detecting nucleic acid of SARS-CoV-2 in human clinical samples. *Biomed Pharmacother*, 140, 111772. doi:10.1016/j.biopha.2021.111772

- Raj, R. (2021). Analysis of non-structural proteins, NSPs of SARS-CoV-2 as targets for computational drug designing. *Biochem Biophys Rep*, 25, 100847. doi:10.1016/j.bbrep.2020.100847
- Rashid, F., Xie, Z., Suleman, M., Shah, A., Khan, S., & Luo, S. (2022). Roles and functions of SARS-CoV-2 proteins in host immune evasion. *Front Immunol*, 13, 940756. doi:10.3389/fimmu.2022.940756
- Saberian, M., Karimi, E., Khademi, Z., Movahhed, P., Safi, A., & Mehri-Ghahfarrokhi, A. (2022). SARS-CoV-2: phenotype, genotype, and characterization of different variants. *Cell Mol Biol Lett*, 27(1), 50. doi:10.1186/s11658-022-00352-6
- Sachdeva, S., Davis, R. W., & Saha, A. K. (2021). Microfluidic Point-of-Care Testing: Commercial Landscape and Future Directions. *Frontiers in Bioengineering and Biotechnology*, 8. doi:10.3389/fbioe.2020.602659
- Safari, F., Zare, K., Negahdaripour, M., Berekati-Mowahed, M., & Ghasemi, Y. (2019). CRISPR Cpf1 proteins: structure, function and implications for genome editing. *Cell Biosci*, 9, 36. doi:10.1186/s13578-019-0298-7
- Sagoe, K. O., Kyama, M. C., Maina, N., Kamita, M., Njokah, M., Thiong'o, K., . . . Gitaka, J. (2023). Application of Hybridization Chain Reaction/CRISPR-Cas12a for the Detection of SARS-CoV-2 Infection. *Diagnostics (Basel)*, 13(9). doi:10.3390/diagnostics13091644
- Sharma, A., Ahmad Farouk, I., & Lal, S. K. (2021). COVID-19: A Review on the Novel Coronavirus Disease Evolution, Transmission, Detection, Control and Prevention. *Viruses*, 13(2). doi:10.3390/v13020202
- Sharma, A., Balda, S., Apreja, M., Kataria, K., Capalash, N., & Sharma, P. (2021). COVID-19 Diagnosis: Current and Future Techniques. *Int J Biol Macromol*, 193(Pt B), 1835-1844. doi:10.1016/j.ijbiomac.2021.11.016
- Shi, Y., Fu, X., Yin, Y., Peng, F., Yin, X., Ke, G., & Zhang, X. (2021). CRISPR-Cas12a System for Biosensing and Gene Regulation. *Chem Asian J*, 16(8), 857-867. doi:10.1002/asia.202100043
- Shihong Gao, D., Zhu, X., & Lu, B. (2021). Development and application of sensitive, specific, and rapid CRISPR-Cas13-based diagnosis. *J Med Virol*, 93(7), 4198-4204. doi:10.1002/jmv.26889

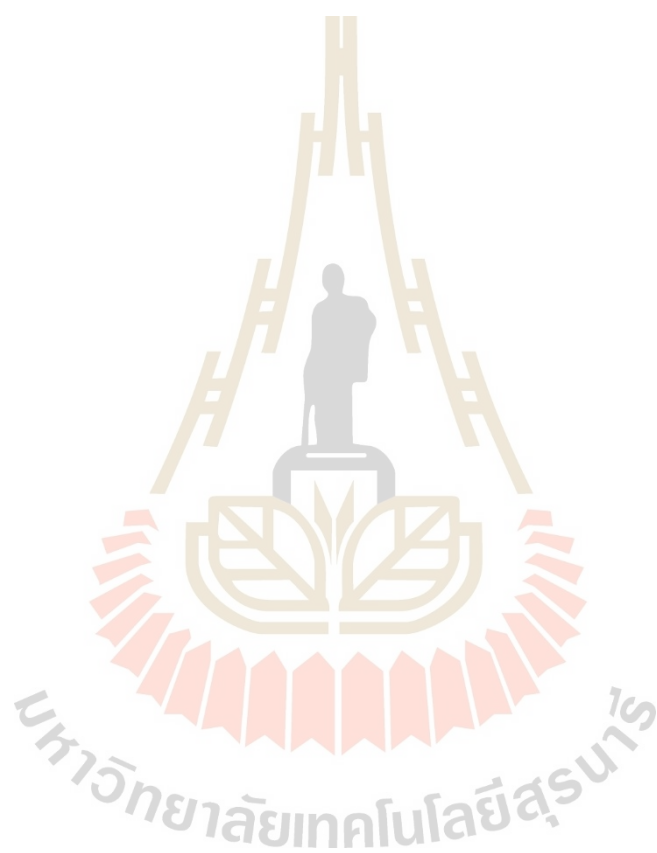
- Shmakov, S., Abudayyeh, O. O., Makarova, K. S., Wolf, Y. I., Gootenberg, J. S., Semenova, E., . . . Koonin, E. V. (2015). Discovery and Functional Characterization of Diverse Class 2 CRISPR-Cas Systems. *Mol Cell*, *60*(3), 385-397. doi:10.1016/j.molcel.2015.10.008
- Shmakov, S., Smargon, A., Scott, D., Cox, D., Pyzocha, N., Yan, W., . . . Koonin, E. V. (2017). Diversity and evolution of class 2 CRISPR-Cas systems. *Nat Rev Microbiol*, *15*(3), 169-182. doi:10.1038/nrmicro.2016.184
- Song, Q., Sun, X., Dai, Z., Gao, Y., Gong, X., Zhou, B., . . . Wen, W. (2021). Point-of-care testing detection methods for COVID-19. *Lab Chip*, *21*(9), 1634-1660. doi:10.1039/d0lc01156h
- Su, S., Zhao, Y., Zeng, N., Liu, X., Zheng, Y., Sun, J., . . . Lu, L. (2023). Epidemiology, clinical presentation, pathophysiology, and management of long COVID: an update. *Mol Psychiatry*. doi:10.1038/s41380-023-02171-3
- Sullivan, T. J., Dhar, A. K., Cruz-Flores, R., & Bodnar, A. G. (2019). Rapid, CRISPR-Based, Field-Deployable Detection Of White Spot Syndrome Virus In Shrimp. *Sci Rep*, *9*(1), 19702. doi:10.1038/s41598-019-56170-y
- Sun, Y., Yu, L., Liu, C., Ye, S., Chen, W., Li, D., & Huang, W. (2021). One-tube SARS-CoV-2 detection platform based on RT-RPA and CRISPR/Cas12a. *J Transl Med*, *19*(1), 74. doi:10.1186/s12967-021-02741-5
- Tahamtan, A., & Ardebili, A. (2020). Real-time RT-PCR in COVID-19 detection: issues affecting the results. *Expert Rev Mol Diagn*, *20*(5), 453-454. doi:10.1080/14737159.2020.1757437
- Talwar, C. S., Park, K. H., Ahn, W. C., Kim, Y. S., Kwon, O. S., Yong, D., . . . Woo, E. (2021). Detection of Infectious Viruses Using CRISPR-Cas12-Based Assay. *Biosensors (Basel)*, *11*(9). doi:10.3390/bios11090301
- Tam, D., Lorenzo-Leal, A. C., Hernández, L. R., & Bach, H. (2023). Targeting SARS-CoV-2 Non-Structural Proteins. *International Journal of Molecular Sciences*, *24*(16), 13002. Retrieved from <https://www.mdpi.com/1422-0067/24/16/13002>
- Tan, M., Liao, C., Liang, L., Yi, X., Zhou, Z., & Wei, G. (2022). Recent advances in recombinase polymerase amplification: Principle, advantages, disadvantages

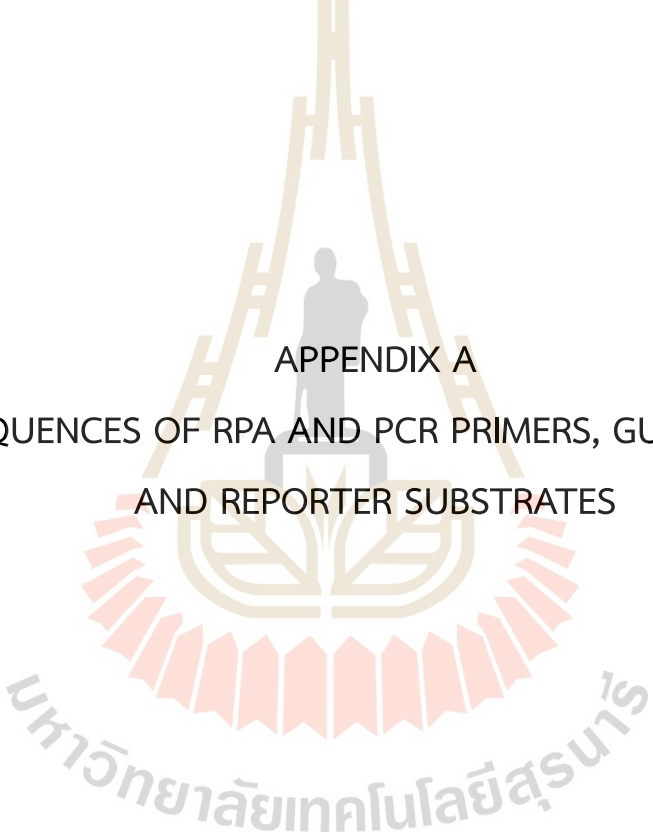
- and applications. *Front Cell Infect Microbiol*, *12*, 1019071. doi:10.3389/fcimb.2022.1019071
- Teymouri, M., Mollazadeh, S., Mortazavi, H., Naderi Ghale-Noie, Z., Keyvani, V., Aghababaei, F., . . . Mirzaei, H. (2021). Recent advances and challenges of RT-PCR tests for the diagnosis of COVID-19. *Pathol Res Pract*, *221*, 153443. doi:10.1016/j.prp.2021.153443
- Tsou, J. H., Leng, Q., & Jiang, F. (2019). A CRISPR Test for Detection of Circulating Nuclei Acids. *Transl Oncol*, *12*(12), 1566-1573. doi:10.1016/j.tranon.2019.08.011
- Udugama, B., Kadhiresan, P., Kozlowski, H. N., Malekjahani, A., Osborne, M., Li, V. Y. C., . . . Chan, W. C. W. (2020). Diagnosing COVID-19: The Disease and Tools for Detection. *ACS Nano*, *14*(4), 3822-3835. doi:10.1021/acsnano.0c02624
- V'Kovski, P., Kratzel, A., Steiner, S., Stalder, H., & Thiel, V. (2021). Coronavirus biology and replication: implications for SARS-CoV-2. *Nat Rev Microbiol*, *19*(3), 155-170. doi:10.1038/s41579-020-00468-6
- van Kasteren, P. B., van der Veer, B., van den Brink, S., Wijsman, L., de Jonge, J., van den Brandt, A., . . . Meijer, A. (2020). Comparison of seven commercial RT-PCR diagnostic kits for COVID-19. *Journal of Clinical Virology*, *128*, 104412. doi:<https://doi.org/10.1016/j.jcv.2020.104412>
- Vinjamuri, S., Li, L., & Bouvier, M. (2022). SARS-CoV-2 ORF8: One protein, seemingly one structure, and many functions. *Front Immunol*, *13*, 1035559. doi:10.3389/fimmu.2022.1035559
- Wang, X., Ji, P., Fan, H., Dang, L., Wan, W., Liu, S., . . . Liao, M. (2020). CRISPR/Cas12a technology combined with immunochromatographic strips for portable detection of African swine fever virus. *Commun Biol*, *3*(1), 62. doi:10.1038/s42003-020-0796-5
- Wölfel, R., Corman, V. M., Guggemos, W., Seilmaier, M., Zange, S., Müller, M. A., . . . Wendtner, C. (2020). Virological assessment of hospitalized patients with COVID-2019. *Nature*, *581*(7809), 465-469. doi:10.1038/s41586-020-2196-x
- Wu, A., Peng, Y., Huang, B., Ding, X., Wang, X., Niu, P., . . . Jiang, T. (2020). Genome Composition and Divergence of the Novel Coronavirus (2019-nCoV) Originating in China. *Cell Host Microbe*, *27*(3), 325-328. doi:10.1016/j.chom.2020.02.001

- Wu, F., Zhao, S., Yu, B., Chen, Y.-M., Wang, W., Song, Z.-G., . . . Zhang, Y.-Z. (2020). A new coronavirus associated with human respiratory disease in China. *Nature*, *579*(7798), 265-269. doi:10.1038/s41586-020-2008-3
- Xiong, D., Dai, W., Gong, J., Li, G., Liu, N., Wu, W., . . . Tang, G. (2020). Rapid detection of SARS-CoV-2 with CRISPR-Cas12a. *PLoS Biol*, *18*(12), e3000978. doi:10.1371/journal.pbio.3000978
- Yadav, R., Chaudhary, J. K., Jain, N., Chaudhary, P. K., Khanra, S., Dhamija, P., . . . Handu, S. (2021). Role of Structural and Non-Structural Proteins and Therapeutic Targets of SARS-CoV-2 for COVID-19. *Cells*, *10*(4). doi:10.3390/cells10040821
- Yan, W., Zheng, Y., Zeng, X., He, B., & Cheng, W. (2022). Structural biology of SARS-CoV-2: open the door for novel therapies. *Signal Transduct Target Ther*, *7*(1), 26. doi:10.1038/s41392-022-00884-5
- Yan, Z., Yang, M., & Lai, C. L. (2021). Long COVID-19 Syndrome: A Comprehensive Review of Its Effect on Various Organ Systems and Recommendation on Rehabilitation Plans. *Biomedicines*, *9*(8). doi:10.3390/biomedicines9080966
- Yip, C. C., Ho, C. C., Chan, J. F., To, K. K., Chan, H. S., Wong, S. C., . . . Yuen, K. Y. (2020). Development of a Novel, Genome Subtraction-Derived, SARS-CoV-2-Specific COVID-19-nsp2 Real-Time RT-PCR Assay and Its Evaluation Using Clinical Specimens. *Int J Mol Sci*, *21*(7). doi:10.3390/ijms21072574
- Yüce, M., Filiztekin, E., & Özkaya, K. G. (2021). COVID-19 diagnosis -A review of current methods. *Biosens Bioelectron*, *172*, 112752. doi:10.1016/j.bios.2020.112752
- Zandi, M. (2022). ORF9c and ORF10 as accessory proteins of SARS-CoV-2 in immune evasion. *Nat Rev Immunol*, *22*(5), 331. doi:10.1038/s41577-022-00715-2
- Zandi, M., Shafaati, M., Kalantar-Neyestanaki, D., Pourghadamyari, H., Fani, M., Soltani, S., . . . Abbasi, S. (2022). The role of SARS-CoV-2 accessory proteins in immune evasion. *Biomed Pharmacother*, *156*, 113889. doi:10.1016/j.biopha.2022.113889
- Zetsche, B., Gootenberg, J. S., Abudayyeh, O. O., Slaymaker, I. M., Makarova, K. S., Essletzbichler, P., . . . Zhang, F. (2015). Cpf1 is a single RNA-guided endonuclease of a class 2 CRISPR-Cas system. *Cell*, *163*(3), 759-771. doi:10.1016/j.cell.2015.09.038

- Zhang, F. (2019). Development of CRISPR-Cas systems for genome editing and beyond. *Quarterly Reviews of Biophysics*, 52, e6. doi:10.1017/S0033583519000052
- Zhang, J., Ejikemeuwa, A., Gerzanich, V., Nasr, M., Tang, Q., Simard, J. M., & Zhao, R. Y. (2022). Understanding the Role of SARS-CoV-2 ORF3a in Viral Pathogenesis and COVID-19. *Front Microbiol*, 13, 854567. doi:10.3389/fmicb.2022.854567
- Zhang, L., Li, G., Zhang, Y., Cheng, Y., Roberts, N., Glenn, S. E., . . . Qi, Y. (2023). Boosting genome editing efficiency in human cells and plants with novel LbCas12a variants. *Genome Biology*, 24(1), 102. doi:10.1186/s13059-023-02929-6
- Zhang, Y.-m., Zhang, Y., & Xie, K. (2020). Evaluation of CRISPR/Cas12a-based DNA detection for fast pathogen diagnosis and GMO test in rice. *Molecular Breeding*, 40(1), 11. doi:10.1007/s11032-019-1092-2
- Zhang, Y., Chai, Y., Hu, Z., Xu, Z., Li, M., Chen, X., . . . Liu, J. (2022). Recent Progress on Rapid Lateral Flow Assay-Based Early Diagnosis of COVID-19. *Front Bioeng Biotechnol*, 10, 866368. doi:10.3389/fbioe.2022.866368
- Zhang, Y., Huang, Z., Zhu, J., Li, C., Fang, Z., Chen, K., & Zhang, Y. (2022). An updated review of SARS-CoV-2 detection methods in the context of a novel coronavirus pandemic. *Bioeng Transl Med*, 8(1), e10356. doi:10.1002/btm2.10356
- Zhao, J., Zhai, X., & Zhou, J. (2020). Snapshot of the evolution and mutation patterns of SARS-CoV-2. *bioRxiv*. doi:10.1101/2020.07.04.187435
- Zhou, P., Yang, X. L., Wang, X. G., Hu, B., Zhang, L., Zhang, W., . . . Shi, Z. L. (2020). A pneumonia outbreak associated with a new coronavirus of probable bat origin. *Nature*, 579(7798), 270-273. doi:10.1038/s41586-020-2012-7
- Zhou, Y., Zhang, L., Xie, Y. H., & Wu, J. (2022). Advancements in detection of SARS-CoV-2 infection for confronting COVID-19 pandemics. *Lab Invest*, 102(1), 4-13. doi:10.1038/s41374-021-00663-w
- Zhu, N., Zhang, D., Wang, W., Li, X., Yang, B., Song, J., . . . Tan, W. (2020). A Novel Coronavirus from Patients with Pneumonia in China, 2019. *N Engl J Med*, 382(8), 727-733. doi:10.1056/NEJMoa2001017

Zhu, Y., Zhang, M., Jie, Z., & Tao, S. (2022). Nucleic acid testing of SARS-CoV-2: A review of current methods, challenges, and prospects. *Front Microbiol*, 13, 1074289. doi:10.3389/fmicb.2022.1074289



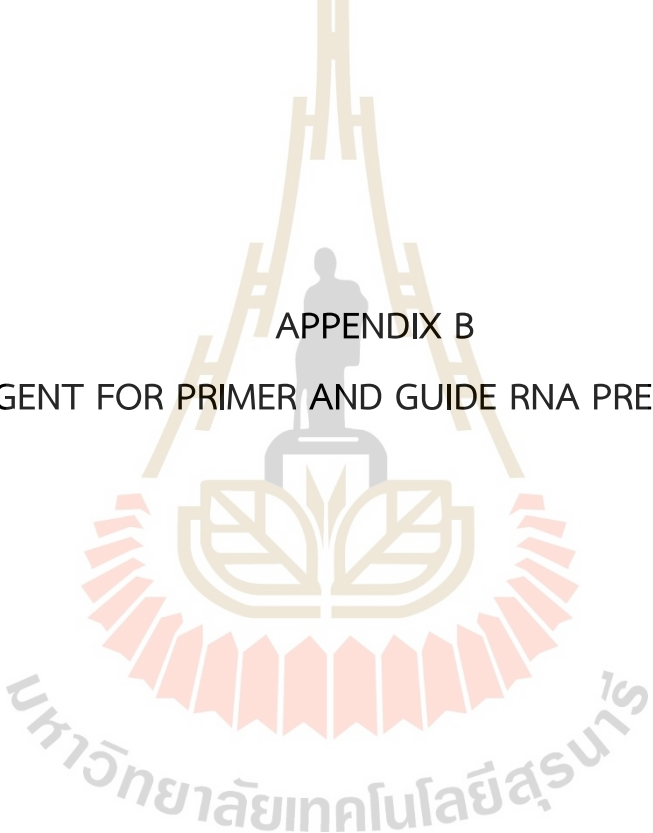


APPENDIX A
SEQUENCES OF RPA AND PCR PRIMERS, GUIDE RNA,
AND REPORTER SUBSTRATES

มหาวิทยาลัยเทคโนโลยีสุรนารี

Sequences of RPA and PCR primers, guide RNA, and reporter substrates

Primers for RPA and PCR	
NSP2_F	ATGTTGCTCGAAATCAAAGA
NSP2_R	TTAAGTACTTTTATCAATCCT
Guide RNA	Sequence (5'->3')
crRNA-NSP2	UAAUUUCUACUAAGUGUAGAAGGUGAUGACACUGUGAUAGA
Substrates	Sequence (5'->3')
ssDNA-Probe1 reporter	BIOTIN/TTATTATTATTATTATT/FITC



APPENDIX B
REAGENT FOR PRIMER AND GUIDE RNA PREPARATION

Reagent for primer and guide RNA preparation

1. Forward Primer (100 μ M stock)

The stock of Forward Primer was prepared by dissolving the below ingredients in 100 μ L of ultrapure deionized water (UDW):

100 μ M Forward Primer (Ward medic)	10	μ L
UDW (HyClone)	90	μ L

Working Forward Primer was prepared by diluting 10 μ L of the Forward Primer with 90 μ L of UDW.

2. Reverse Primer (100 μ M stock)

The stock of Reverse Primer was prepared by dissolving the below ingredients in 100 μ L of ultrapure deionized water (UDW):

100 μ M Reverse Primer (Ward medic)	10	μ L
UDW (HyClone)	90	μ L

Working Reverse Primer was prepared by diluting 10 μ L of the Reverse Primer with 90 μ L of UDW.

3. Lba Cas12a crRNA (2 nmol stock)

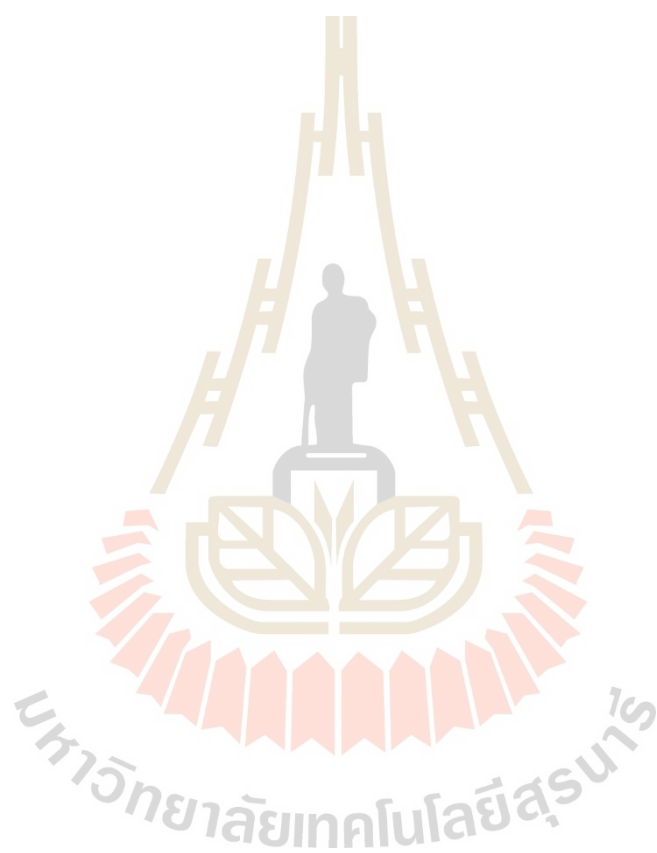
The preparation of amount of Lba Cas12a crRNA was prepared by dissolving 100 μ L of ultrapure deionized water (UDW) in 2 nmol of Lba Cas12a crRNA.

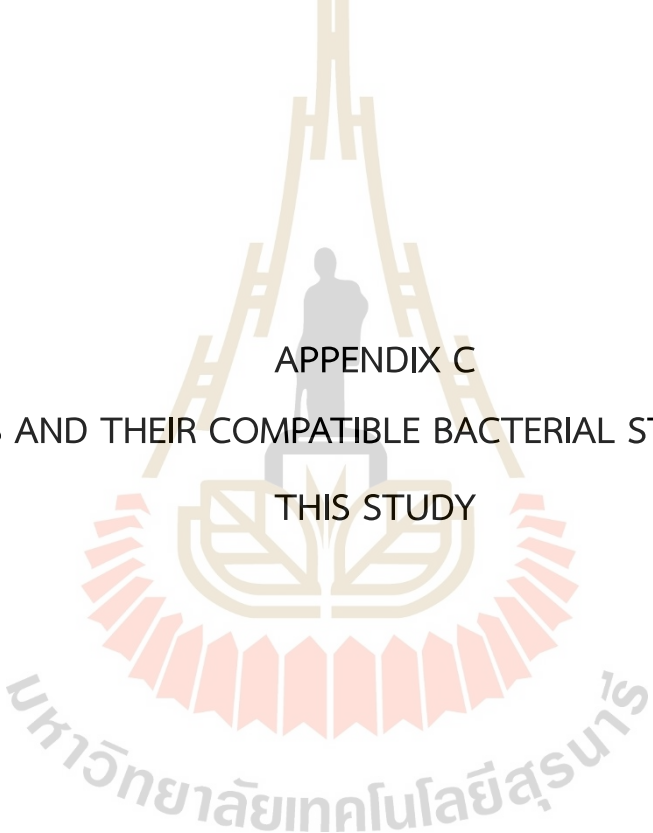
4. 300 nM Lba Cas12a crRNA (10^{-5} M stock)

The stock of Lba Cas12a crRNA was prepared by dissolving the below ingredients in 100 μ L of ultrapure deionized water (UDW):

2 nmol of NSP2 Guide Sequence (Ward medic)	3	μ L
UDW (HyClone)	97	μ L

Working 300 nM Lba Cas12a crRNA was prepared by diluting 3 μL of the Lba Cas12a crRNA with 97 μL of UDW.



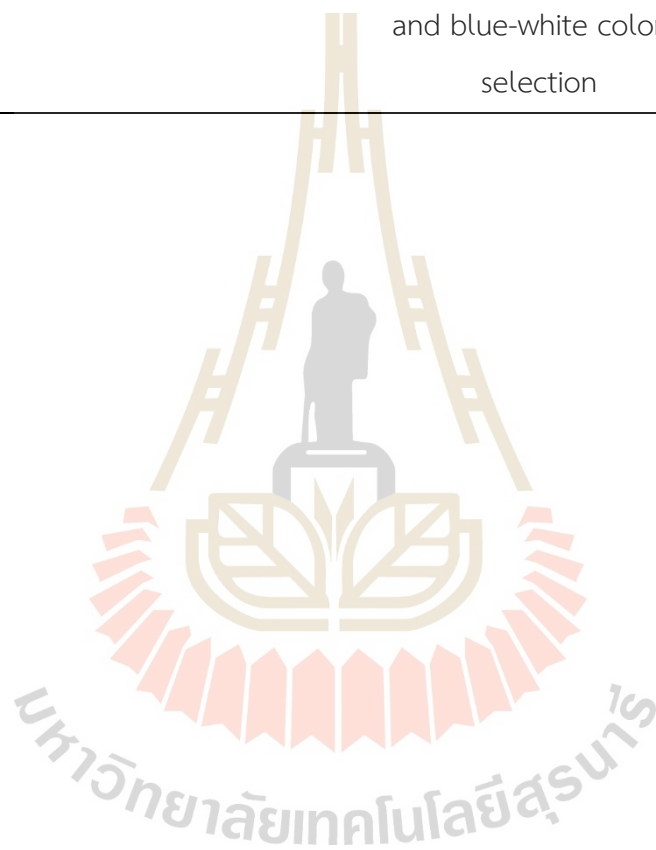
The logo of Sakon Nakhon Rajabhat University is a large, faint watermark in the background. It features a central figure of a person standing on a platform, flanked by two stylized figures. Above them are several 'H' shapes. The entire emblem is enclosed in a circular border with a scalloped edge. The Thai text 'มหาวิทยาลัยเทคโนโลยีสุรนารี' is written in a curved path around the bottom of the emblem.

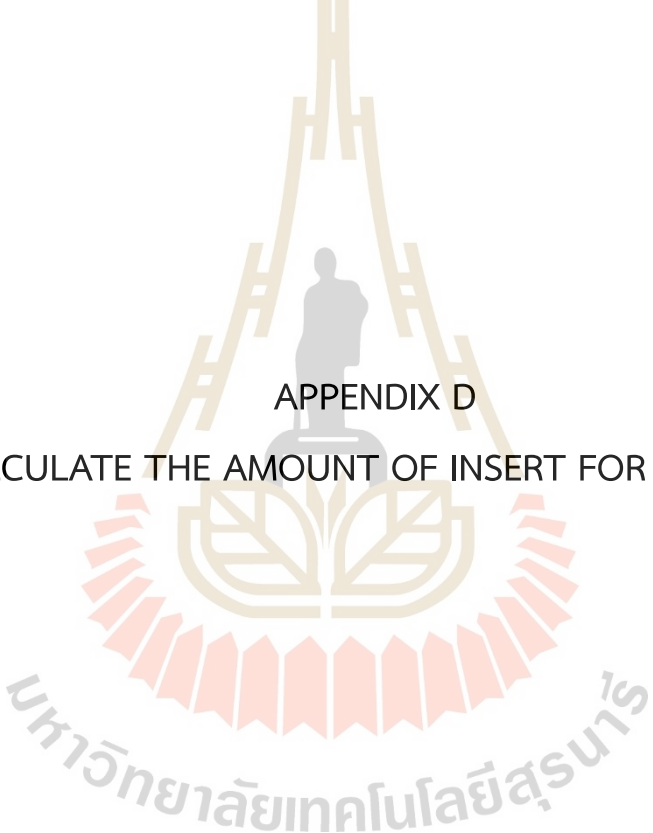
APPENDIX C

PLASMIDS AND THEIR COMPATIBLE BACTERIAL STRAINS USED IN
THIS STUDY

Plasmids and their compatible bacterial strains used in this study

Plasmid	Application	Promoter	Selection marker	Compatible <i>E. coli</i> strain
pTG19-T	Gene cloning	T7	Ampicillin resistance and blue-white colony selection	DH5 α





APPENDIX D
CALCULATE THE AMOUNT OF INSERT FOR LIGATION

Calculate the amount of insert for ligation

1. Calculate the amount of insert for ligation based on the example below

For 500bp insert with 50ng of pTG19-T vector (2880bp)

$$\frac{2880 \text{ bp}}{500 \text{ bp}} = 5.76$$

(Vector is 5.76x larger than insert, you need 5.76x less insert)

For 50ng pTG19-T vector

$$\frac{50 \text{ ng}}{5.76} = 8.68 \text{ ng}$$

8.68 ng of insert for 1:1 ratio

$$\frac{50 \text{ ng}}{5.76} = 8.68 \text{ ng}$$

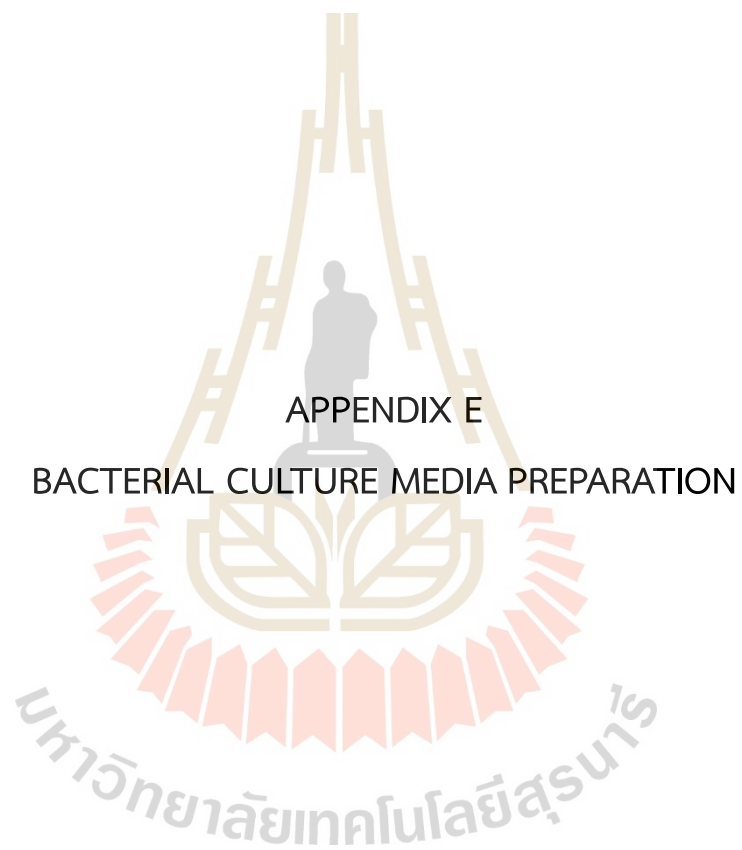
$$= 8.68 \text{ ng} \times 3$$

$$= 26.04 \text{ of insert for 1:1 ratio}$$

มหาวิทยาลัยเทคโนโลยีสุรนารี

2. Conversion table for amount of PCR product required per ligation reaction

Size of PCR product (bp)	Amount needed for 1:3 vector and insert molar ratio
100	5.21 ng
300	15.63 ng
500	26.04 ng
1000	52.08 ng
1500	78.13 ng
2000	104.17 ng
3000	156.25 ng



APPENDIX E

BACTERIAL CULTURE MEDIA PREPARATION

Bacterial culture media preparation

1. Luria-Bertani (LB) broth

The medium was prepared by dissolving the following ingredients in 1000 mL of UDW and autoclaved:

Tryptone Type-1 (Casitose Type-I (Himedia)	10	g
Yeast extract powder (Himedia)	5	g
NaCl (1 st Base)	5	g

2. LB-ampicillin (LB-A) broth

The LB broth prepared as described above was added with ampicillin to a final concentration of 100 $\mu\text{L}/\text{mL}$. The medium was kept at 4°C until use.

3. LB agar

This agar was prepared by dissolving the following ingredients in 1000 mL of UDW.

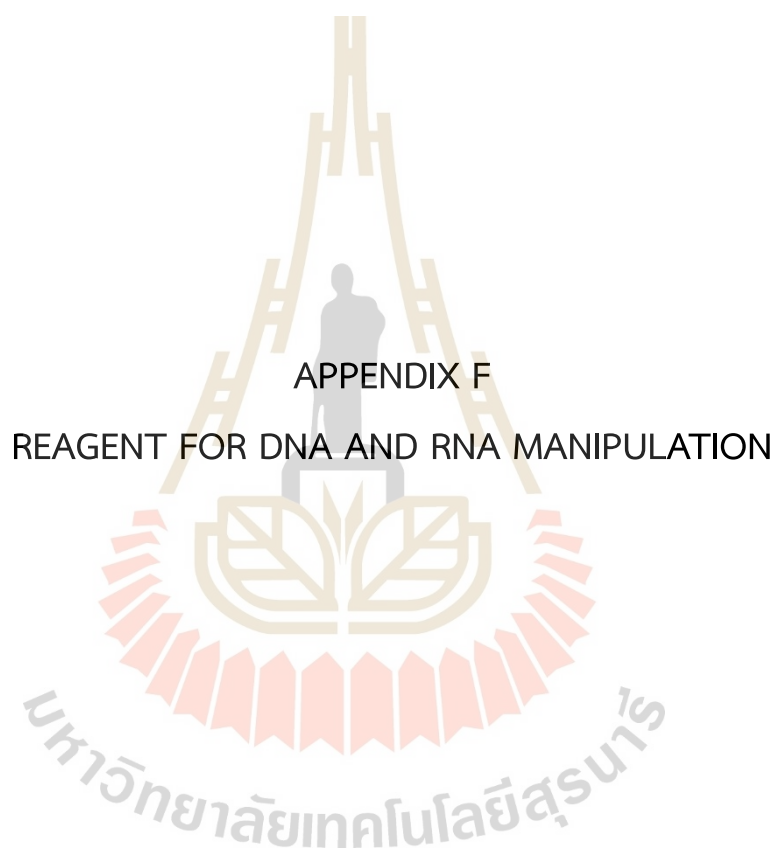
Bacto-tryptone (Himedia)	10	g
Bacto-yeast extract (Himedia)	5	g
NaCl (1 st Base)	5	g
Agar powder (Himedia)	15	g

The preparation was sterilized by autoclaving. After cooling down to ~55-60 °C, 25 mL aliquots were poured into 90-15 mm Petri-dishes. The agar was allowed to set in a biosafety cabinet. The plates were kept at 4 °C. The agar surface was dried appropriately before use.

4. LB-ampicillin (LB-A) and LB-ampicillin agar

For preparing the LB-A agar and the LB agar were prepared as described above in (3). After cooling down ~55-60 °C, ampicillin was added to the final concentration of 100 μ L/mL. Twenty-five mL aliquots of the preparation were poured into 90-15 mm petri dishes; the agar was allowed to set and the plates were kept at 4 °C until use.





APPENDIX F

REAGENT FOR DNA AND RNA MANIPULATION

Reagent for DNA and RNA manipulation

1. dNTPs

The dNTPs for master mix PCR reaction were prepared by dissolving all of below ingredients in of ultrapure deionized water (UDW):

100 mM of dATP (Themoscientific)	2	μL
100 mM of dATP (Themoscientific)	2	μL
100 mM of dATP (Themoscientific)	2	μL
100 mM of dATP (Themoscientific)	2	μL
UDW (HyClone)	92	μL

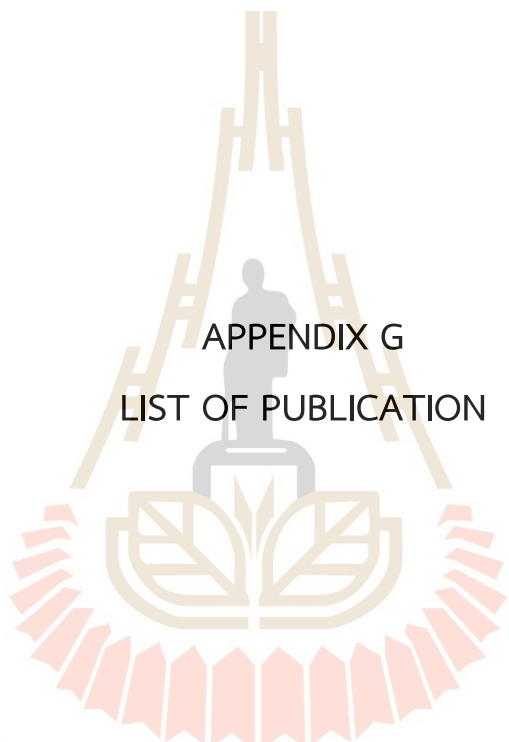
The volume was made to 100 μL with UDW

2. Tris-acetate-EDTA (TAE) (50X stock)

The stock of TAE buffer was prepared by dissolving the below ingredients in 1,000 mL of UDW:

TAE (Themoscientific)	20	mL
UDW (HyClone)	980	mL

Working TAE (1X) was prepared by diluting 20 mL of the stock buffer with 980 mL of UDW.

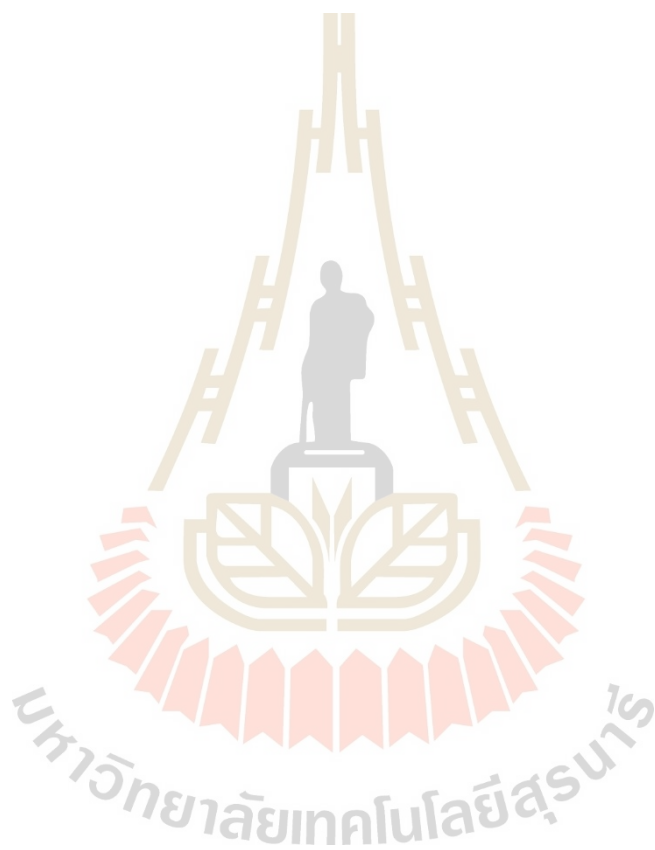
The logo of Suranaree Technological University is a circular emblem. At the top, there is a stylized golden structure resembling a traditional Thai roof or a monument. Below this, a grey silhouette of a person stands on a pedestal. Underneath the person is a golden lotus flower. The entire emblem is surrounded by a decorative border of red and orange segments. The text 'มหาวิทยาลัยเทคโนโลยีสุรนารี' is written in Thai script along the bottom curve of the emblem.

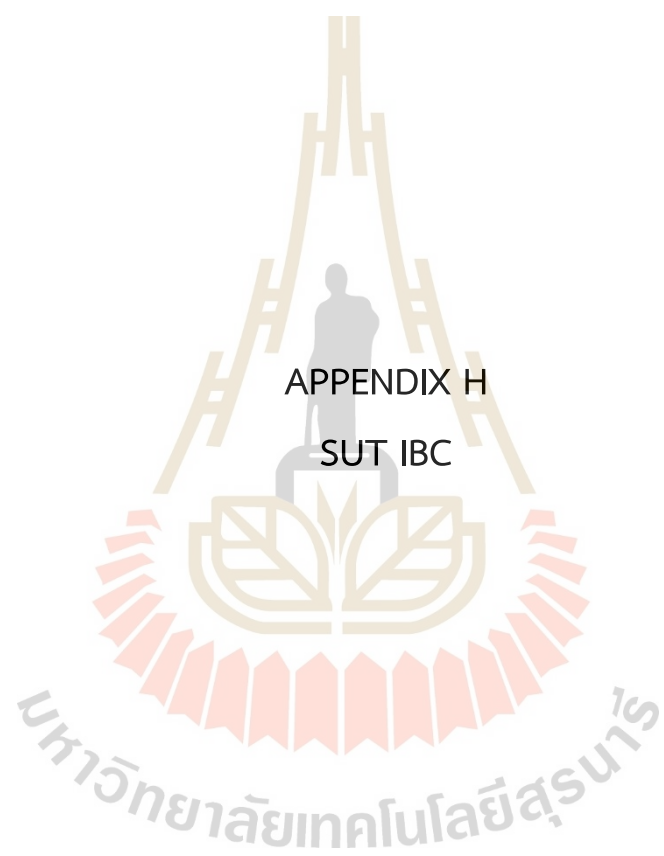
APPENDIX G
LIST OF PUBLICATION

มหาวิทยาลัยเทคโนโลยีสุรนารี

List of Publication

Naewwan, N., Surasiang, T., Jamklang, M., Namvichaisirikul, N., Thueng-in, K.
“Development of CRISPR-Cas12a based assay for the detection of SARS-CoV-2 NSP2”
The 3rd International Conference on Science Technology & Innovation Maejo
University Hybrid conference (3rd ICSTI 2023), 11th August 2023, Chiang Mai, Thailand.





APPENDIX H

SUT IBC

มหาวิทยาลัยเทคโนโลยีสุรนารี



เลขที่รับรอง SUT-IBC-008/2022

ใบรับรองการดำเนินงานด้านความปลอดภัยทางชีวภาพ
มหาวิทยาลัยเทคโนโลยีสุรนารี

ชื่อโครงการ : การพัฒนาชุดตรวจโรคติดเชื้อไวรัสโคโรนา 2019 ด้วยเทคนิค CRISPR-Cas12a
รหัสโครงการ : IBC-65-08
หัวหน้าโครงการ : นายนพพร แนวนวัน
อาจารย์ที่ปรึกษา : อาจารย์ ดร.กัญญารัตน์ ถึงอินทร์
สังกัด : สำนักวิชาแพทยศาสตร์
ประเภทงานวิจัย : งานวิจัยประเภทที่ 2
ระดับห้องปฏิบัติการ : Biosafety Level 2 (BSL 2)
รายงานความก้าวหน้า : ส่งรายงานความก้าวหน้าอย่างน้อย 1 ครั้ง/ปี

ข้อเสนอโครงการวิจัยและเอกสารประกอบของข้อเสนอโครงการวิจัยนี้ ได้รับการพิจารณาจากคณะกรรมการควบคุมความปลอดภัยทางชีวภาพ มหาวิทยาลัยเทคโนโลยีสุรนารีแล้ว คณะกรรมการฯ ลงความเห็นว่าย ข้อเสนอโครงการวิจัยที่จะดำเนินการมีความสอดคล้องกับแนวทางปฏิบัติเพื่อความปลอดภัยทางชีวภาพ และพระราชบัญญัติเชื้อโรคและพิษจากสัตว์ พ.ศ. 2558 จึงเห็นสมควรให้ดำเนินการวิจัยตามข้อเสนอการวิจัยนี้ได้

กรณีที่มีการปฏิบัติอย่างหนึ่งอย่างใดนอกเหนือจากที่กรอกไว้ในข้อมูลและที่เสนอไว้ในโครงการ คณะกรรมการฯ จะดำเนินการตใบรับรองนี้ และแจ้งมายังคณะกรรมการควบคุมความปลอดภัยทางชีวภาพ มทส.หรือหน่วยงานที่เกี่ยวข้องทราบ

ลงชื่อ..... 

(รองศาสตราจารย์ ดร.ระพี อุณหเคอ)

ประธานคณะกรรมการควบคุมความปลอดภัยทางชีวภาพ

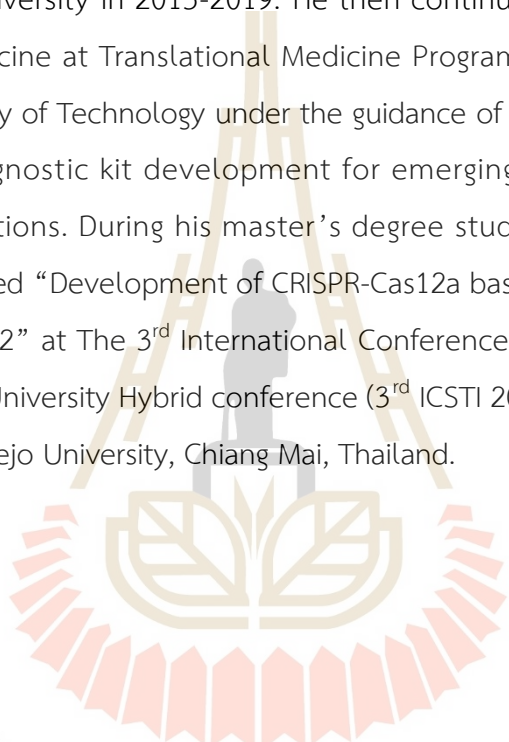
มหาวิทยาลัยเทคโนโลยีสุรนารี

วันที่ออกใบรับรอง 3 พฤศจิกายน 2565

วันที่ใบรับรองหมดอายุ 2 พฤศจิกายน 2566

CURRICULUM VITAE

Mr. Nopporn Naewwan was born on July 1, 1996 in Nakhon Ratchasima Province, Thailand. He earned his Bachelor's Degree in Bachelor of Science from Maharakham University in 2015-2019. He then continued his Master's Degree in Translational Medicine at Translational Medicine Program, Institute of Medicine at Suranaree University of Technology under the guidance of Dr. Kanyarat Thueng-in. His expertise was diagnostic kit development for emerging/re-emerging and sexual transmission infections. During his master's degree study, he presented one oral presentation entitled "Development of CRISPR-Cas12a based assay for the detection of SARS-CoV-2 NSP2" at The 3rd International Conference on Science Technology & Innovation Maejo University Hybrid conference (3rd ICSTI 2023) to be held during 11th August, 2023 at Maejo University, Chiang Mai, Thailand.



มหาวิทยาลัยเทคโนโลยีสุรนารี